DIASTEREOSELECTIVE GOLD (I) AND BISMUTH (III) CATALYZED CYCLIZATIONS OF 1,4 AND 1,5-DIOLS IN THE FORMATION OF SUBSTITUTED 1,3-DIOXOLANES, 1,3-DIOXANES, AND 3,6-DIHYDRO-2H-PYRANS

By

CARL FRANCIS BALLESTEROS

A DISSERTATION PRESENTED TO THE GRADUATE SCHOOL
OF THE UNIVERSITY OF FLORIDA IN PARTIAL FULFILLMENT
OF THE REQUIREMENTS FOR THE DEGREE OF
DOCTOR OF PHILOSOPHY

UNIVERSITY OF FLORIDA

2013

To my beautiful wife Elin and my wonderful children Carl Junior, Brielle, and Carolynn

ACKNOWLEDGMENTS

I thank my wife Elin for all of her love, support, and encouragement over the entirety of my graduate career. She has been my greatest source of strength and support. She amazes me each day in her undertaking of raising our two living children Carl Junior and Carolynn on top of working a full time job. I am most grateful for her perseverance and faith in me.

I thank my parents for all of their help in getting to this point of my life. Without their love and support, I would have never even thought to pursue a graduate level degree. To this day I rely upon their advice and loving support.

I thank Dr. Aaron Aponick for building an organic synthetic driven research group here at the University of Florida, thus giving me the opportunity of a lifetime in studying chemistry in my field of choice. Not only has he built a group that daily works to expand the state of the art, but he has made this research group a powerhouse of learning synthetic chemistry. It is my humble opinion that this research group is the most knowledgeable in the construction of complex molecules in the entire division of organic chemistry at the University of Florida. The group Dr. Aponick has built has even attracted many other like-minded, very talented, and smart students whom I also thank for their constant positivity. Everyone of these students, past and present, has made this endeavor one of one of joy, shared learning, and great fun.

TABLE OF CONTENTS

page

LIST OF TABLES

LIST OF FIGURES

LIST OF ABBREVIATIONS

Ac	Acetyl
Anhyd	Anhydrous
aq	Aqueous
Ar	Aromatic
Atm	Atmosphere
BBN (9-BBN)	9-Borabicyclo[3.3.1]nonane (9-BBN)
Bn	Benzyl
Boc	t-Butyloxycarbonyl
BOM	Benzyloxymethyl
bp	Boiling Point
BQ	Benzoquinone
Bz	Benzoyl
Bu (nBu)	n-Butyl
c	speed of light
ca	Circa (approximately)
CAN	Cerium (IV) Ammonium Nitrate
Calcd	Calculated
cat.	Catalytic
Cbz	Benzyloxycarbonyl
conc.	Concentrated
Cond	Conditions
COD	1,5-Cyclooctadiene
Cp	Cyclopentadienyl
Cp*	Pentamethylcyclopentadienyl

CSA	Camphorsulfonic Acid
Cy	Cyclohexyl
Δ	Heat
d	Days (length of reaction time)
DBU	1,8-diazabicclo[5.4.0]undec-7-ene
DCC	dicyclohexylcarbodiimide
DCD	Dewar-Chatt-Duncanson model
DCE	1,1-Dicycloethane
DDQ	2,3-Dichloro-5,6-Dicyano-1,4-Benzoquinone
DHP	3,4-Dihydro-2H-Pyran
DIAD	Diisopropyl Azodicarboxylate
DIBAL-H	Diisobutylaluminum Hydride
DMAP	N,N-4-Dimethylamineopyridine
DMF	N,N-Dimethylformamide
DMS	Dimethylsulfide
DMSO	Dimethylsulfoxide
dr	Diastereomeric Ratio
E^+	Electrophile
E2	Bimolecular Elimination
ee	Enantiomeric Excess
Et	Ethyl
EWG	Electron Withdrawing Group
g	Gas
GC	Gas Chromatography
h	Hours (length of reaction time)

Het	Heterocycle
HMDS	1,1,1,3,3,3-Hexamethyldisilazane
HOMO	Highest Occupied Molecular Orbital
HPLC	High-Pressure Liquid Chromatography
HWE	Horner-Wadworth-Emmons
i	Iso
IPA	Isopropyl Alcohol
Ipc	Isopinocamphenyl
IR	infrared spectroscopy
L	ligand
LA	Lewis Acid
LAH	Lithium Aluminim Hydride
liq.	Liquid
LUMO	Lowest Unoccupied Molecular Orbital
m	Meta
m-CPBA	3-Chloroperbenzoic Acid
Me	Methyl
MOM	Methyoxymethyl
mp	Melting Point
MS	Molecular Sieve
n	Normal (e.g. unbranched alkyl chain)
NMR	Nuclear Magnetic Resonance
NR	No Reaction
Nuc	Nucleophile
o	Ortho

Oxone	Potassium Peroxymonosulfate
p	Para
PCC	Pyridinium Chlorochromate
Ph	Pheynyl
Piv	Pivaloyl
PMB	4-Methoxybenzyl
PPTS	Pyridinium p-Toluenesulfonate
psi	Pounds Per Square Inch
P.T.	Proton Transfer
PTSA (or TsOH)	p-Toluenesulfonic Acid
Py	Pyridine
rt	Room Temperature
rac	Racemic
RDS	Rate Determining Step
Red-Al	Sodium Bis(2-methoxyethoxy) Aluminium Hydride
R_f	Retention Factor
s	Solid
Sia	1,2-Dimethylpropyl
Sec	Secondary
TBAF	Tetra-n-Butylammonium Floride
TBS	t-Butyldimethlsilyl
TBDPS	t-Butyldiphenylsilyl
TEA	Triethylamine
TES	Triethylsilyl
TFA	Trifluoroacetic Acid

THF	Tetrahydrofuran
THP	2-Tetrahydropyranyl
TMS	Trimethylsilyl
TP	bis[2-(diphenylphosphino)-phenyl]phosphine
TS	Transition State
Tos	p-Toluenesulfonyl
TOF	turn over frequency

Abstract of Dissertation Presented to the Graduate School
of the University of Florida in Partial Fulfillment of the
Requirements for the Degree of Doctor of Philosophy

DIASTEREOSELECTIVE GOLD (I) AND BISMUTH (III) CATALYZED CYCLIZATIONS OF 1,4 AND 1,5-DIOLS IN THE FORMATION OF SUBSTITUTED 1,3-DIOXOLANES, 1,3-DIOXANES, AND 3,6-DIHYDRO-2H-PYRANS

By

Carl Francis Ballesteros

May 2013

Chair: Aaron Aponick
Major: Chemistry

Gold (I) catalyzed reactions are of growing importance in the synthetic community. They have been shown to be widely applicable in the nucleophilic addition of C, N, O, P, and S species to a variety of unsaturated C-C bonds. This is due in large part to the role of ligands among other factors. Surprisingly, few reports on the effects of various ligands are reported. Moreover, there are no known reports of the effects of electron withdrawing ligands in gold catalysis. In this work, the effects of ligands in gold (I) catalysis are discussed, while ligands with electron withdrawing capability are given special attention. In addition, two new methodologies are reported based on the application of electron deficient gold (I) catalyst systems.

Diastereoselective gold (I) and bisthmuth (III) catalyzed tandem hemiacetalization and ketalization/dehydrative cyclization was developed. In this method, easily prepared 1,4 and 1,5-monoallyic diols are transformed into cis-1,3-dioxolanes and dioxanes. This transformation may have practical use in the synthesis of protected syn-1,2 and 1,3 diols in natural products. This method is the first to show a cooperative nature between bismuth and gold which are both capable of catalyzing the transformation, but only

when the other catalyst cannot. It also represent the first known use of a phosphite ligand in gold (I) catalysis to be able to activate both a C-C double bond and a C-O double bond towards nucleophilic attack.

Diastereoselective gold (I) catalyzed synthesis of 3,6-dihydro-2H-pyrans was also developed. This methodology has the potential to becoming a new strategy in natural product synthesis for the facile production of these interesting dihydropyran moieties which are found in many marine natural products. Most of which have been shown to posses important biological activity and are currently the subject of great interest as potential new antifungals, antibiotics, and even anticancer treatments. These important biological functions are believed to stem from the structural shape and rigidity of the dihydro-2H-pyranyl moiety.

CHAPTER 1
ELECTRON-DEFICIENT LIGANDS IN HOMOGENEOUS GOLD (I) CATALYSIS

1.1 Ubiquity of Gold Catalysis

Gold-catalyzed reactions are an increasingly powerful tool in the synthesis of a wide variety of compounds. Over the past two decades, there has been an explosion of reports that exemplify this phenomenon. According to the online science database "Web of Science," there were 18 reports for gold catalysis in 1991 while in 2011 there were 800 (Figure 1-1).[1]

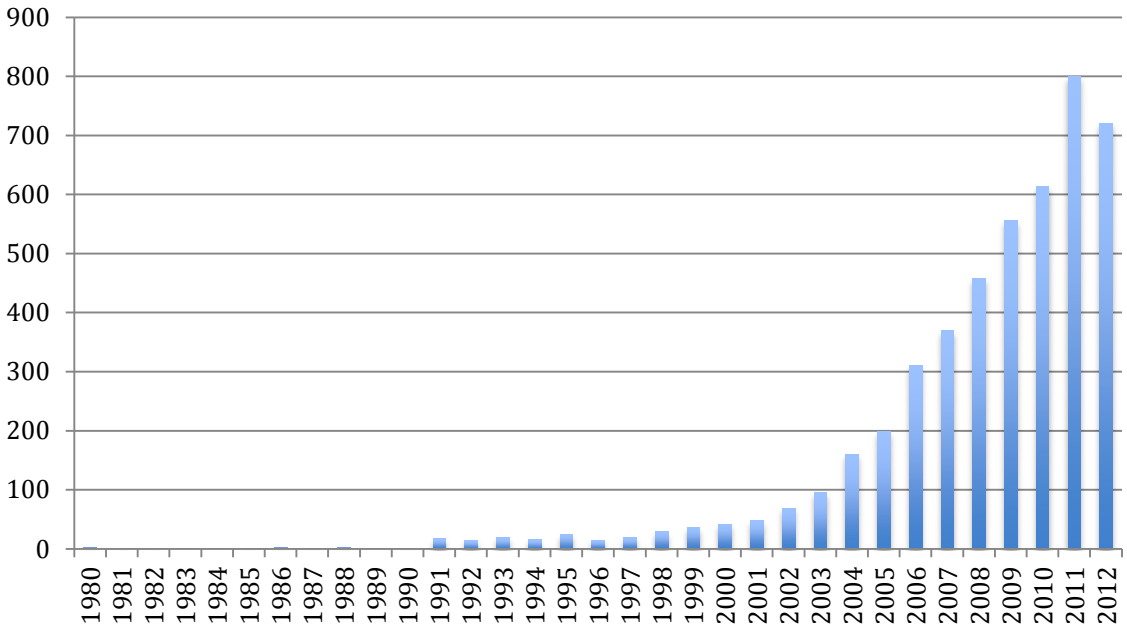

Figure 1-1. Number of publications found on "Web of Science" for gold catalysis.

The reasons for this growth in the utility of gold are fourfold: 1) Gold is a carbophilic Lewis acid and thus can activate all manner of C-C π bonds toward nucleophilic attack. 2) Gold is air and water stable and does not need stringent measures for handling. 3) Gold has been shown to be a mild catalyst, tolerant to a wide variety of functional groups. 4) Gold can be coordinated to a variety of ligands; which

allows for increased catalyst lifetime, the possibility of stereochemical induction, and also electronic tuning of the catalyst system.

Because of the exponential growth in the field of gold catalysis, a large number of reviews are published annually in order to keep up with the state of the art. These are in large part an appendix of new transformations[2-7] and only a few reviews address the fundamental questions that drive innovation in the field.[8-10] One such review from Toste[11] is the latest review on ligand effects in homogenous gold catalysis. Since its publication in 2008, there have been over 3,000 new reports in the field. It therefore seems that an updated review is needed as the role of ligands is now more clearly defined and better understood. This is especially true for electron deficient ligands, which have promising reactivity, but are scarcely reported in the literature while electron rich ligands are ubiquitous. In fact, there are already a large number of reviews on electron rich ligands in gold (I) catalysis. This chapter will therefore strive to not only include examples of electron deficient ligands in various transformations, but also to give clear insight into the ligand's effect on the reactivity of gold (I) catalysis.

1.2 The Nature of Gold (I) Catalysis

As previously described, gold has been shown to catalyze a large number of transformations. These include, but are not limited to: oxidations, condensations, cyclizations, ring openings, cross-couplings, pericyclic transformations, and even tandem processes which combine these transformations. All of these are the result of nucleophilic attack on a given π-system that is activated by coordination to the gold catalyst. The nucleophile can be C, N, O, S, or even P. The following subsections will discuss four major pillars for understanding gold (I) catalysis, and the impact ligands

contribute to this reactivity. These are relativistic effects, common mechanistic steps, electronic and steric effects of the ligand, and lastly the silver cocatalysts.

1.2.1 Relativistic Effects of Gold.

Relativistic effects are an important facet to gold (I) catalysis. They have been evoked to explain the preference of gold (I) complexes interaction with substrates to be orbitally controlled rather than charge controlled.[12] These effects are also used to explain why gold forms stronger gold-ligand (Au-L) bonds than the other group 11 and period 6 metals,[13] and also explains the linear coordination geometry of gold (I) complexes. Below is a brief explanation of what these effects are, and the consequences they incur on gold (I) catalysis.

Group 11 metals all have completely filled f orbitals. As a result, electrons in the 1s orbital are traveling at such great velocity that they are moving at a significant fraction of the speed of light (c) and therefore subject to the special theory of relativity. This theory stated simply, means that mass increases towards infinity as velocity approaches c. Because the Bohr radius of an electron orbital is inversely proportional to its mass; electrons in 1s orbital are pulled closer towards the nucleus of the atom - contracting this and all other s and p orbitals. Since gold (0) has the electron configuration [Xe] 4f14 5d10 6s1, electrons in the d and f orbitals are shielded from the nucleus by electrons in the s and p orbitals, they are not contracted as much. Practically this means that overall gold, regardless of oxidation state, experiences a contraction of its 6s orbital and relative expansion of its 5d orbitals compared to the other group 11 elements copper and silver (Figure 1-2).[14,15] The consequence of this relative change in size of orbitals is that gold can form very strong bonds with ligands and interacts preferentially with C-C unsaturated bonds due to the improved orbital overlap.

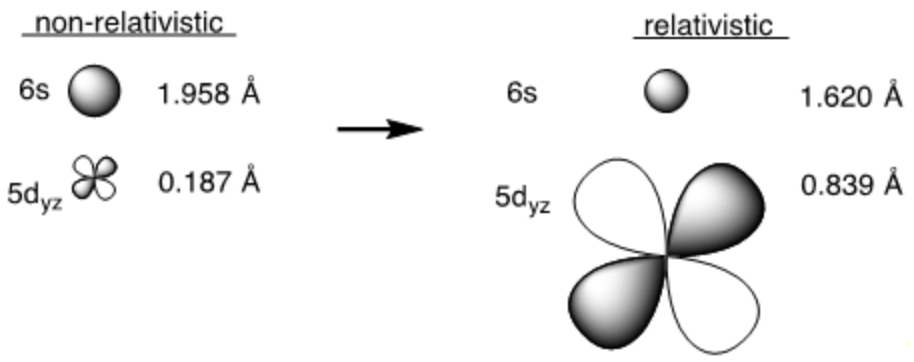

Figure 1-2. Contraction of 6s orbital and expansion of 5d orbitals.

According to the Dewar-Chatt-Duncanson (DCD) model,[16] substrates with π-systems (S) share electrons with π-Lewis acidic metals (M) in two important ways, substrate to metal donation (S → M, or σ-donation) as well as metal to substrate back donation (M → S, or π-back bonding). It was previously believed that when gold (I) interacts with a π-system, the σ-donation is the largest contributing factor to the bond.[17] However, a recent theoretical study by Tarantelli and coworkers showed that the nature of this interaction is based equally on σ-donation and π-back donation for gold (I) chloride.[18] This is directly due to relativistic effects. The result of equally sized contribution between σ-donation and π-back donation is that the interaction does not cause a build up of charge nor does it cause significant distortion of the C-C unsaturated bond typically seen with other metals such as platinum or palladium. It is for this reason that gold (I) catalysis is orbitally controlled rather than charge controlled.

It is also important to note that the degree in which σ-donation and π-back donation plays a role in bonding depends also upon the electronic and structural nature of the ligand. This was demonstrated when the contribution of π-back bonding was measured for a carbene ligand and was found to be one-half less than that of a chloride

ligand. Electron deficient ligands such as phosphites, fluorine enriched phosphines, and phosphoramidites were not examined. The tunability of π-back donation was also shown in a report from Toste,[19] who showed that NHC-ligated gold complexes were better at stabilizing the carbocation that arises from the metal-catalyzed ring opening of cyclopropenes.

The bond gold (I) makes with ligands has been shown to be markedly strong. In a report from Zank et al.,[20] dimethylsulfide gold (I) chloride (DMSAuCl) is treated with an equivalent of bis[2-(diphenylphosphino)-phenyl]phosphine (TP) to generate the phosphine gold (I) complex (TPAuCl, **1-1**) (Table 1-1). The phosphine to gold bond is 2.32 Å, which is significantly shorter than the silver phosphine bond (2.46Å) shown in the corresponding silver-complex (TpAgCl, **1-2**). This is also due to the change in orbital size caused by relativistic effects. Because the 6s orbital is smaller, it can better overlap with carbene and phosphorous containing ligands in addition to other non-metal elements of the p-block elements.[8] A consequence of this tight bond between gold (I) and phosphine is that gold (I) salts are primarily dicoordinate, linear molecules.[21]

Table 1-1. M-P bond lengths in gold (I) and silver (I) Tp salts.

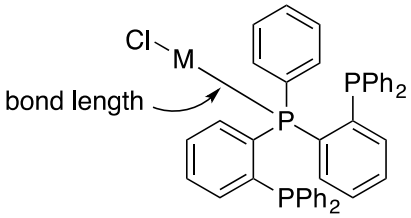

entry	M	length (Å)
1-1	Au	2.32
1-2	Ag	2.46

1.2.2 Common Mechanistic Steps in Homogenous Gold (I) Catalysis.

Commonly, gold (I) is used to catalyze a nucleophilic attack on a π-system. Most gold (I) catalyzed reactions share the same four common mechanistic steps (Figure 1-3 **a-d**). The first step, activation of catalyst (**a**) is usually accomplished through counterion

exchange with a silver cocatalyst. This presumably makes the gold (I) catalyst more cationic since the new counterion is non-coordinating or less coordinating than chloride. The next step is usually coordination to, and activation of the π-system (**b**). This is then followed by nucleophilic attack on the π-system (**c**) in an *anti* fashion. Lastly, regeneration of the cationic catalyst (**d**) allows the catalytic cycle to begin again. This last step is most commonly accomplished by protodeauration but can also occur in other ways. Each of these steps is greatly affected by ligand effects which will be discussed at length in the following two sections.

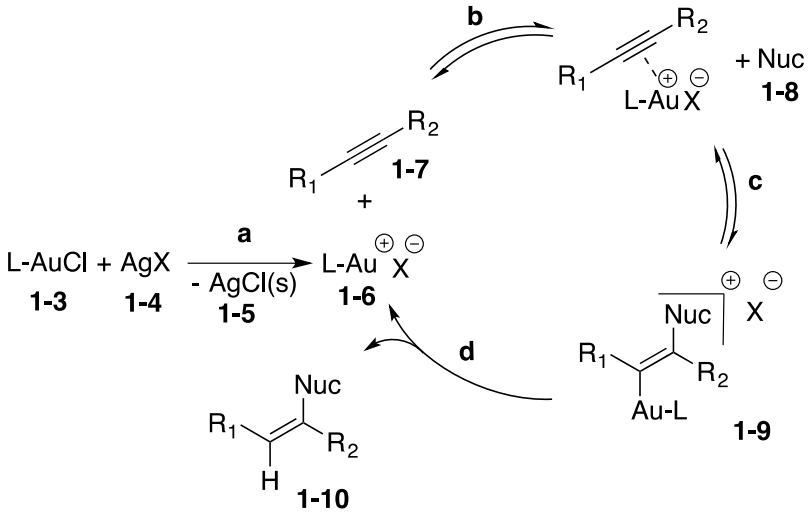

Figure 1-3. Common mechanism for gold (I) catalyzed nucleophilic attack of an alkyne. a) Activation of gold (I) complex. b) Coordination and activation of C-C unsaturated bond. c) Nucleophilic attack of complex **1-8**. d) Protodeauration of complex **1-9**.

1.2.3 Electronic and Steric Effects of the Ligand

It is well known that the reactivity of transition metals is greatly altered by ligands. In a recent report from Wang,[22] common phosphorous and NHC-ligands in gold (I) catalysis were categorized into one of four groups depending upon their effect on protodeauration, activation of unsaturated C-C bonds, and catalyst lifetime. This was

accomplished by measuring the rates of these three steps through ^{31}P-NMR. The results were then compared by ligand.

To measure the rate of protodeauration, a series of complexes (Figure 1-4,**1-11 a-f**) were first made between a gold (I) catalyst and a substrate beforehand. The complex was then treated with trifluoroacetic acid to promote protodeauration. The percent conversion was measured over time by NMR. To measure the rate of activation of a C-C unsaturated bond, the same NMR technique was used to observe the formation of a gold (I) cation-substrate complex over time. This was done with a series of gold (I) cations (Figure 1-5, **1-13 a-f**) that varied by ligand.

Catalyst lifetime was also measured similarly by treating a series of catalysts (Figure 1-6, **1-13 a-f**) with 10 equivalents of an alkyne (**1-17**) and observing the formation of twice ligated gold (I) complex (Ln_2Au^+, **1-19**) which comes about by transmetallation between two of the same catalyst species. The byproduct of this reaction is gold (0), which precipitates out of solution.

It was observed that the rate of protodeauration is favored when the ligand is electron donating (Figure 1-4). The fastest results came from an NHC-ligand (**I**) while the slowest by a wide margin came from an electron deficient, fluorinated phosphine ($(p\text{-}CF_3\text{-}C_6H_4)_3P$). Sterics were also shown to play a role in this as bulky Buchwald-type ligands also showed higher rates of reactivity (**II,** and **III**). These ligands typically feature a biphenyl phosphine, which has been shown to interact with the gold metal center remotely at the biphenyl moiety. This interaction changes the P-Au-C bond angle from about 180˚ to about 169˚.[23] However, bulky ligands that did not have a biphenyl phosphine were slower than their counterparts.

The rate of C-C unsaturated bond activation was favored by ligands that are electron withdrawing, although by a much smaller extent than what is seen in protodeauration (Figure 1-5, **II** vs. (p-CF_3-C_6H_4)$_3$P). This is probably due to the fact that all gold (I) species can activate C-C unsaturated bonds due to relativistic effects, regardless of electron donating or withdrawing ability of the ligand.

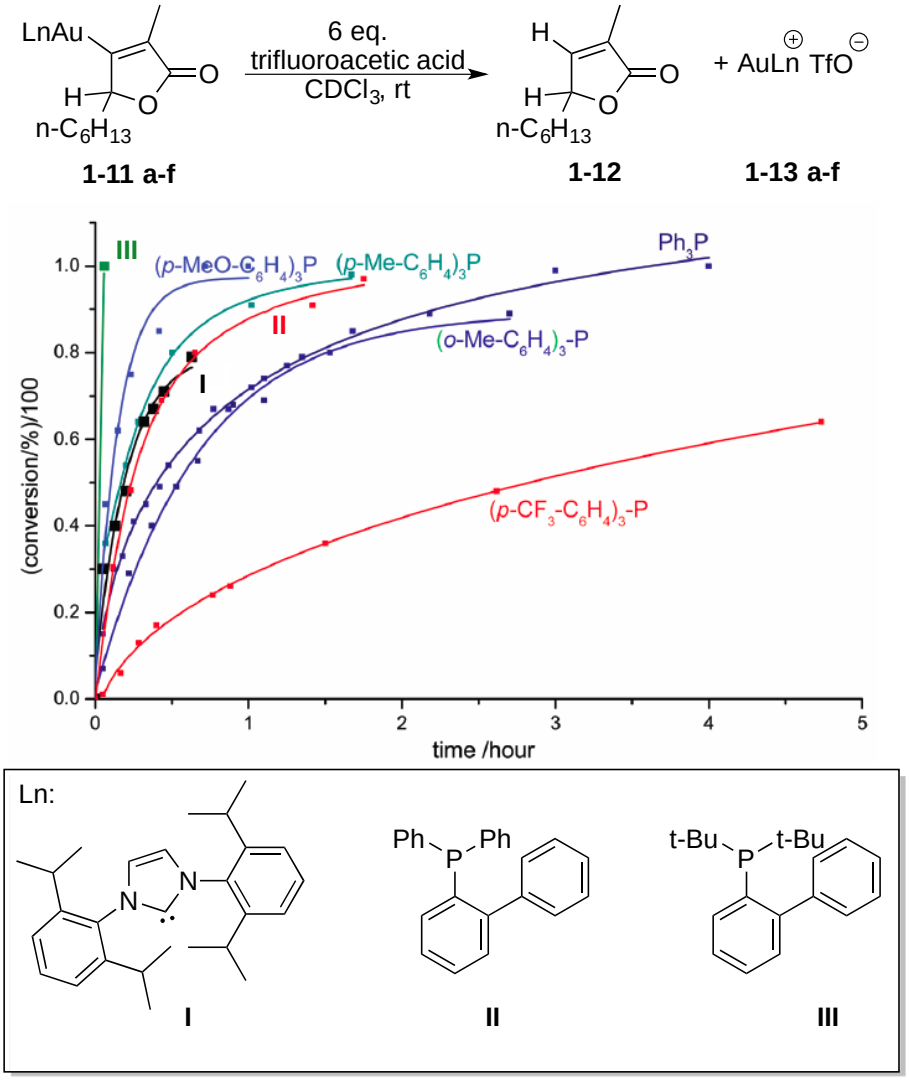

Figure 1-4. Rates of protodeauration of common ligands in gold (I) catalysis. Reprinted with permission from Wang W.; Hammond, G. B.; Xu, B. *J. Am. Chem. Soc.* **2012**, *134*, 5697-5705. Copyright 2012 American Chemical Society.

Catalyst lifetimes were found to be prolonged by increasing bulk about the metal center (Figure 1-6). Particularly ligand **II**, which features a biphenyl moiety was shown to have very little decomposition over 250 hours. This compares favorably to the other tested symmetric triarylphosphines, which were shown to lose active catalyst (**1-13**) within 24 hours.

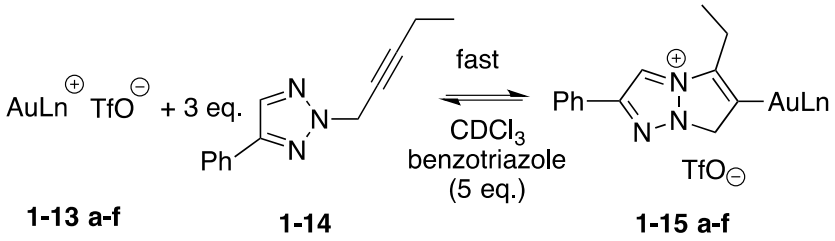

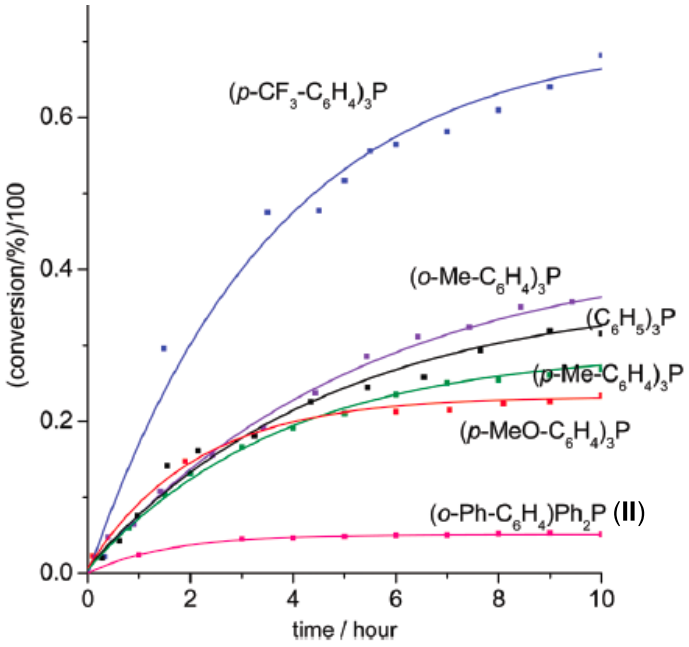

Figure 1-5. Rates of C-C unsaturated bond activation of common ligands in gold (I) catalysis. Reprinted with permission from Wang W.; Hammond, G. B.; Xu, B. *J. Am. Chem. Soc.* **2012**, *134*, 5697-5705. Copyright 2012 American Chemical Society.

In addition, the electronic nature of the ligand is also responsible for affecting the Lewis acidity of transition metal complexes. This is due to the polarization of metal-ligand bond orbitals.[24] This is especially true in gold (I) catalysis where the ligand-metal-

substrate bond is linear. When a given transition metal is ligated to an electron withdrawing ligand, its Lewis acidity is increased.[25] However, due to relativistic effects of gold, it is always π Lewis acidic (or soft Lewis acid), but when an electron withdrawing ligand is present on a gold (I) catalyst then it becomes a hard Lewis.

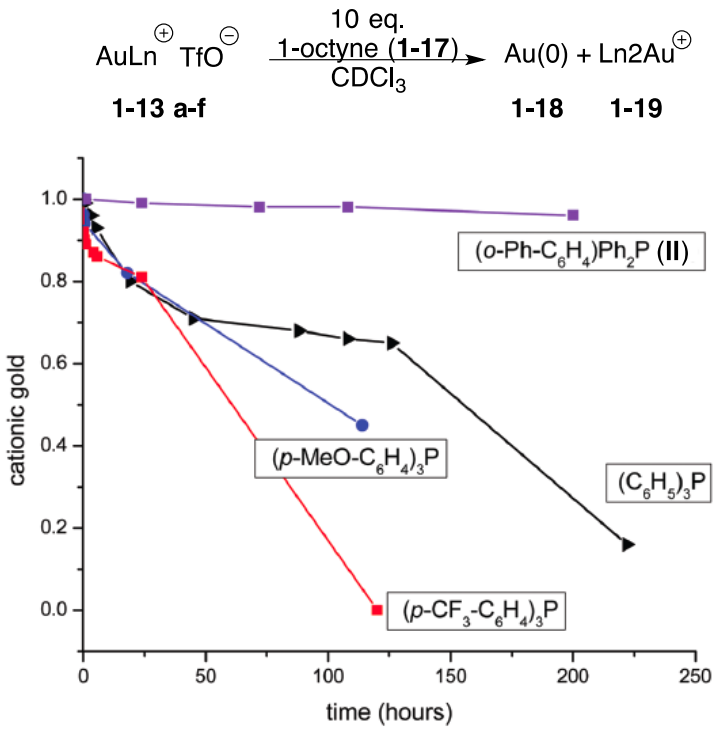

Figure 1-6. Catalyst lifetimes of common ligands in gold (I) catalysis. Reprinted with permission from Wang W.; Hammond, G. B.; Xu, B. *J. Am. Chem. Soc.* **2012**, *134*, 5697-5705. Copyright 2012 American Chemical Society.

It is somewhat novel for a Lewis acid to be both hard and soft Lewis acidic.[26] Classical Lewis acids are typically hard acids, favoring coordination with a lone pair rather than a π bond. Examples include titanium, boron, and cerium. Gold complexes however, are among a relatively new class of Lewis acids that can be both hard and soft Lewis acidic. Other examples include platinum, palladium, copper, mercury, and silver complexes.

For example, gold (I) chloride has been shown to be both hard and soft Lewis acidic but triphenylphosphine gold (I) trifluromethanesulfonate [(Ph_3P)AuOTf] is shown

to be only soft Lewis acidic.[26] When the latter catalyst system was mixed with a stoichiometric amount of benzaldehyde, benzamine, phenylacetylene, and styrene, the resulting complexes formed crystals and were subjected to x-ray analysis. These x-ray data are shown in Figure 1-7. When mixed with benzaldehyde, this gold catalyst is shown not to coordinate with the oxygen atom of the aldehyde. Instead, it only coordinates with the nitrogen of the benzamine, and the C-C triple bond of phenylacetylene. This example demonstrates the dichotomy in the Lewis acidity of gold complexes. They can be either soft Lewis acidic or both hard and soft Lewis acidic by selecting the appropriate ligands and counter anion.

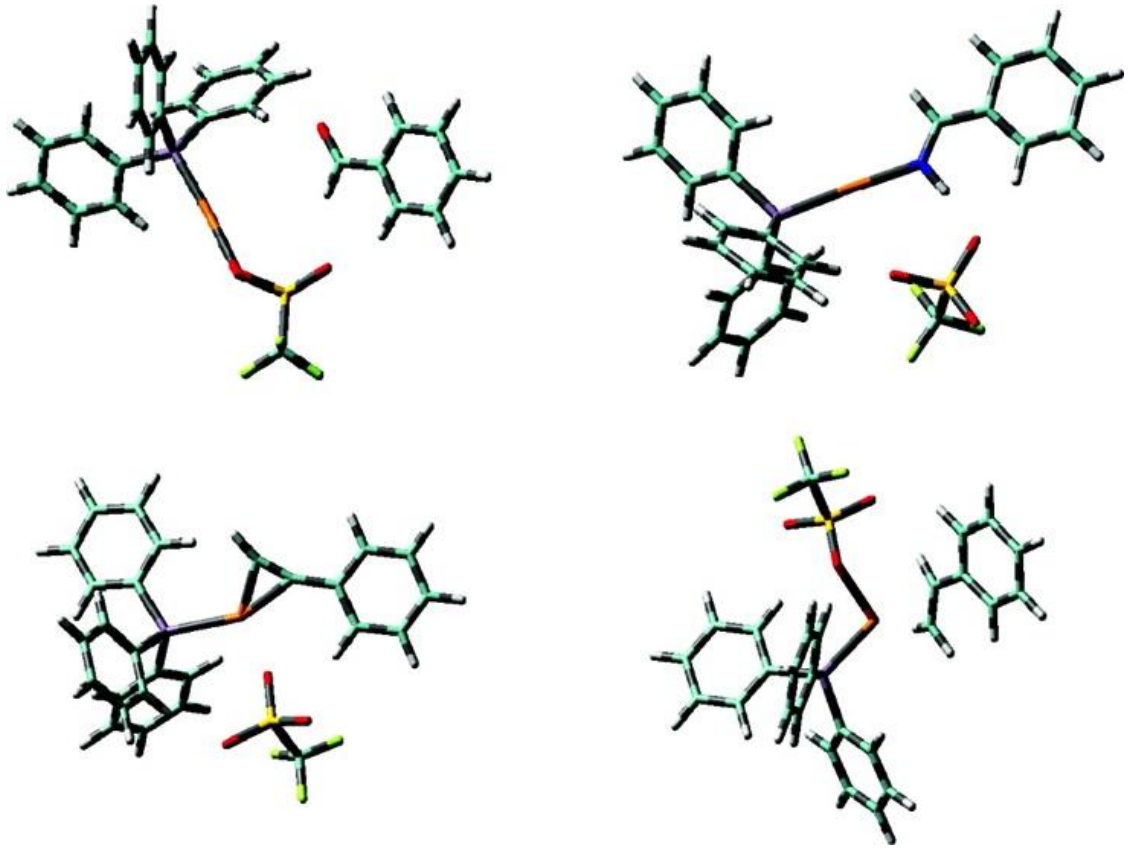

Figure 1-7. Optimized structures (B3LYP/SDD) of the complexes of $(Ph_3P)AuOTf$ with benzaldehyde (upper left), benzamine (upper right), phenylacetylene (lower left), and styrene (lower right). Gold (orange), phosphorous (violet), oxygen (red), nitrogen (blue), fluorine (green), sulfur (yellow). Reprinted with

permission from Yamamoto, Y. *J. Org. Chem.* **2007**, *72*, 7817-7831. Copyright 2007 American Chemical Society.

1.2.4 Silver Cocatalyst

Activation of a gold (I) catalyst is not always needed, but is widely used for the purpose of increasing the cationic nature of the gold center. This is typically accomplished by mixing a gold (I) chloride species with a silver salt as a cocatalyst because silver is a known chloride scavenger. The end result is the presumed precipitation of silver chloride, and exchange of the counter anion to the gold (I) catalyst. Usually, the new counter anion is selected to be non-coordinating. Examples include trifluoromethansulfonate (triflate, TfO^-), tetrafluoroborate (BF_4^-), hexafluorophosphonate (PF_6^-), and hexafluoroantimonate (SbF_6^-). Although the silver is usually presumed not to be involved in a given gold (I) catalyzed reaction, a recent report has shown it can play a crucial role.[27] In the report from Shi, it was theorized that for any given 'gold-catalyzed' reaction, it could actually be one of three types: true gold catalysis, gold and silver bimetallic catalysis, or silver assisted catalysis.

Wang then classified a number of known gold (I) catalyzed reactions by screening them with only gold, only silver, and with both metals present in solution. The yields for all three tests were subsequently compared. Reactions where 'gold only' yields matched the yields of 'both gold and silver' were deemed to be true gold catalysis. When reaction yields did not match, then one of two scenarios had to be determined. If the 'gold only' yield was less than combined two metals yield, then the reaction was deemed to be silver assisted. If however the 'gold only' and 'silver only' both gave no yields, yet together they gave moderate to good yields; then these were deemed bimetallic. It should be noted that none of the reactions tested were ever observed to be promoted

by silver alone. The authors were able to find multiple working examples of all three reaction classifications thus demonstrating that the role of the silver cocatalysts is inherently more complex than previously thought.

1.3 Applications of Electron Deficient Ligands in Gold Catalysis

In homogeneous gold (I) catalysis, the use of electron withdrawing ligands is much less common than the use of electron donating ligands. This may be somewhat expected considering the above discussion regarding the effect of electron donating ligands on protodeauration. However, by using an electron poor ligand, a change in Lewis acidity occurs which opens the door for the possibility of expanding the reactivity of gold (I) catalysis. Typically, electron poor ligands in homogeneous gold (I) catalysis are fluorinated phosphines however phosphites are known to be more electron deficient than phosphines when coordinated to a metal.

In a review from Tolman, a 'steric and electronic map' of phosphorous ligands is presented (Figure 1-8).[28] In the figure, phosphorous ligands are plotted by Θ (a steric parameter also known as ligand cone angle) versus v (an electronic parameter). The ligand cone angle is determined from x-ray crystal structures to be the apex angle of a cylindrical cone 2.28Å from the center of the P atom to the van der Waals radii of the outermost atoms. If the ligand is not symmetric, then the ligand cone angle is determined by an equation, which minimizes the sum of half-angles. The electronic parameter, v is measured from the absorbed IR frequency that corresponds to the C-O triple bond mode of vibration that is observed in $Ni(CO)_3L$ dissolved in methylene chloride. When the ligand (L) is electron poor, the observed IR frequency increases while the reverse is true for electron rich ligands. If one compares the plots of

triphenylphosphine versus triphenylphosphite, the phosphite is less bulky, but more electron deficient. This trend holds for most phosphites in comparison to phosphines.

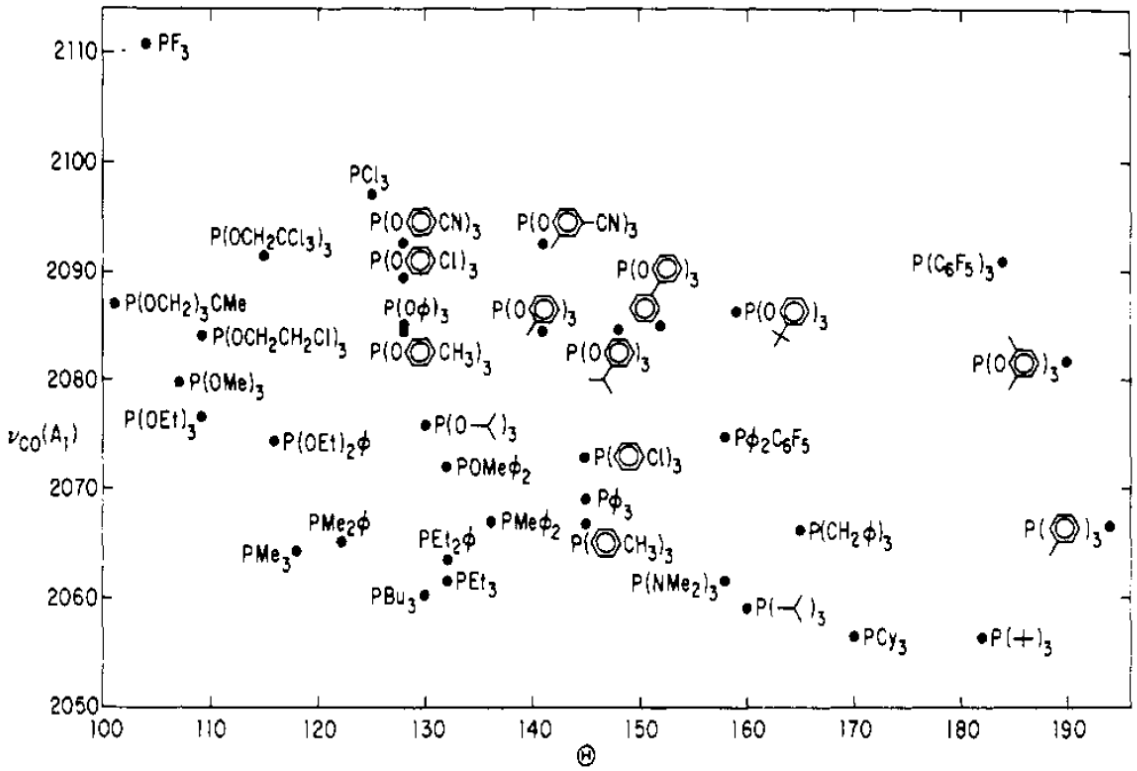

Figure 1-8. Sterics and electron deficiency of various phosphorous ligands. Reprinted with permission from Tolman, C. A. *Chem. Rev.* 1977, *77*, 313-348. Copyright 1977 American Chemical Society.

Below are some examples where electron poor gold (I) complexes were found to better catalyze the transformation than a more electron rich complexes in homogeneous gold (I) catalysis.

1.3.1 C, N, and O nucleophilic attack of non-activated olefins

A report from Tokunaga showed how electron deficient ligands were better able to activate a hydroalkoxylation of a non-activated olefin (**1-20**, Table 1-2).[29] The authors speculated that the electron withdrawing ability of the fluorinated arylphosphine was the reason for the increased reactivity compared to the non-fluorinated triphenylphosphine (entry 1) or even the tri-(4-fluoromethylphenyl)phosphine ($(p\text{-}CF_3\text{-}C_6H_4)_3P$, entry 2).

However, it was unclear to the authors why the addition of extra phosphine made such an improvement on reaction yield (entry 4). This improvement may be due to the extra ligand's ability to improve catalyst lifetime by preventing the formation of gold (0).

Table 1-2. Gold (I) catalyzed hydroalkoxylation of non-activated olefins.

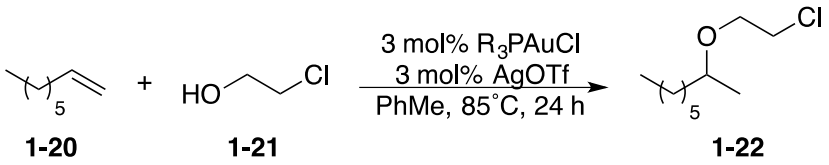

1-20 **1-21** **1-22**

entry	gold catalyst	yield (%)
1	Ph_3PAuCl	54
2	$(p\text{-}CF_3C_6H_4)_3PAuCl$	56
3	$(C_6F_5)_3PAuCl$	79
4	$(C_6F_5)_3PAuCl + P(C_6F_5)_3$	92

In another report on non-activated olefins, a hydroamination is reported by Nájera using very low catalyst loadings (Figure 1-9).[30] Triphenylphosphite was shown to give vastly improved results compared to triphenylphosphine (entries 1 and 2). Because the reactivity was so high in this method, the authors were able to reduce the catalyst loading to as little as 0.01 mol %. When these same conditions were used on non-activated dienes, the reaction did not require heating.

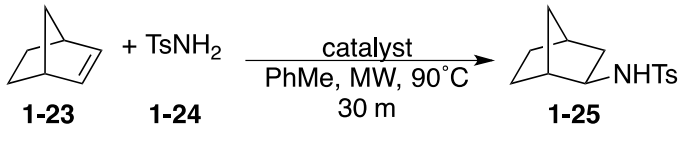

1-23 **1-24** **1-25**

entry	catalyst (mol %)	yield (%)
1	$Ph_3PAuCl/AgOTf$ (0.1)	58
2	$(PhO)_3PAuCl/AgOTf$ (0.1)	99
3	$(PhO)_3PAuCl/AgOTf$ (0.05)	94
4	$(PhO)_3PAuCl/AgOTf$ (0.01)	60

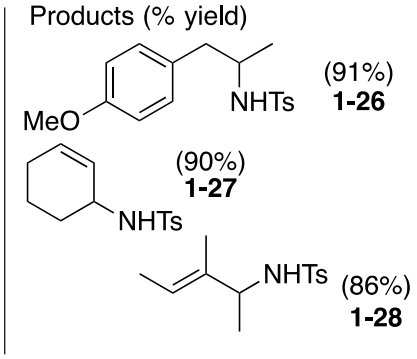

Figure 1-9. Nájera's hydroamination of non-activated olefins by various catalysts and catalyst loadings.

In analogous fashion, Che used triphenylphosphine as a ligand in an earlier report of gold (I) catalyzed hydroamination of non-activated olefins. The nitrogen compounds

were also sulfonamides (Figure 1-10).[31] The triphenylphosphine gold (I) chloride/silver triflate catalyst system had to be run at a significantly higher catalyst loading (100 times as much), higher temperature, and longer reaction time to get similar yields to Nájera's method.

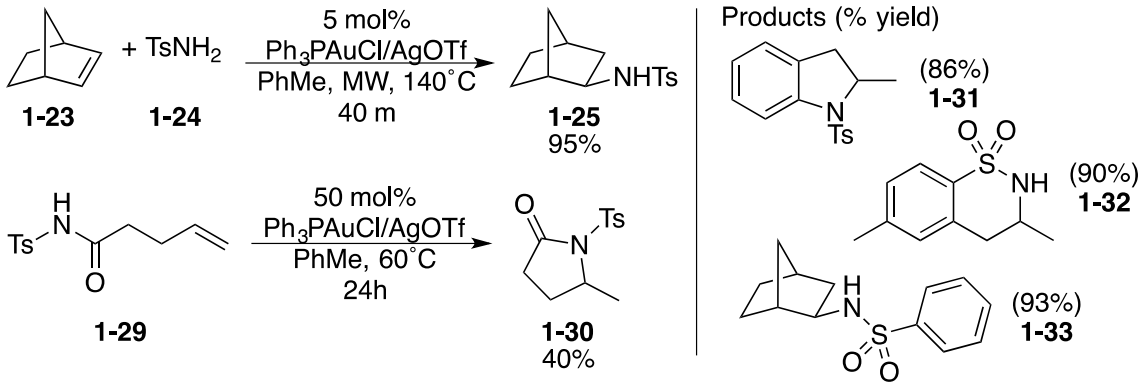

Figure 1-10. Che's hydroamination of terminal olefins by sulfonamides.

Phosphite ligands were also able to show efficacy towards the hydroarylation of allylic alcohols in a report by Bandini and coworkers (Table 1-3).[32] In this example, other ligands were not compared to the phosphite ligand but interesting reactivity was observed nonetheless. The methodology only works for the Z-olefin as the E-olefin led mostly to decomposition. Allylic ethers were shown not to work at all. The authors

Table 1-3. Bandini's hydroarylation of allylic alcohols.

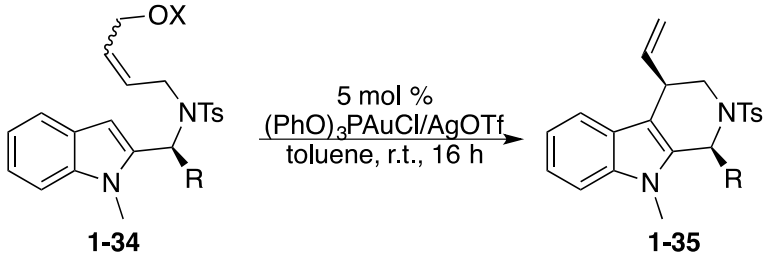

entry	substrate (R/X)	yield (%)	d.r.
1	Z (allyl / H)	88	> 95 : 5
2	E (allyl / H)	-	-
3	Z (Bn / H)	89	> 95 : 5
4	Z (allyl / TBS)	-	-

propose that the free hydroxyl group is hydrogen bonded to the sulfonyl moiety of the sulfonamide which facilitates the dehydrative cyclization on the Z olefin. This is in spite the fact that the hydrogen would have to interact with an oxygen nine atoms away. For a more detailed understanding of leaving groups in gold (I) catalyzed dehydrative cyclizations see selected works from Aponick and coworkers.[33,34]

1.3.2 C and O nucleophilic attack of alkynes.

Echavarren and coworkers found a phosphite ligand (Table 1-4, entry 2) was found to be optimal rather than a Buchwald-type biphenylphosphine or even an NHC-carbene (entries 1 and 6) in the reaction of a tandem enyne cyclization/electron-rich aromatic addition methodology.[35] The reason why an electron withdrawing ligand is favored is unclear. In the mechanism (Figure 1-11), it is believed that the gold cation first activates the alkyne towards nucleophilic attack by the olefin thus cyclizing the substrate to a five membered ring intermediate **1-40**. The authors then postulate the formation of a fused cyclopropane ring by donating electrons from the gold atom to form a carbenoid **1-41**. However, this step must be reversible which sets up an interesting equilibrium. If the gold (I) catalyst has an electron donating group attached, then the forward direction must be favored and thus giving rise to the cyclopropane, gold carbenoid **1-41**. When the nucleophile attacks, it attacks the carbenoid giving rise to product **1-38b**.

On the other hand, if the ligand is electron withdrawing and the R group is electron rich then the reverse direction must be favored. This gives rise to a secondary carbocation (Figure 1-11, **1-40**) that can then be subsequently attacked by the nucleophile, giving rise to product **1-38a**. This would seem to indicate that electron deficient ligands do not favor formation of gold carbenoids thus pushing the equilibrium

towards the carbocation **1-40**. However, it has been shown that these ligands do in fact form stronger Au-C carbenoid bonds than electron rich ligands.[23] This poses an interesting question and should be examined more thoroughly.

Table 1. Echavarren's tandem cyclization/nucleophilic ring opening.

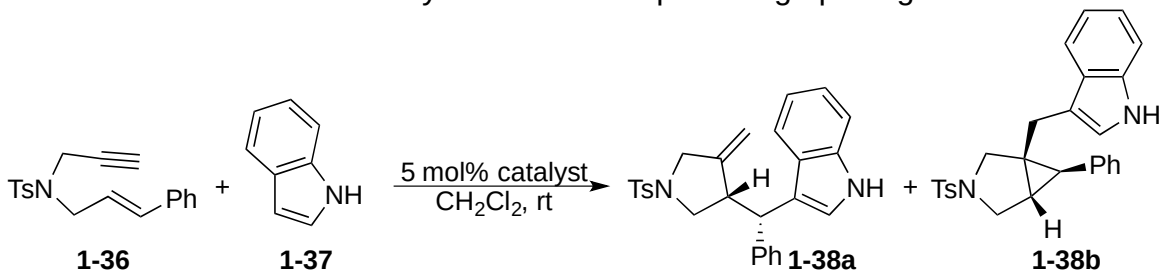

entry	catalyst	time	product (ratio)	yield (%)
1	**IV**	1	a + b (4 : 1)	74
2	**V**/$AgSbF_6$	1	a + b (10 : 1)	68
3	**V**	60	-	-
4	AuCl	192	-	-
5	$AuCl_3$	192	-	-
6	**VI**/$AgSbF_6$	19	a + b (0.8 : 1)	72
7	$AgSbF_6$	60	-	-

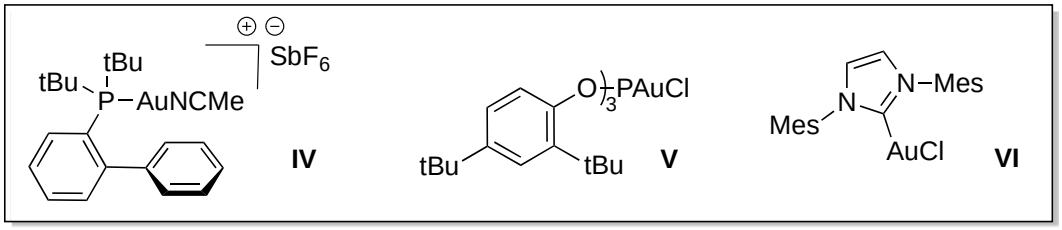

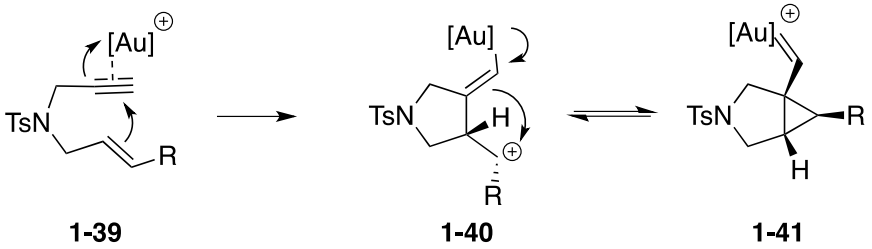

Figure 1-11. Proposed mechanism for the tandem enyne cyclization/nucleophilic attack.

In a report from Toste, a fluorinated arylphosphine ligand was found to be superior to triphenylphosphine in the synthesis of indenyl ethers from alkynes.[36] In fact, Ph_3PAuCl gave no reaction, while (p-CF_3-C_6H_4)$_3$PAuCl/$AgBF_4$ was shown to give 81%

yield. Interestingly, the methodology was even shown to transfer chirality with little loss of ee (Table 1-5, **1-42** into **1-42**).

Table 1-5. Synthesis of indenyl ethers from alkynes.

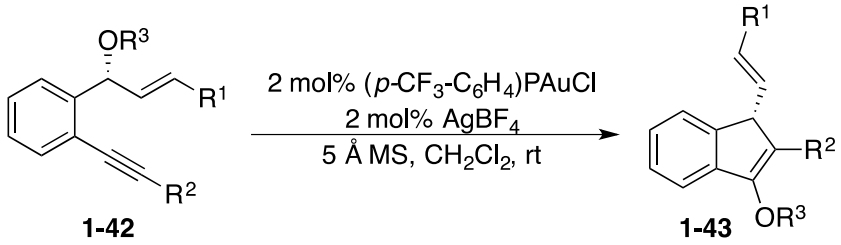

1-42 **1-43**

entry	substrate	yield (%)	ee (%)
1	R^1=Ph, R^2=CO_2CH_3, R^3=CH_3 (82% ee)	99	81
2	R^1=H, R^2=Ph, R^3=CH_3 (99% ee)	92	95
3	R^1=Ph, R^2=CO_2CH_3, R^3=allyl (73% ee)	92	59

1.3.3 Cycloadditions and C, O nucleophilic attack of allenes.

Phosphites have also been shown by Gagne and coworkers to activate allenes towards intramolecular hydroarylation by electron rich aryl groups (Figure 1-12).[37] Initially, the authors used an electron rich BINAP-type phosphine ligand which was shown to achieve full conversion after 16 hours. The phosphite ligand was shown to work in 6 hours for near full conversion. This methodology was later extended to an intermolecular variant using the same catalyst system.[38]

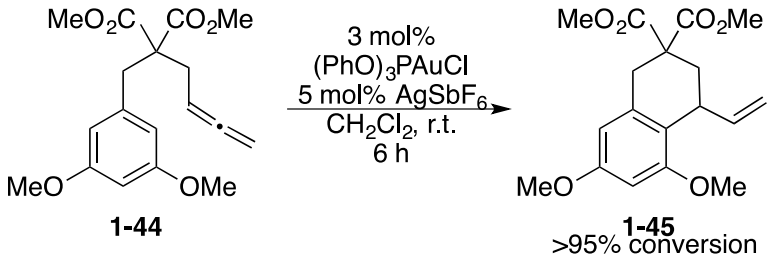

1-44 **1-45**
>95% conversion

Figure 1-12. Gagne's intramolecular hydroarylation of allenes.

In another example, phosphites were again shown to be more reactive than electron rich NHC ligand. González and coworkers[39] were able to furnish the intermolecular [2 +2] cycloaddition of N-allenylsulfonamids with enol ethers and

styrenes with as little as 0.5 mol% catalyst loadings at room temperature in just 5 minutes (Figure 1-13). The methodology also applied to allenylsilylethers with enol ethers. In the same report, the authors were even able to dimerize the N-allenylsulfonamides by adding a catalytic amount of norbornene.

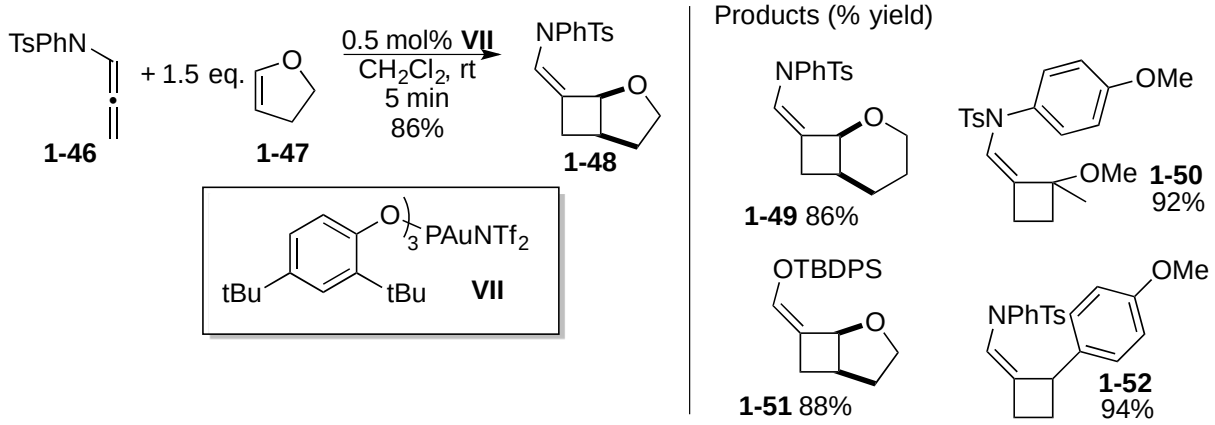

Figure 1-13. Intermolecular [2 + 2] cycloaddition of N-allenylsulfonamides with enol ethers.

A phosphite ligand was also shown to work best in the cascade cyclization of allenylepoxides from Gagné (Figure 1-13).[40] In this example, the authors believe that gold first coordinates to the allene which activates it towards nucleophilic attack by a pendant epoxide. But because the epoxide is also an electrophile, the ring opening was made into a cascade by attack by another epoxide. However, another plausible mechanism would have the gold (I) catalyst first coordinating to an epoxide, which is

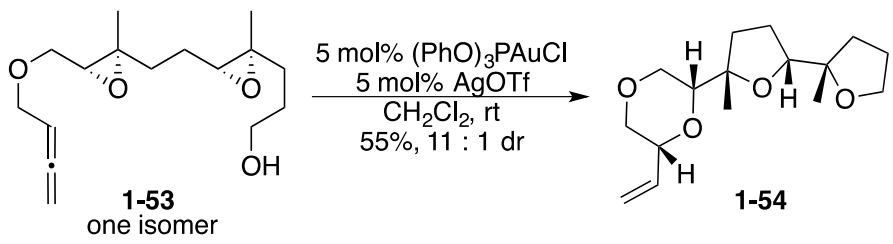

Figure 1-14. Gagne's cascade cyclization of allenylepoxides.

then attacked by a pendant alcohol to make the first tetrahydrofuran. The resulting intermediate can then continue to cascade down the backbone to lastly cyclize with the pendant allene resulting in **1-54**.

In an extremely rare instance in gold (I) catalysis, the choice of the ligand was shown to actually change the outcome of a gold (I) catalyzed reaction as reported by Toste (Figure 1-15).[41] It was found that when 5 mol% $Ph_3PAuCl/AgSbF_6$ catalyst was used, a mixture of both cycloadducts (**1-56** and **1-57**) were formed in 2:1 ratio in favor of the [4 + 2] product **1-56**. However, when a phosphite ligand (**VIII**) was used, only the [4 + 2] product is observed. In addition, if an electron rich ligand such as a Buchwald-type (**IX**) ligand is used – then the [4 + 3] product **1-57** is almost exclusively formed over the [4 + 2] in ratio of 96:4.

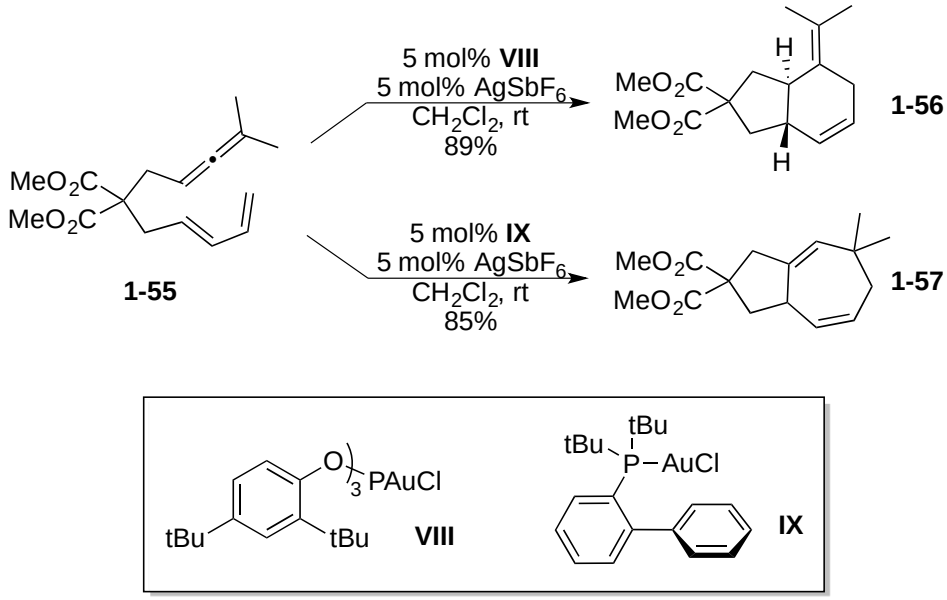

Figure 1-15. Ligand controlled access to [4 + 2] or [4 + 3] cycloadditions of allenyldienes.

The reason for this difference in products is believed to stem from a single intermediate **1-58** (Figure 1-16). This intermediate comes about from a [4 + 3]

cycloaddition that can then either undergo a 1,2-hydride shift or a 1,2-alkyl shift depending upon the nature of the ligand bound to gold.

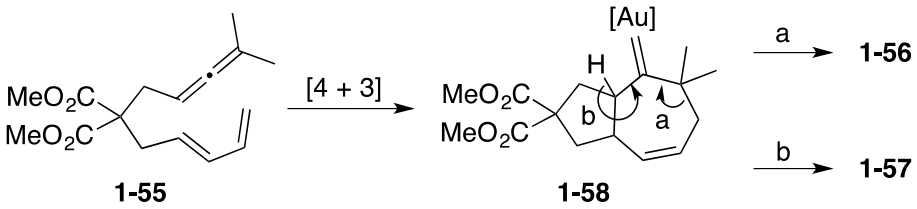

Figure 1-16. Proposed common intermediate between products **1-56** and **1-57** resulting from arrow a or b.

In a study,[23] it was found that this bifurcation of mechanism comes from both the electronic and steric nature of the ligand. In the study, Toste and Goddard compared three ligands; PPh_3, $P(OPh)_3$, and $P(t\text{-}Bu)_2(o\text{-}biPh)$ to find that all three were shown to have about the same activation barrier for an alkyl shift of 6.1, 6.0, and 5.7 kcal/mol respectively for $[AuP(t\text{-}Bu)_2(o\text{-}biPh)]^+$, $[AuP(OPh)_3]^+$, and $[AuPPh_3]^+$ cations. Therefore, all three of these ligands should be capable of undergoing [4 + 2] cycloaddition.

The key to the bifurcation of mechanism therefore lies in the difference of each ligand's ability to facilitate the 1,2-hydride shift. The bond angle between P-Au-C is about 169˚ in the $[AuP(t\text{-}Bu)_2(o\text{-}biPh)]^+$. This is due to a remote steric interaction of the biphenyl moiety with the gold metal center. Because this angle is significantly different from 180˚, the Au 5d orbital electrons have less overlap with the C sp^2 π-orbitals and thus the gold carbenoid has more carbene character than a carbenoid stabilized by a gold cation with a symmetric ligand (i.e. PPh_3 or $P(OPh)_3$). This then favors a 1,2-hydride shift over an alkyl shift and is in agreement with the calculated activation barriers. The hydride shift of a free carbene was found to be 1.3 kcal/mol, while the $[AuP(t\text{-}Bu)_2(o\text{-}biPh)]^+$ was 2.6 kcal/mol, and the $[AuP(OPh)_3]^+$ was 6.9 kcal/mol.

The $[AuP(OPh)_3]^+$ seems to only favor the 1,2-alkyl shift as no [4 + 3] product is ever observed. This appears to be due to the gold cation's ability to better stabilize the carbene. It has a snap bond energy (which is a type of calculated bond energy) of 92 kcal/mol versus the 78 kcal/mol of the $[AuP(t\text{-}Bu)_2(o\text{-}biPh)]^+$. This increased stabilization polarizes the Au-C bond, thus favoring the 1,2-alkyl shift completely.

Toste followed this work by using electron deficient ligands to do an enantioselective intramolecular [4 + 2] cycloaddition of allenes.[42] After a thorough catalyst screening and conditions optimization, high yields and selectivity were observed at room temperature for cyclization of the dimethylmalonate (Figure 1-17). Even more impressively, the authors report that they were able to recover and reuse the catalyst without degradation to ee.

In the same report, Toste was also able to show that allenyldiene sulfonamides could also work but required the use of another electron deficient, phosphoramidite ligand in higher loading (Figure 1-18). The higher catalyst loading was needed because of the coordinating ability of the nitrogen moiety.

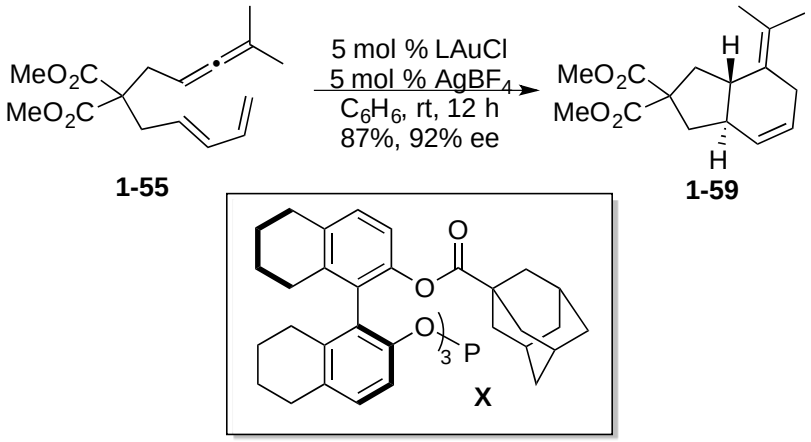

Figure 1-17. Enantioselective [4 + 2] cycloaddition of allenyl-diene malonates.

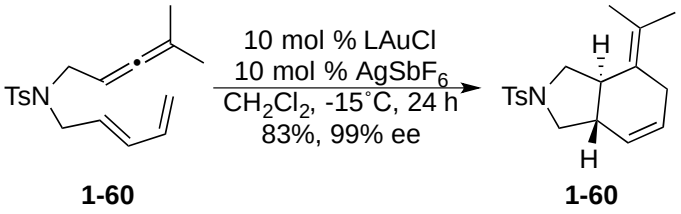

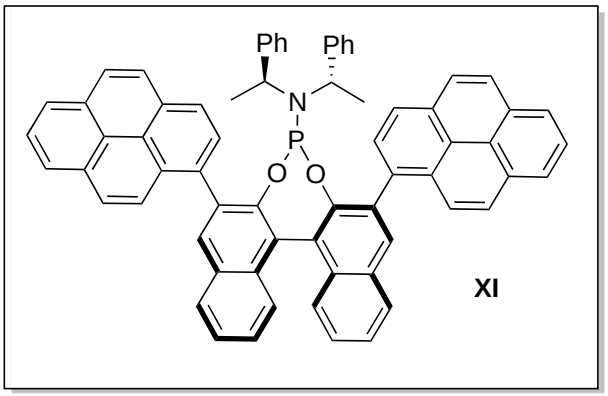

Figure 1-18. Enantioselective [4 + 2] cycloaddition of allenyl-diene sulfonamides.

1.4 Conclusions

From these examples, one can conclude that C, O, and N nucleophilic attack on non-activated alkenes and alkynes can be accomplished by electron rich or poor gold (I) catalysts, but that electron poor catalysts can do so more efficiently in all the above cases. This results in lower catalyst loadings, reaction times, temperatures, and sometimes higher yields. Presumably, this is because of the increased Lewis acidity of the electron poor catalyst, which can better activate the alkene or alkyne towards nucleophilic attack.

Use of electron deficient ligands in gold (I) catalysis remains relatively under explored. However from the examples above, these ligands have been shown to be advantageous and have even led to the development of highly enantioselective catalyst systems. Even more promising is the effect that electron withdrawing ligands have on the Lewis acidity of the gold cation. This phenomenon seems well-suited for allowing a given gold (I) cation to serve as both a σ and π-Lewis acid, and may be able to catalyze

multiple bond forming events in a given reaction – thus harnessing the potential dual activity of the catalyst. This could be a new and unexplored frontier in the vast expanse of reactivity in gold (I) catalysis.

In the following chapters, the dual Lewis acidity of electron deficient ligands in homogeneous gold (I) catalysis is utilized in the tandem hemiacetalization and hemiketalization/dehydrative cyclization of 1,4 and 1,5-monoallylic diols as well as in the cyclization of these same diols into 3,6-dihydro-2H-pyrans.

CHAPTER 2
DIASTEREOSELECTIVE GOLD (I) AND BISMUTH (III) TANDEM HEMIACETAL FORMATION/HYDROALKOXYLATION REACTIONS OF 1,4 AND 1,5-MONOALLYLIC DIOLS TO FURNISH 1,2-DIOXOLANES AND 1,3-DIOXANES

2.1 Introduction

In 2008, Aponick and coworkers reported gold (I) catalyzed dehydrative cyclization of 1,7-monoallylic diols (Figure 2-1, **2-1**) to produce substituted tetrahydropyrans (**2-2**).[43] The method was shown to have tolerance to a wide variety of functional groups and catalyst loadings as low as 0.1 mol% to promote the reaction at room temperature. Interestingly, the catalyst does not appear to be working through a cationic mechanism. When two isomeric substrates (Figure 2-2, **2-3** and **2-4**) were subjected to the same conditions – only **2-3** produced tetrahydropyran **2-5**. Even when diol **2-4** was treated with higher catalyst loading and heating, no reaction was observed. Instead, the reaction appears to undergo the proposed stepwise S_N2' addition and elimination of the gold (I) cation (Figure 2-2). After coordination of the gold (I) cation to the olefin, nucleophilic attack by the pendant alcohol produces intermediate **2-7**. Thereafter, water and gold are eliminated producing product **2-8**. At the time of this report, it was not yet clear how the elimination of water or gold (I) cation took place.

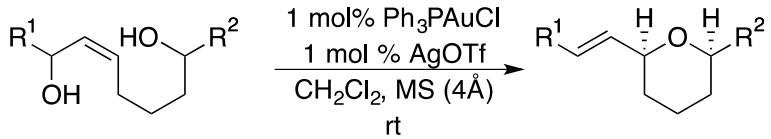

2-1 **2-2**

79-99%, dr up to >25 : 1

Figure 2-1. Diastereoselective dehydrative cyclizations of 1,7-monoallylic diols.

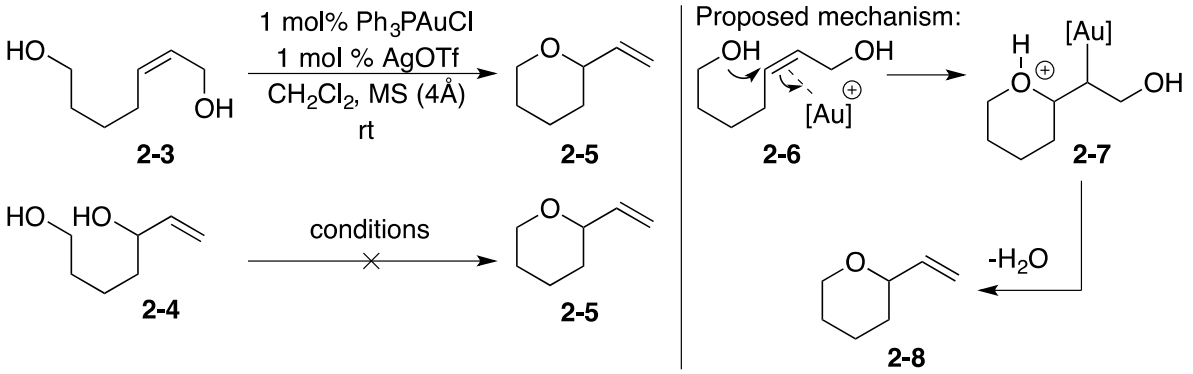

Figure 2-2. First investigation of and proposed mechanism of dehydrative cyclization.

In a subsequent report, Aponick showed that this methodology was also applicable in the transfer of chirality.[44] In fact, it was observed that when the geometry of the allylic alcohol moiety is changed; so too is the stereochemical outcome (Figure 2-3). The transfer of chirality was shown to work on a number of substrates, showing little to no loss of enantiomeric excess (ee).

The most plausible way for chirality to transfer from the allylic alcohol moiety to the newly formed tetrahydropyran without loss of ee is if the gold (I) cation were adding and eliminating in anti fashion to the incoming hydroxyl group. Thus, the proposed mechanism for the methodology was first proposed in greater detail (Figure 2-4). After coordination with the gold (I) cation, the substrate then undergoes nucleophilic attack of the pendant alcohol moiety to the olefin in an anti or syn-fashion to produce intermediate **2-14** or **2-15**. Presumably, this is actually occurring as an anti addition due to the incoming nucleophile encumbering a syn addition pathway.

It was also proposed that in either of these intermediates, **2-14** or **2-15** that formation of **2-16** might be facilitated by a hydrogen bond between the protonated ether and free alcohol moieties. These intermediates then undergo elimination of gold (I) cation and water to furnish the *Z* olefin product **2-17**. Again, if the addition is presumed

to be anti, then the elimination would occur in anti fashion. If this is the true mechanism at work, then it represents a rare example of gold (I) catalysis that does not require protodeauration for the regeneration of catalytic gold (I) cation.[45]

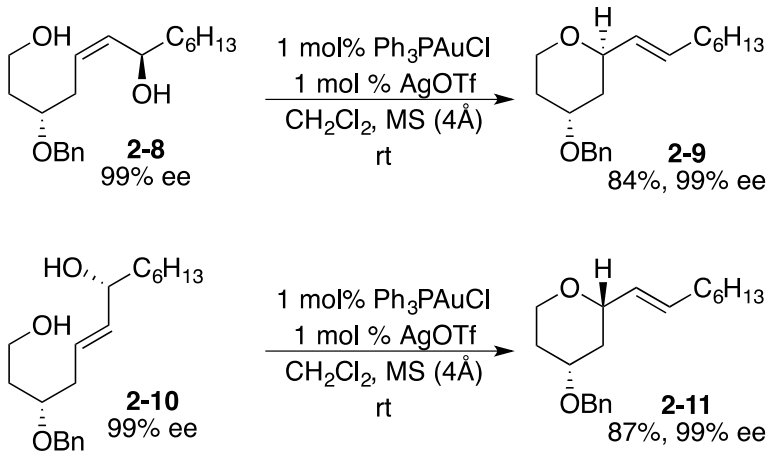

Figure 2-3. Chirality transfer study of dehydrative cyclization methodology.

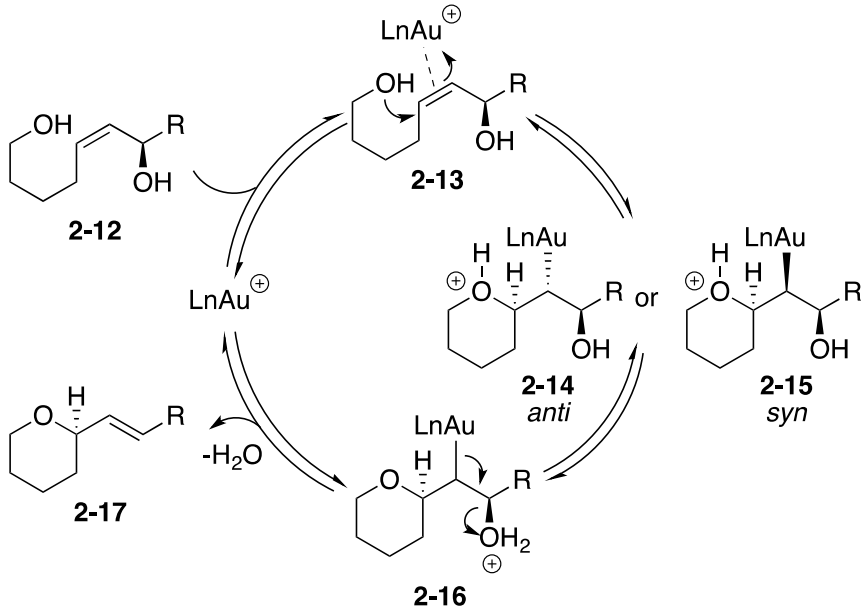

Figure 2-4. Proposed mechanism for the dehydrative cyclization methodology.

To investigate the possibility of hydrogen bonding in the above proposed mechanism, a study was undertaken to investigate the types of leaving groups that this methodology could tolerate.[33] Various allylic ethers were subjected to standard

conditions (Figure 2-5). The rate of the reaction was monitored by gas chromatography (GC) as follows. Aliquots were removed from the reaction and treated with Reaxa Quadrapure™ MPA resin beads. These serve to irreversibly bind the active gold (I) cation catalyst and thereby stop any further reaction progress. The sample was then diluted and chromatographed via GC. Peak area ratios were then used to calculate reaction progress and thus rates of conversion. This was the first report to show this utility of the resin beads.

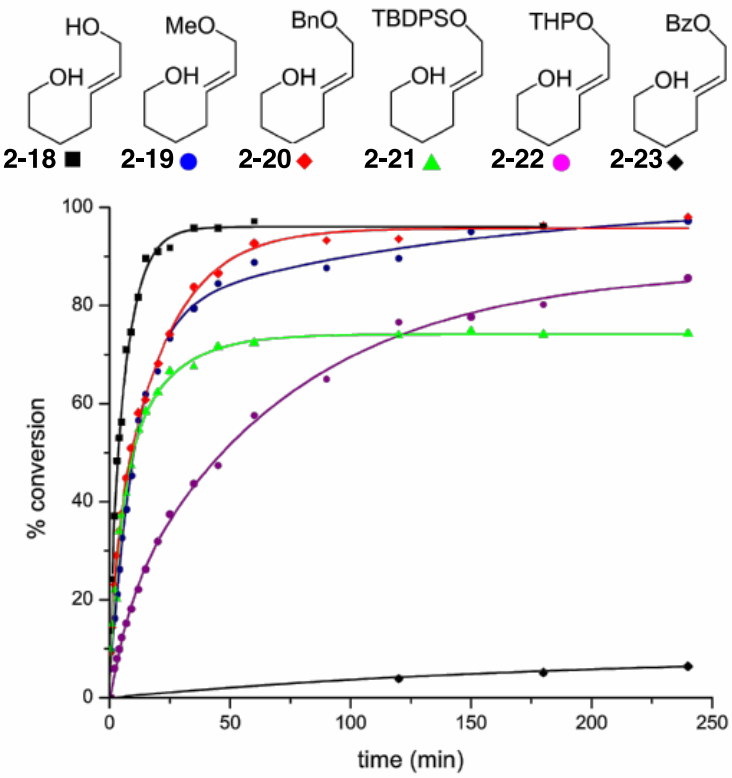

Figure 2-5. Rates of dehydrative cyclization of various allylic ethers.[33]

It was found that a traditional leaving group, such as benzoyl (Figure 2-5, **2-23**) showed very little conversion while poor leaving groups such as hydroxyl, methoxy, and even benzyl (**2-18**, **2-19**, and **2-20**) gave highest conversions. Furthermore, tert butyldiphenylsilyl (TBDPS) ether and tetrahydropyranyl (THP) ether (**2-21** and **2-22**)

also gave good conversion but took longer to reach moderate to good yields. These results give further support for a hydrogen-bonded motif described in the proposed mechanism for this transformation, as the most reactive leaving groups tend to be the best hydrogen bond acceptors.

Finally, full elucidation of the proposed mechanism was achieved through a calculations study.[34] In this last report of the dehydrative cyclization methodology, DFT calculations were performed in collaboration with Ess group. These calculations not only corroborate the stepwise anti-addition/elimination of gold (I) cation, but also show the importance of hydrogen bonding in the dehydrative cyclization.

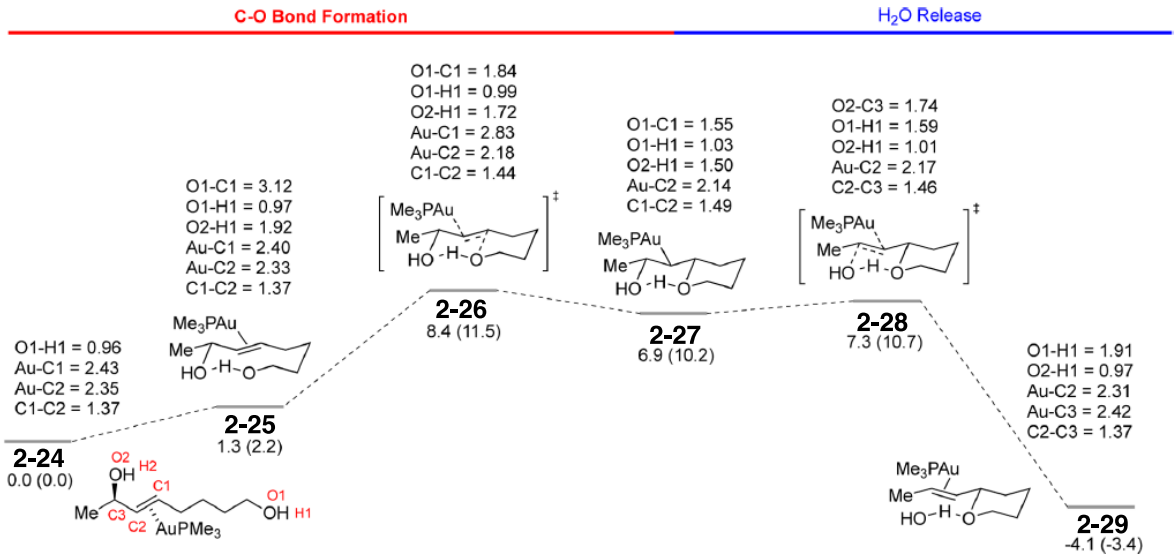

Figure 2-6. The complete enthalpy/free energy reaction coordinate profile gold (I) catalyzed dehydrative cyclization of **2-24** by Me_3PAu^+ cation. Bond lengths are written above each structure while relative energies are given below.[34]

A hydrogen bond was found to occur even before nucleophilic attack of the alcohol on the activated olefin (Figure 2-6, **2-25**). Furthermore, once this hydrogen bond is established, it is very unlikely to break throughout the course of the reaction. This adds rigidity to the complex, thus acting as a trans-decalin-like template for the next steps in the reaction mechanism. After hydrogen bond formation, the mechanism proceeds

through the anti-addition nucleophilic attack of the olefin (**2-26**), followed by proton transfer (**2-27**), then subsequent anti-elimination of gold (I) cation and concomitant elimination of water (**2-28** to **2-29**).

The above dehydrative cyclization methodology was extended into several other methodologies. Aponick and coworkers were able to show a gold (I) catalyzed dehydrative spiroketalization methodology (Figure 2-7 A).[46] Additionally, a gold catalyzed tandem dehydrative cyclization/aromatization (B),[47] and also a gold (I) catalyzed dehydrative cyclization of monoallylic alcohol containing phenols to furnish chromenes (C)[48] methodologies were developed.

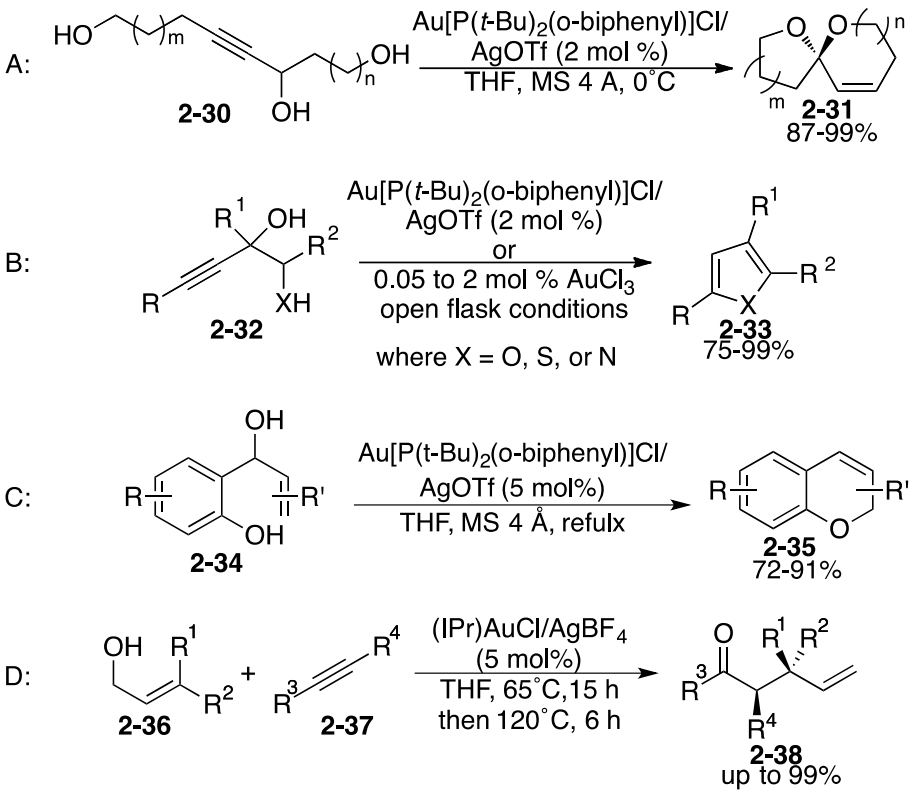

Figure 2-7. Other gold (I) catalyzed dehydrative methodologies from Aponick group.

More recently, Aponick reports a gold (I) catalyzed-tandem intermolecular hydroalkoxylation/Claisen rearrangement (Figure 2-7, D).[49] This is the first report from Aponick that shows a gold (I) catalyzed intermolecular reaction, in this case for the

formation of an enol ether. However, the impetus for studying a tandem hemiacetalization/hydroalkoxylation (this work) was to address this very issue. The original hypothesis was to see if it would be possible to extend the dehydrative cyclization to an intermolecular variant such that the gold (I) catalyst not only served to activate a C-C unsaturated bond, but also to catalyze further bond forming events. In this way, the new methodology would serve to add increasingly complex molecules from very simple ones.

The original hypothesis stemmed from the idea that a monoallylic diol (Figure 2-8, **2-39**) could first attack an electrophile with such functionality as to create a pendant nucleophile that could then undergo subsequent dehydrative cyclization. It was thought that this could best be accomplished by using aldehydes (**2-40**) as these are known to undergo facile hydration to form hemiacetals (**2-41**).[50] Overall, the transformation would produce a protected diol in the form of an acetal.

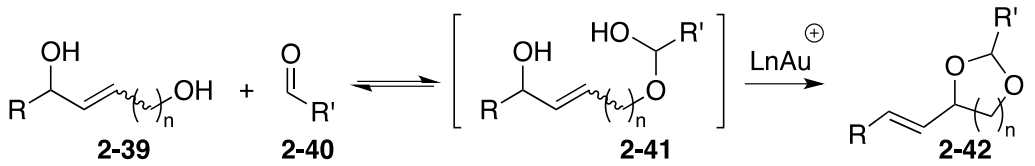

Figure 2-8. Original hypothesis for the formation of protected diols.

To date, no gold (I) catalyzed transformations of this kind have yet been reported. However similar reaction mechanisms or products have been reported as early as 1977. In a report from Bartlett, homoallylic alcohols are functionalized by a process referred to as “phosphate extension.”[51] In the method, the homoallylic alcohol is first converted to a phosphate and then subsequently treated with elemental iodine (Figure 2-9, **2-43** to **2-44**). This new cyclic phosphate (**2-43**) can then be treated with sodium ethoxide to produce epoxide **2-44**.

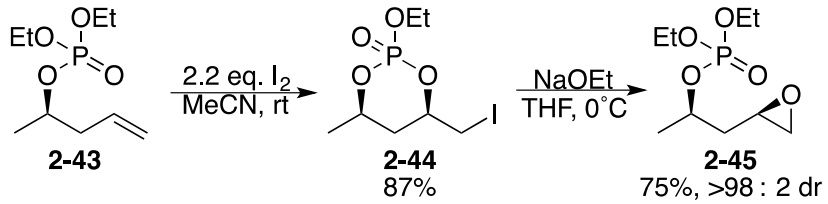

Figure 2-9. Bartlett's phosphate extension methodology.

Unfortunately, the phosphate extension methodology suffers from one drawback. It is very difficult to remove the phosphate via hydrolysis. Instead, Bartlett later found that carbonates were able to undergo the same type of reactivity, yet easily furnish the desired 1,3-diol.[52] This new methodology was referred to as "carbonate extension." Much like before (Figure 2-10), a homoallylic alcohol is converted to the tert butylcarbonate **2-46**, then subsequently treated with elemental iodine to produce the cyclic carbonate **2-47**. The selectivity for the new methodology is not as good as the previous method, but can be easily converted into an array of compounds ranging from various substituted diols to epoxides.

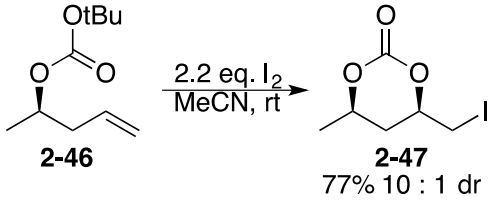

Figure 2-10. Bartlett's carbonate extension methodology.

In 1993, Evans was also interested in the synthesis of protected 1,3-diols for use in macrolide antibiotics.[53] In analogous fashion, homoallylic alcohols were subjected to basic conditions in order to prepare benzylidene acetals **2-49** (and cyclic carbamates **2-51**) via conjugate addition. The method was shown to work in good yields and diastereoselectivities, which is greatly improved from Bartlett's carbonate extension. Interestingly, when p-anisaldehyde was used, the reaction was sluggish, but when p-nitrobenzaldyde was used, the reaction proceeded smoothly to give multiple products.

Aliphatic aldehydes were shown to work, but not with any diastereoselectivity. These observations implicate hemiacetalization may be the rate determining step.

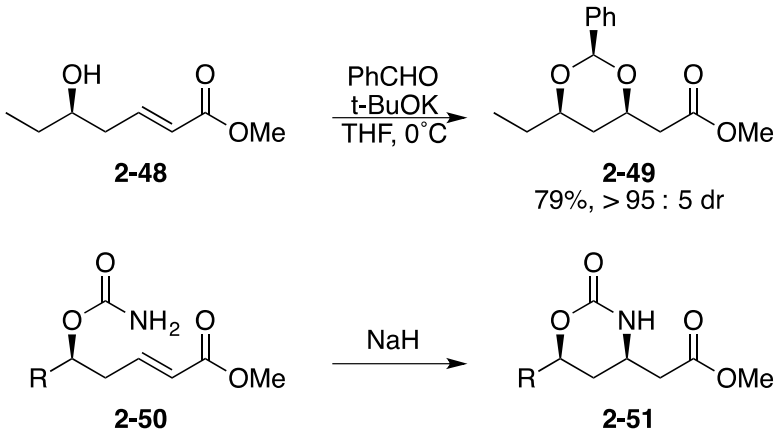

Figure 2-11. Evans diastereoselective synthesis of protected 1,3 diols and carbamates.

The above methodology has since become the standard protocol for formation of syn-1,3-diols in natural product synthesis. As such, the methodology was employed in the formation of many natural products including (+)-roxaticin, leucascandrolide A, cochleamycin A, and (-)-apiclaren A.[54-57] Additionally, the Evan's methodology has been expanded to similar methodologies that differ in substrate and in catalyst, but still undergo the same hemiacetal formation followed by conjugate addition motif.[58-61]

In an entirely different approach, Zakarian reports formation of protected syn-1,3-diols by way of a rhenium catalyzed transposition of allylic alcohols.[62] In the method, 1-5-monoallylic diols (Figure 2-12, **2-52**) are treated with Re_2O_7 and dimethoxy acetals or ketals to furnish the desired acetonide **2-53** or PMP-acetal **2-54**. Though the mechanism is not yet known, the method shows tolerance for a variety of functional groups, however is sufficiently Lewis acidic to deprotect silyl-protected alcohols and preexisting acetals or ketals present in the substrate.

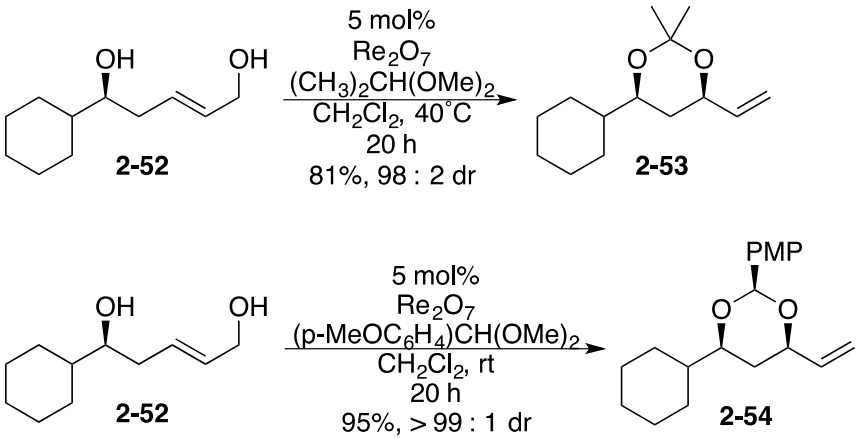

Figure 2-12. Zakarian's transposition of 1,5-monoallylic diols to produce protected syn 1,3-diols.

2.2. Results

To test our hypothesis, the commercially available reagents cis-1,4-butenediol (Figure 2-13, **2-55**), benzaldehyde (**2-56**), and cyclohexane carboxaldehyde (**2-58**) were treated with 5 mol% of **I**/AgOTf. After 36 hours, acetals **2-57** and **2-59** were found on the first attempt of our proposed methodology.

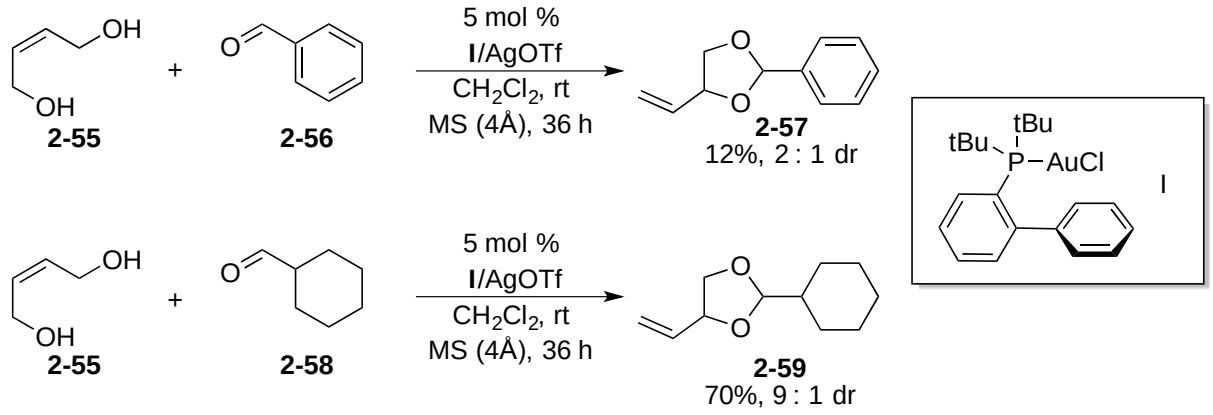

Figure 2-13. First attempt at proposed methodology

2.2.1 Catalyst Screening

We next sought to determine which catalyst was optimal for the transformation (Table 2-1). The best yielding catalysts were found to be gold salt **I**/AgOTf (entry 10) and also the trimeric gold (I) oxonium catalyst (entry 9, $[(Ph_3P)Au]_3BF_4$). However, the best diastereoselectivity came from gold salt **V**/$AgSbF_6$ (entry 12).

Table 2-1. Catalyst screening of various catalysts.

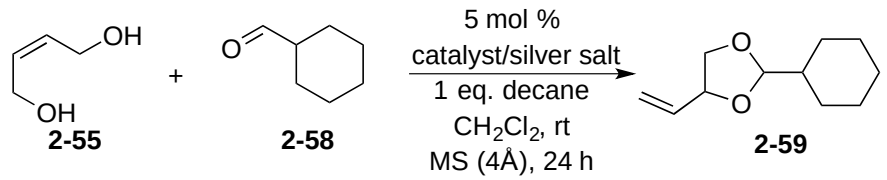

entry	catalyst	silver salt	yield (%)[a]	dr[a]
1	Ph_3PAuCl	AgOTf	36	1:15
2	$Pd(NCMe)_2Cl_2$	-	30	1:1
3	**I**	$AgBF_4$	37	1:11
4	**I**	$AgSbF_6$	43	1:7
5	**II**	$AgBF_4$	45	1:15
6	**III**	$AgBF_4$	60	1:10
7	$Ph_3PAuNTf_2$	-	n.r.	n/a
8	**IV**	**-**	70	1:7
9	$[(Ph_3P)Au]_3OBF_4$	-	92	1:7
10	**I**	AgOTf	92	1:17
11	$AuCl_3$	-	n/a	n/a
12	**V**	$AgSbF_6$	19	1 : >25

[a] Yields and dr measured by GC as compared to decane as an internal standard.

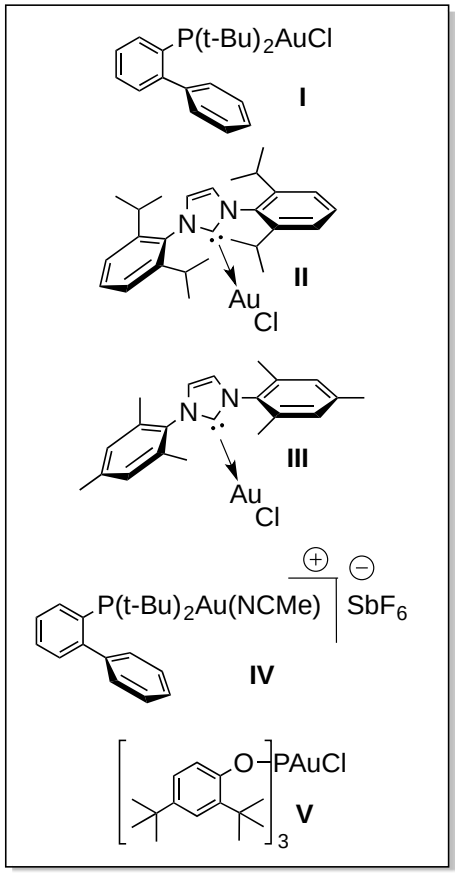

2.2.2 1,3-Dioxolane Conditions Optimization

Before an examination of reaction scope could be conducted, we sought to first determine the best reaction conditions (Table 2-2). For the formation of **2-59**, the best conditions were found in entry 10. Interestingly, increasing the number of aldehyde equivalents decreased the reaction time, thus suggesting that formation of the hemiacetal is the rate-determining step. The cis-diastereomer was found to be the major diastereomer as confirmed by nOe.

Table 2-2. 1,3-dioxolane conditions optimization

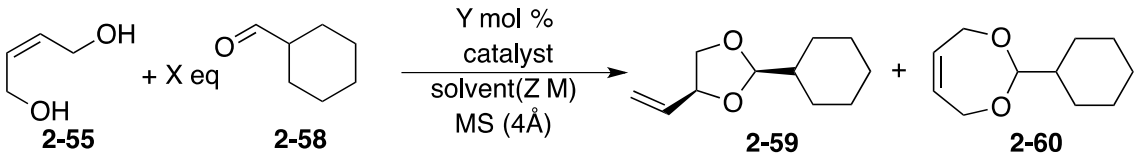

2-55 **2-58** **2-59** **2-60**

entry	X	Y	catalyst	solvent	Z (M)	MS	temp. (˚C)	time (h)	yield **2-59** (%)[a]	*dr*[b]
1	1	5	**I**/AgOTf	CH_2Cl_2	0.2	Y	rt	36	70	1 : 7
2	1.5	5	**I**/AgOTf	CH_2Cl_2	0.2	Y	rt	23	88	1 : 6
3	1.5	2.5	**I**/AgOTf	CH_2Cl_2	0.2	Y	rt	72	78	1 : 6
4	1.5	5	**I**/AgOTf	Et_2O	0.2	Y	rt	22	29	1 : 8
5	1.5	5	**I**/AgOTf	NCMe	0.2	Y	rt	24	n.r.	-
6	1.5	5	**I**/AgOTf	CH_2Cl_2	0.4	N	rt	24	mostly **2-60**	-
7	1.6	5	**I**/AgOTf	CH_2Cl_2	0.8	N	rt	24	mostly **2-60**	-
8	1.5	5	**I**/AgOTf	THF	0.2	N	66	6.5	n.r.	-
9	5	5	**I**/AgOTf	CH_2Cl_2	0.2	N	rt	7	inseperable mixture	-
10	3	5	**I**/AgOTf	CH_2Cl_2	0.2	Y	rt	8	93	1 : 6
11	3[c]	5	**I**/AgOTf	CH_2Cl_2	0.2	Y	rt	8	30	1 : 4
12	3	2.5	**I**/AgOTf	CH_2Cl_2	0.2	Y	rt	23	42	1 : 5
13	3	5	**V**/$AgSbF_6$	CH_2Cl_2	0.2	Y	rt	24	72	1 : 5

[a]Isolated yields. [b]Determined from crude NMR. [c]Freshly distilled.

2.2.3 Aldehyde Scope

Using the conditions found above, various aldehydes were screened. Our results turned out to be exactly opposite of Evans methodology.[53] In fact, branched aliphatic aldehydes not only gave the best yields, but also the highest selectivity (Table 2-3, entries 1-4). Oddly, aromatic aldehydes show little to no reactivity despite the presence of electron donating or electron withdrawing moieties (entries 7-9). Chloral hydrate was found to be the most reactive, but also gave the lowest selectivity (entry 6).

Table 2-3. Aldehyde scope.

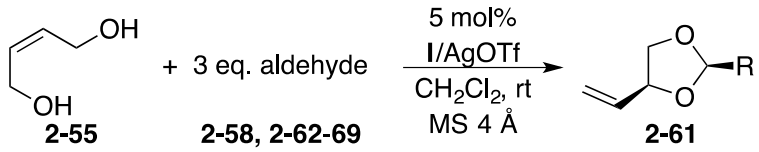

2-55 **2-58, 2-62-69** **2-61**

entry	aldehyde		time (h)	yield (%)[a]	dr[b]
1	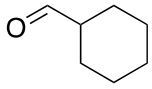	**2-58**	8	93[c]	1 : 8
2	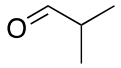	**2-62**	8	80	1 : 8
3	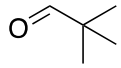	**2-63**	24	70	1 : 18
4	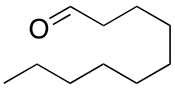	**2-64**	1	81[c]	1 : 3
5	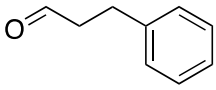	**2-65**	7	68[c]	1 : 5
6	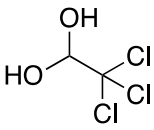	**2-66**	8	98	2 : 3
7	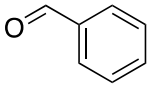	**2-67**	21.5	55[c]	1 : 2
8	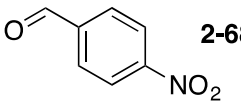	**2-68**	7.5	< 3	-
9	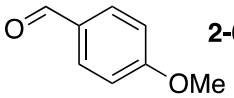	**2-69**	24	n.r.	-

[a] Isolated yields. [b]Determined by ^{1}H-NMR. [c]Purified by reduction of excess aldehyde using $NaBH_4$.

2.2.4 Synthesis of 1,5-Monoallylic Diols

In order to determine the substrate scope, diols were prepared in one of two general methods (Figure 2-14). The first method involves an alkynylation of an aldehyde to produce propargylic diols **2-71**. This is usually done without protecting the alkynyl alcohols **2-70**. The propargylic diols are then reduced to 1,5-monoallylic diols by either LAH or Lindlar reduction to afford the corresponding E or Z olefin **2-72**. Alternatively, isomeric 1,5-diols that have a primary allylic alcohol moiety **2-75** were made via allylation with a Grignard reagent to produce homoallylic alcohols **2-74**. This was followed by metathesis with crotonaldehyde and subsequent reduction with sodium borohydride ($NaBH_4$).

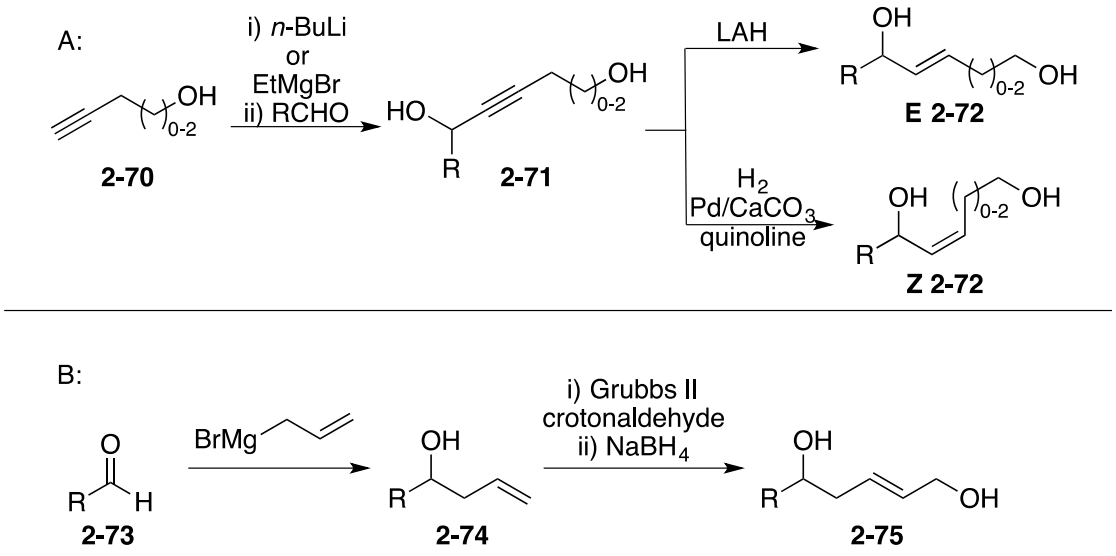

Figure 2-14. General synthesis of 1,5-monoallylic diols.

The first set of diols were prepared as described above. Diol **E 2-55** was made via the lithium aluminum hydride (LAH) reduction of diol **2-76** which was furnished in 70% (Figure 2-15). 1,5-monoallylic diols **E 2-79** and **Z 2-79** were prepared over two steps in

69% and 58% respectively. Isomeric 1,5-monoallylic diol **2-82** was produced in 9% over three steps.

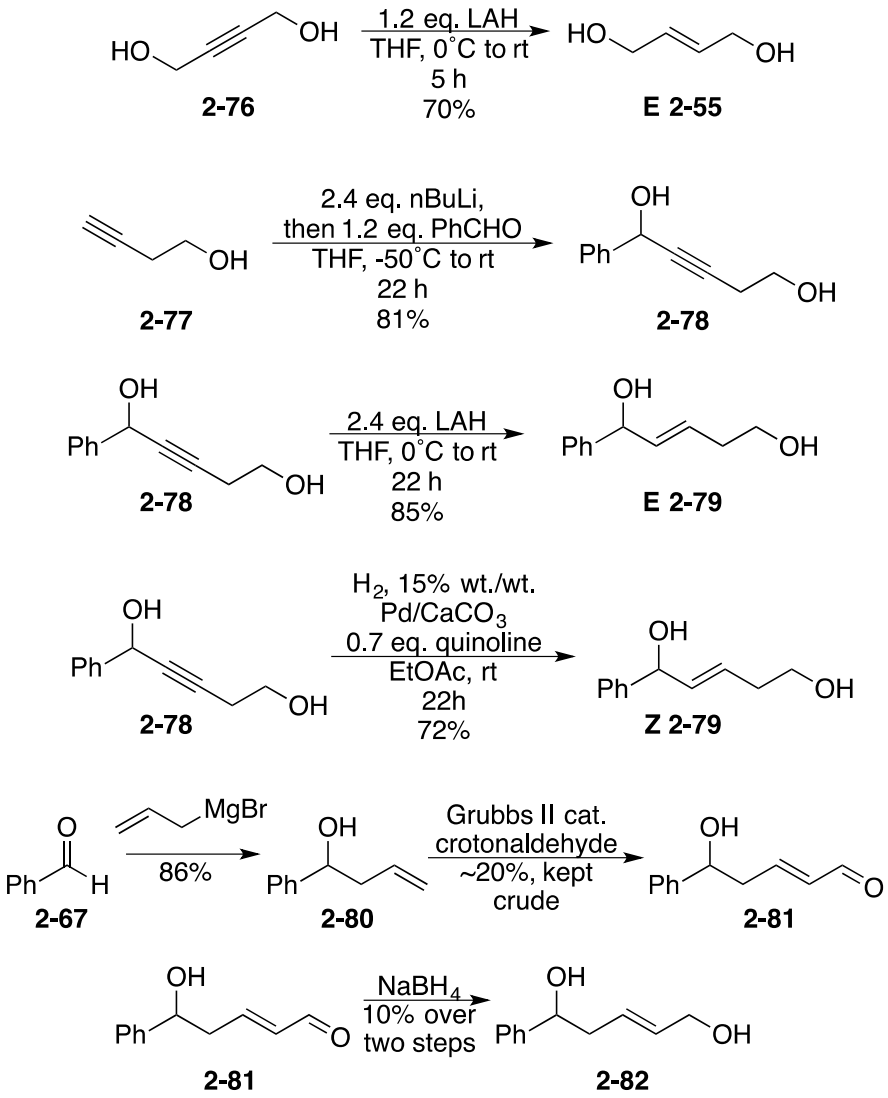

Figure 2-15. Synthesis of 1,5-monoallylic diols.

2.2.5 Diol Scope

Application of the standard conditions found above on an initial diol scope found no reactivity (Table 2-4). It seemed that the conditions optimized for the formation of 1,3-dioxolanes from cis-butene-1,4-diol **z 2-55** would need to be completely changed to furnish the desired reactivity on other substrates. It was thought that investigating

Brønsted acid additives such as camphor sulfonic acid (CSA) or p-toluene sulfonic acid (pTSA) could help. Also, an entirely new catalyst perhaps needed to be considered.

Table 2-4. Initial diol scope.

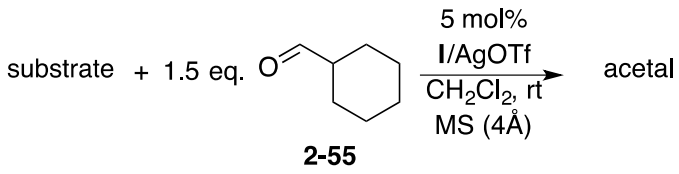

entry	substrate		acetal		yield (%)	time (h)
1	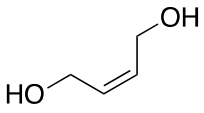	**Z 2-55**	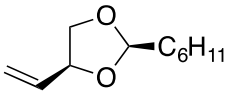	**2-59**	92[a]	92
2	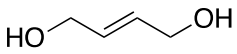	**E 2-55**	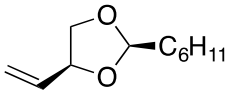	**2-59**	n.r.	n.r.
3	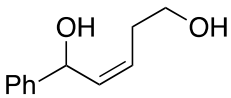	**Z 2-79**	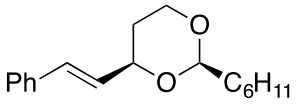	**2-83**	n.r.	n.r.
4	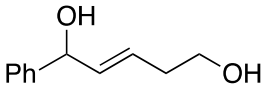	**E 2-79**	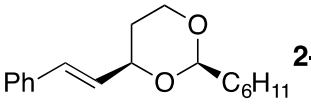	**2-83**	n.r.	n.r.
5	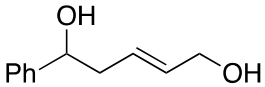	**2-82**	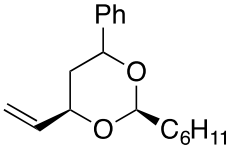	**2-84**	n.r.	n.r.

[a] Isolated yield.

Other metal salts are known to catalyze dehydrative substitution reactions. Two examples were recently reported. Shibasaki found bismuth (III) triflate to catalyze an allylic or propargylic alcohol substitution in good yields on a variety of substrates (Figure 2-16).[63] In a different report, Kitamura found that ruthenium catalyst **2-91** was also able to catalyze the allylic alcohol substitution reaction on allylic alcohols dehydratively (Figure 2-17).

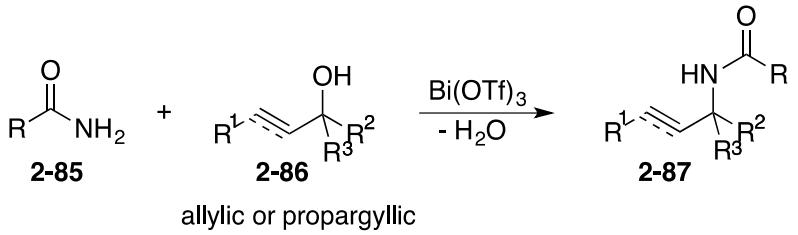

Figure 2-16. Shibasaki's bismuth (III) catalyzed propargylic or allylic alcohol substitution.

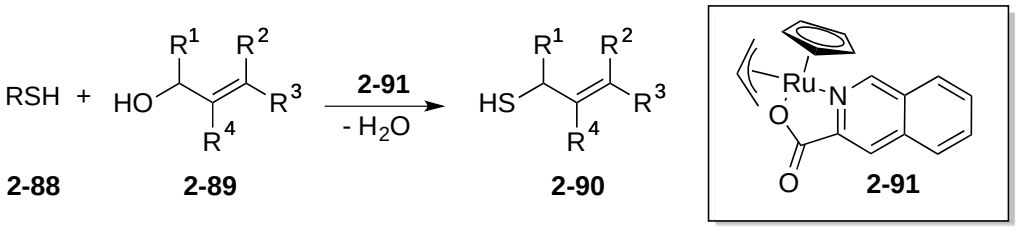

Figure 2-17. Kitamura's ruthenium (III) catalyzed allylic alcohol dehydrative substitution.

Looking back at the catalyst screening results from Table 2-1 entry 12, catalyst **V** was shown to catalyze our tandem hemiacetalization/dehydrative cyclization methodology with high selectivity. It was thought that perhaps this catalyst, if optimized, might yield better results than the phosphine **I**, because phosphites are known to be more electron deficient than phosphines.[28] This might increase the Lewis acidity of the gold (I) cation, which might facilitate formation of the hemiacetal which is believed to be the rate limiting step.

The methodology was then re-optimized using diol **Z 2-79** (Table 2-5). This time, isobutyraldehyde was used because it had previously been shown to give good yields and selectivity in the aldehyde scope (Table 2-3). In addition, excess aldehyde could be easily removed via rotary evaporation of the crude sample. This meant that excess aldehyde did not have to be first reduced with sodium borohydride ($NaBH_4$) then separated from product via flash column chromatography. Because this excess

aldehyde was no longer problematic, the number of equivalents used was raised from 3 to 5 in order to facilitate formation of the hemiacetal.

During the optimization, the addition of pTSA was first investigated (entries 1 and 2). This showed no increase in yield or reactivity, but did sharply decrease diastereoselectivity. Next, temperature and concentration were examined (entries 3-7) only to show no favorable change from entry 1. Finally, phosphite catalyst **V** was tested (entry 8). Because phosphites are known to be more electron poor than phosphines,[28] it was theorized that catalyst **V** might facilitate the formation of the hemiacetal by coordinating to the aldehyde in addition to the substrate.

Table 2-5. Optimization of 1,3-dioxane formation.

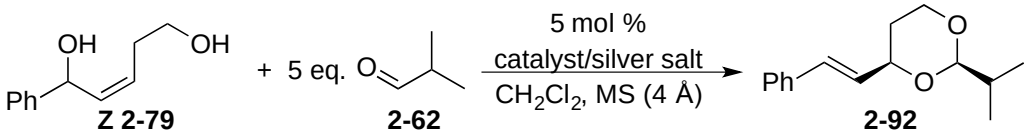

Z 2-79 **2-62** **2-92**

entry	catalyst	conc. (M)	temp. (˚C)	additive (5 mol%)	time (h)	yield (%)[a]	dr[b]
1	**I**/AgOTf	0.2	r.t.	-	20	40	1 : 23
2	**I**/AgOTf	0.2	r.t.	pTSA	3.5	36	1 : 1
3	**I**/AgOTf	0.2	39	-	21	43	all 4 diast.
4	**I**/AgOTf	0.2	39	-	5	40	1 : 15
5	**I**/AgOTf	0.4	39	-	6.5	59	1 : 2
6	**I**/AgOTf	0.8	39	-	4	85	1 : 6
7	**I**/AgOTf	0.8	r.t.	-	20	42	1 : >25
8	**V**/$AgSbF_6$	0.8	r.t.	-	4.5	91	1 : 22

[a] Isolated yields. [b]Determined by crude NMR.

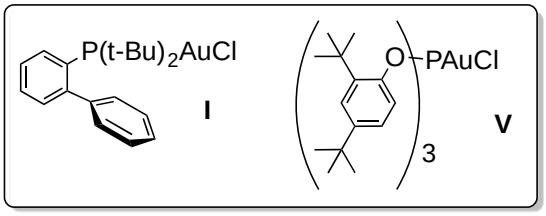

In fact, catalyst **V** was shown to give the highest yields and selectivity without the need for heating. Comparing entries 7 and 8 of Table 2-5, phosphine catalyst **I** was not able to provide nearly the same reactivity as phosphite **V**. Unfortunately, when the E-diol **E 2-79** was treated with these same conditions (Table 2-6, entry 1), the reaction

Table 2-6. Optimization of E-1,5-monoallylic diols.

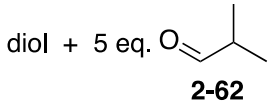

2-62 **2-92** or **2-93**

entry	diol	acetal	conditions[a]	time (h)	yield (%)[b]	dr[c]
1	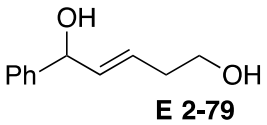 **E 2-79**	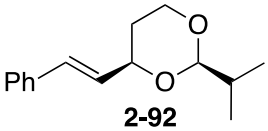 **2-92**	A	23	83	1 : 7
2	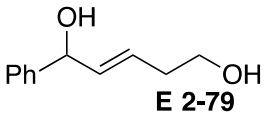 **E 2-79**	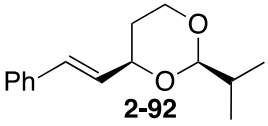 **2-92**	B	0.5	98	1 : >25
3	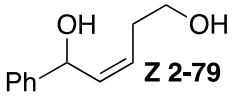 **Z 2-79**	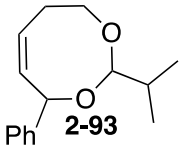 **2-93**	B	0.08	quant.	n.d.

[a] A: 5 mol% **V**/$AgSbF_6$ in 0.8 M CH_2Cl_2, rt, MS (4Å). B: 5 mol% $Bi(OTf)_3$ in 0.2 M CH_2Cl_2, rt,MS (4Å). [b]Isolated yields. [c]Determined by crude NMR.

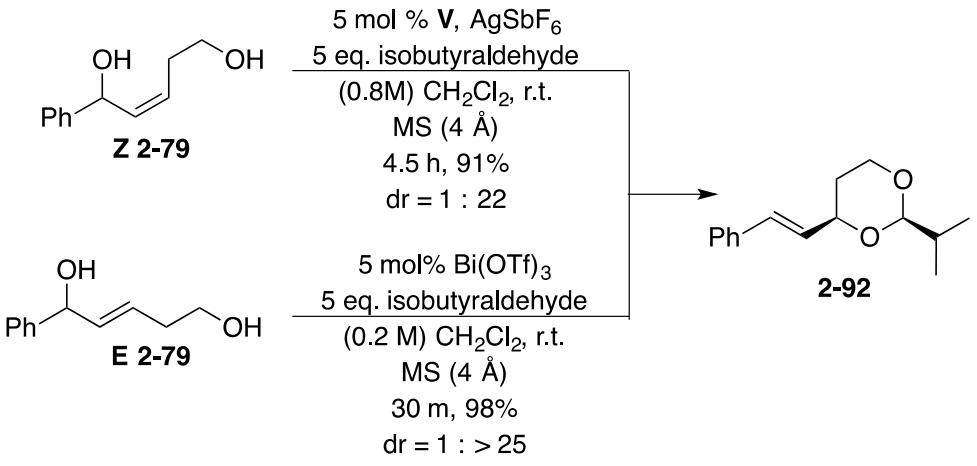

Figure 2-18. Complementary system for the formation of 1,3-dioxanes.

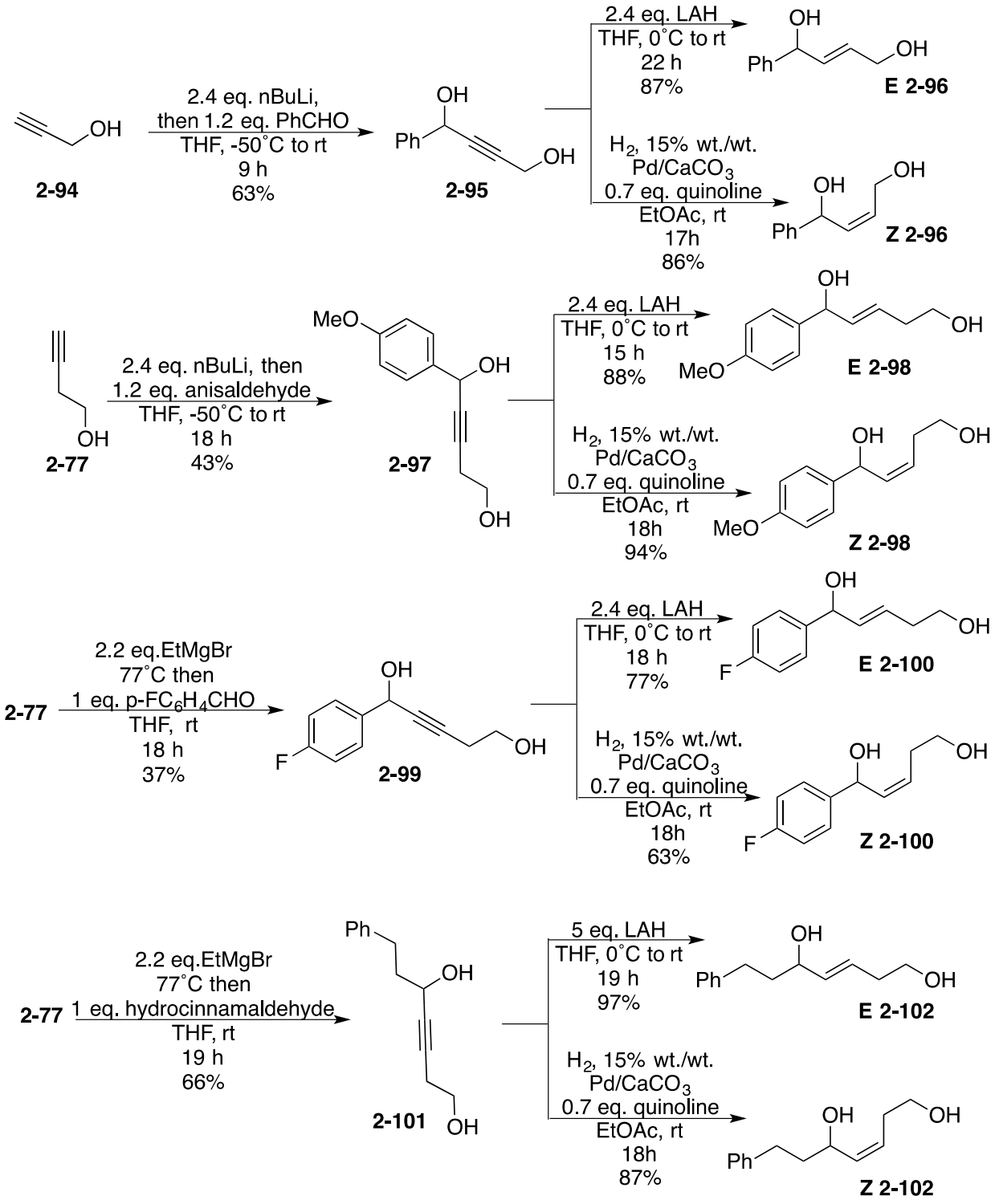

Figure 2-19. Synthesis of diols **2-96**, **2-98**, **2-100**, and **2-102**.

Table 2-7. Diol scope.

1,4 or 1,5-monoallylic diol —conditions A or B→ product

entry	product	olefin[a]	conditions[b]	time (h)[c]	% yield[d]	dr[e]
1	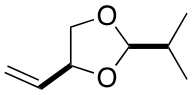 **2-59**	cis	A	4.5	98	1 : 5
2		trans	B	3	dec.	n/a
3		trans	A	5	55	1 : 4
4	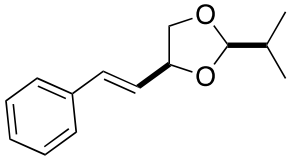 **2-103**		A	4	87	1 : 15
5	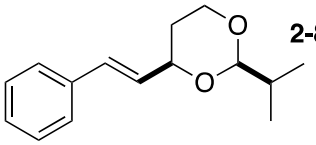 **2-83**	trans	A	23	83	1 : 7
6		trans	B	0.5	98	1 : >25
7		cis	B	0.08	n.o.[f]	n.d.
8		cis	A	4.5	91	1 : 22
9	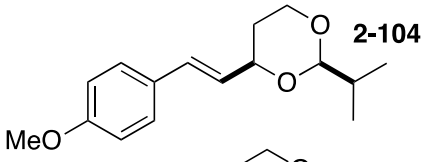 **2-104**	cis	A	18	dec	n/a
10		trans	B	0.01	dec	n/a
11	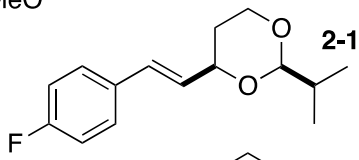 **2-105**	cis	A	3	98	1 : >25
12		trans	B	0.08	80	1 : >25
13	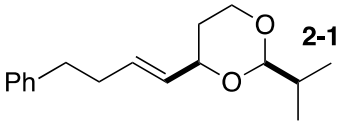 **2-106**	cis	A	4.5	83	1 : >25
14		trans	B	0.5	95	1 : >25

[a] Substrate olefin geometry. [b]A: 5 mol% **V**/$AgSbF_6$ in 0.8 M CH_2Cl_2, rt, MS (4Å).
B: 5 mol% $Bi(OTf)_3$ in 0.2 M CH_2Cl_2 rt,MS (4Å). [c]As indicated by TLC. [d]Isolated yields.
[e]Determined by crude NMR. [f]1,3-dioxepine (**2-83**) instead observed.

was very sluggish. Moreover, the diastereoselectivity was found to be low compared to the results found with **Z 2-79**. Interestingly, bismuth (III) triflate was found to cyclize **E 2-79**, yet it was unable to cyclize **Z 2-79** to produce **2-92**. Thus a complementary system was found for the formation of 1,3-dioxanes (Figure 2-18) between the bismuth (III) triflate and gold (I) phosphite catalyst **V**/$AgSbF_6$.

Additional 1,5-monoallylic diols were prepared (Figure 2-19) in order to determine the role of the R group attached to the internal allylic alcohol moiety. These were prepared in analogous fashion to the general method described previously in Figure 2-14. Thus diols **2-96**, **2-98**, **2-100**, and **2-102** were prepared below.

It was found that when the moiety attached to the internal allylic alcohol was electron rich, complete decomposition was observed. However, when this was an electron withdrawing group or alkane, high yields and diastereoselectivities are observed. Interestingly, the olefin geometry of the starting material did not change the product geometry. Both the E and Z olefin starting materials gave rise to the same cis-1,3-dioxolane or 1,3-dioxane of E olefin geometry. This was confirmed by NMR and nOe observations. The diol scope is given in Table 2-7.

2.2.6 Proposed Mechanism and Origin of Selectivity

By analogy to our previously reported gold (I) catalyzed dehydrative cyclization methodology, we propose the following mechanism (Figure 2-20). First, the gold (I) cation is believed to activate the carbonyl of the aldehyde towards nucleophilic attack(**2-108**) by an incoming diol (**2-107**) to form hemiacetal **2-109** after proton transfer. The gold (I) cation then coordinates to the olefin to make complex **2-110**, which can then cyclize to form intermediate **2-111**. After rotation of the C-C bond, a hydrogen bound conformer **2-112** is formed. It is from this last intermediate that the concomitant loss of gold (I) catalyst and water takes place to produce the cis-1,3-dioxane **2-113**.

The formation of the hemiacetal is believed to be the rate determining step, and it has been shown that gold (I) precatalyst **V** is much more reactive than precatalyst **I**; it is believed that the electron deficient gold (I) cation derived from precatalyst **V** is

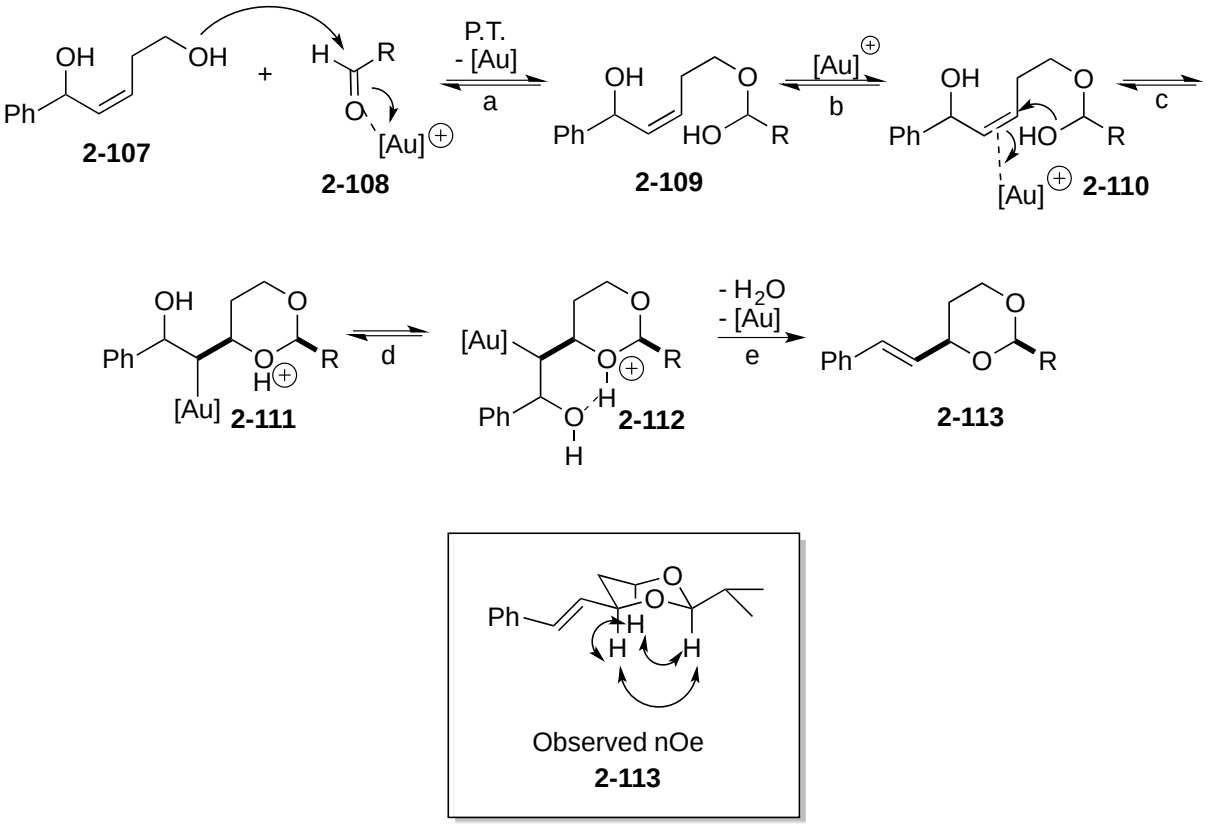

Figure 2-20. Proposed mechanism for the gold (I) catalyzed tandem hemiacetalization/dehydrative cyclization of Z-monoallylic-1,5-diols to form cis-1,3-dioxanes.

working to activate the aldehyde in the formation of hemiacetal. The importance of hydrogen bonding in gold (I) catalyzed dehydrative cyclizations has been previously shown and is therefore thought to also occur in this transformation.[34] This may also be attributed to the formation of E-olefin in the 1,3-dioxane product. Lastly, the major diastereomer formed was shown to be the cis-acetal as observed by nOe. This last piece of evidence suggests the following origin of diastereoselectivity (2-21).

Because previous studies have shown that gold (I) activates nucleophilic addition in anti fashion,[34] it is thought that for the Z-olefin the chair-like conformation that puts the allylic alcohol in pseudo-equatorial position **2-110a** is favored over the pseudo-axial conformation **2-110b**. In the E-olefin case, the same argument is made for bismuth as it

is also able to afford a single diastereomer. It is believed that bismuth might also work for the cis, however it instead follows another path. Gold can also be used for the E-olefin case, though lower selectivity is observed.

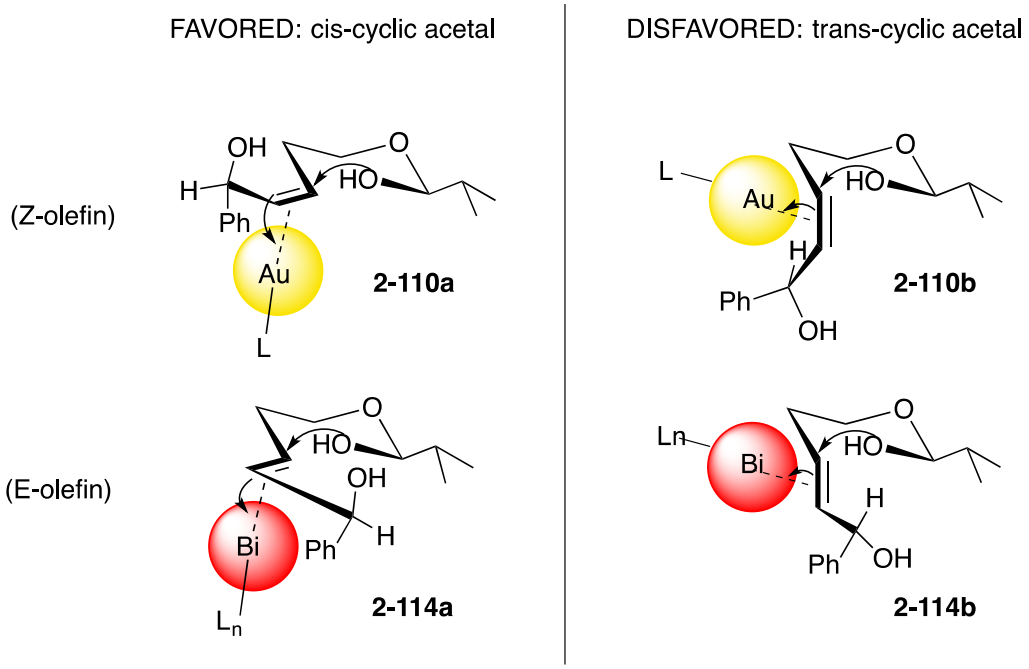

Figure 2-21. Proposed origin of diastereoselectivity.

2.2.7 Application to Natural Product Synthesis

It was originally thought that this new methodology would have utility as a new strategy in the synthesis of natural products containing 1,3-diols. One way of producing syn-1,3-diols **2-118** would be to use an iterative approach (Figure 2-22). In this approach, an asymmetric alkylation can be used to produce homoallylic alcohol **2-116**. After protecting the alcohol and then treating with ozone to produce aldehyde **2-117**, steps 1 and 2 can be repeated to finally yield the protected 1,3-diol after a total of five steps. However, if instead one were to use Roush's double allylboration methodology,[64] in tandem with our proposed methodology, then an analogously protected 1,3-diol **2-121** can be produced in only two steps.

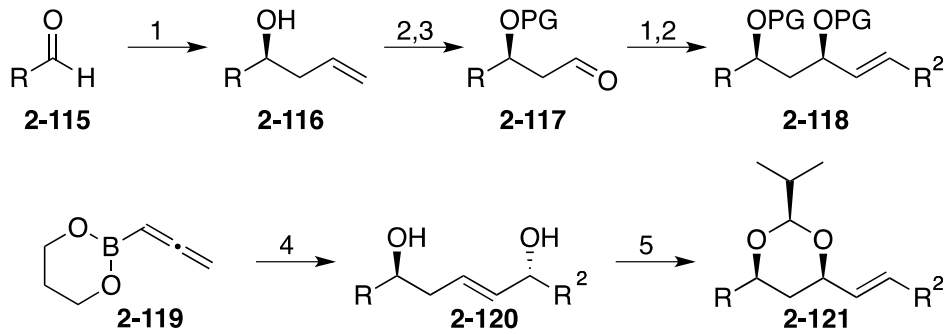

Figure 2-22. Comparison of competing 1,3-diol syntheses. 1) Asymmetric alkylation, 2) alcohol protection, 3) ozone oxidation, 4) Roush's double allylboration, 5) Tandem hemiacetalization/dehydrative cyclization methodology.

This new synthetic strategy could be employed for the synthesis of the following natural products which all feature one or more syn-1,3 diols (Figure 2-23). RK-397 **2-124** features three sets of these moieties, which serve as nearly half of the natural product backbone. As such, this represents an interesting synthetic target that would serve as a great medium for the application of our new methodology.

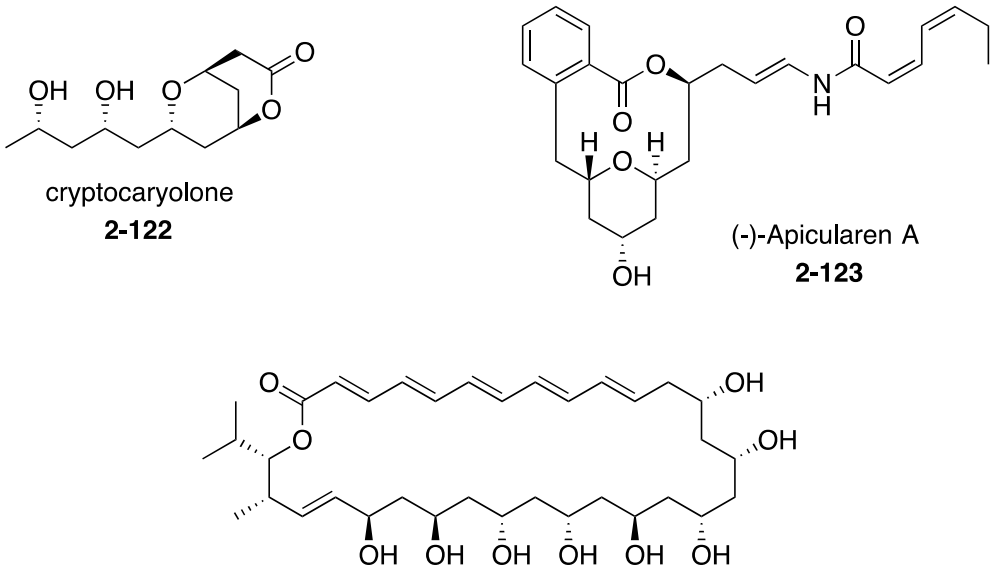

cryptocaryolone
2-122

(-)-Apicularen A
2-123

RK-397
2-124

Figure 2-23. Possible natural product targets.

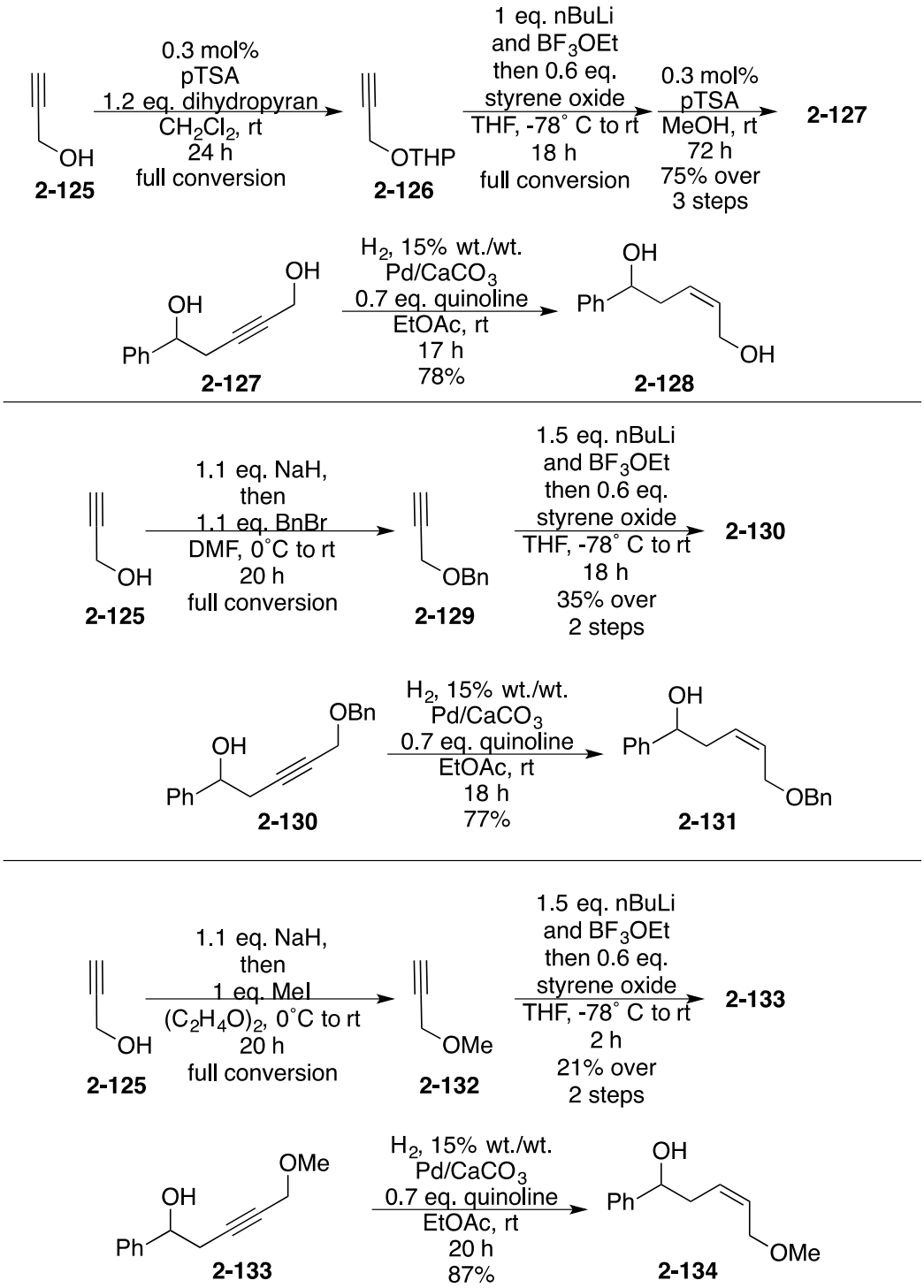

Figure 2-24. Synthesis of isomeric 1,5-monoallylic diol **2-128**, and allylic ethers **2-131** and **2-134**.

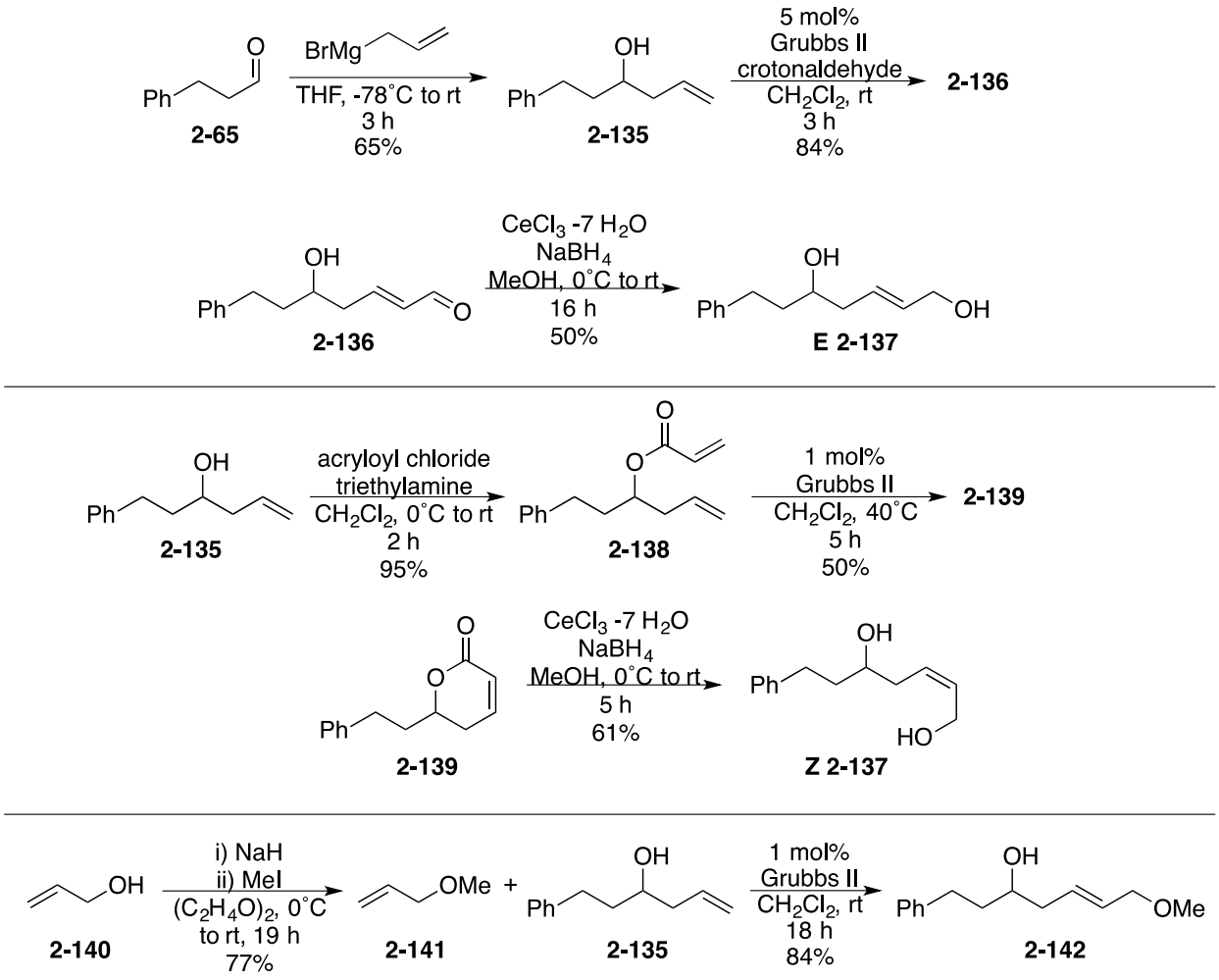

Figure 2-25. Synthesis of diols **2-137** and allylic ether **2-142**.

2.2.8 Investigation of Other Substrates

In order to apply the tandem hemiacetal/dehydrative cyclization methodology towards natural product syntheses, simple experiments served first as a proof of concept (Table 2-8). It was initially thought that a simple trans-positioning of the olefin in the previous1,5-monoallyic diols would not affect the reactivity of the methodology. Because the previous method for forming these diols (by way of cross metathesis) had proven low yielding, a styrene oxide-opening strategy was instead employed. Thus,

isomeric 1,5 monoallylic diol **2-128**, and its analogous allylic ethers **2-131** and **2-134** were prepared (Figure 2-24).

Unfortunately, the styrene oxide-opening reaction did not work well for methyl or benzyl ethers which were produced in 27% and 18% overall. Therefore, the metathesis strategy was again employed for the synthesis of diol **E 2-137** which also was produced in 27% overall (Figure 2-25). This strategy was also employed in the synthesis of allylic ether **2-142**.

Thus, the isomeric 1,5-monoallylic diols **2-128** and **2-137** were subjected to various conditions (Table 2-8). No reaction or decomposition was largely observed. It was then thought that hemiacetalization was occurring predominantly at the terminal alcohol but not at the internal alcohol. This would decrease the amount of activated aldehyde available for the internal alcohol to attack, thus the overall result would be the slower formation of the hemiacetal at the secondary alcohol position - if it is even occurring at all.

To test this theory, the primary allylic alcohol was protected as various ethers since these had previously been shown to be effective leaving groups in other gold (I) catalyzed dehydrative cyclizations.[33] Unfortunately, little to no reactivity was observed except in entries 6 and 14 which were not optimized further as entry 6 gave only 20% yield and entry 14 gave only 40% yield.

Although the reactivity and selectivity is low, it is hoped that upon deprotection of the acetal that only a single diastereomer of the 1,3-diol will be found. If this is the case then the formation of these tri-substituted dioxanes needs only an optimization of

reaction conditions to try and improve the yield. Though the relative stereochemistry of the diol backbone has not yet been determined.

Table 2-8. Trial of proposed strategy in natural product synthesis.

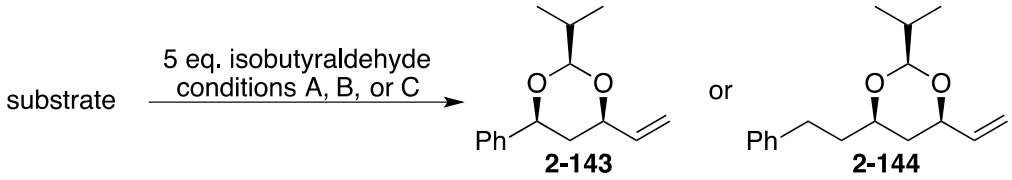

entry	substrate	olefin	conditions[a]	temp (˚C)	time (h)	% yield[b]	dr[c]
1	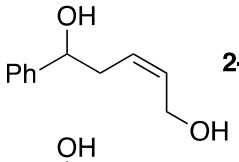 **2-128**		A[d]	rt	24	nr	-
2			A	rt	24	nr	-
3			A[e]	83	24	dec	-
4			A	rt	4	nr	-
5	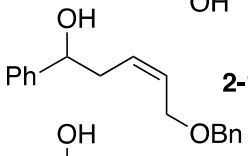 **2-131**		B	rt	24	nr	-
6			B	40	24	20	nd
7			B[e]	55	22	nr	-
8			C	55	22	nr	-
9	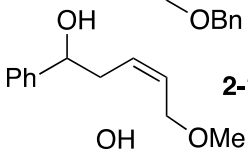 **2-134**		B	rt	18	nr	-
10	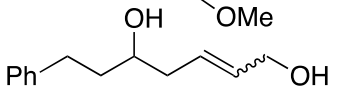 **2-137**	E	D	rt	0.5	dec	-
11		E	D	-78 to 10	16	nr	-
12		E	B	rt	5	nr	-
13		Z	B	rt	48	dec	-
14	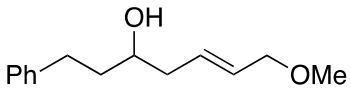 **2-142**		A	rt	23	40	1 : 1

[a]A: 5 mol% **I**/AgOTf, CH_2Cl_2 (0.8 M), MS (4Å). B: 5 mol% **V**/$AgSbF_6$, CH_2Cl_2 (0.8 M), MS (4Å). C: 5 mol% Ph_3PAuCl/AgOTf, $(CH_2)_2Cl_2$ (0.8 M), MS (4Å). D: 5 mol% $Bi(OTf)_3$, CH_2Cl_2 (0.2 M), MS (4Å). [b]Isolated yields. [c]Measured by crude NMR. [d]Used 0.1 M concentration. [e]Used $(CH_2)_2Cl_2$ instead of CH_2Cl_2.

In a new trial, it was then hoped that substituted 1,5-diols made from the Roush double allylboration methodology might be able to undergo the tandem hemiacetalization/dehydrative cyclization; if only the conditions could be optimized for the transformation. These were prepared from commercially available propargyl bromide **2-145** and (-)-alpha-pinene **2-150** (Figure 2-26). Bromide **2-145** was converted

into boronate ester **2-149**, which was hydroborated by borane **2-151** that had been prepared from the alpha-pinene **2-150**. The Roush one-pot double allylboration proceeded smoothly to afford both diols **2-152** and **2-153**.

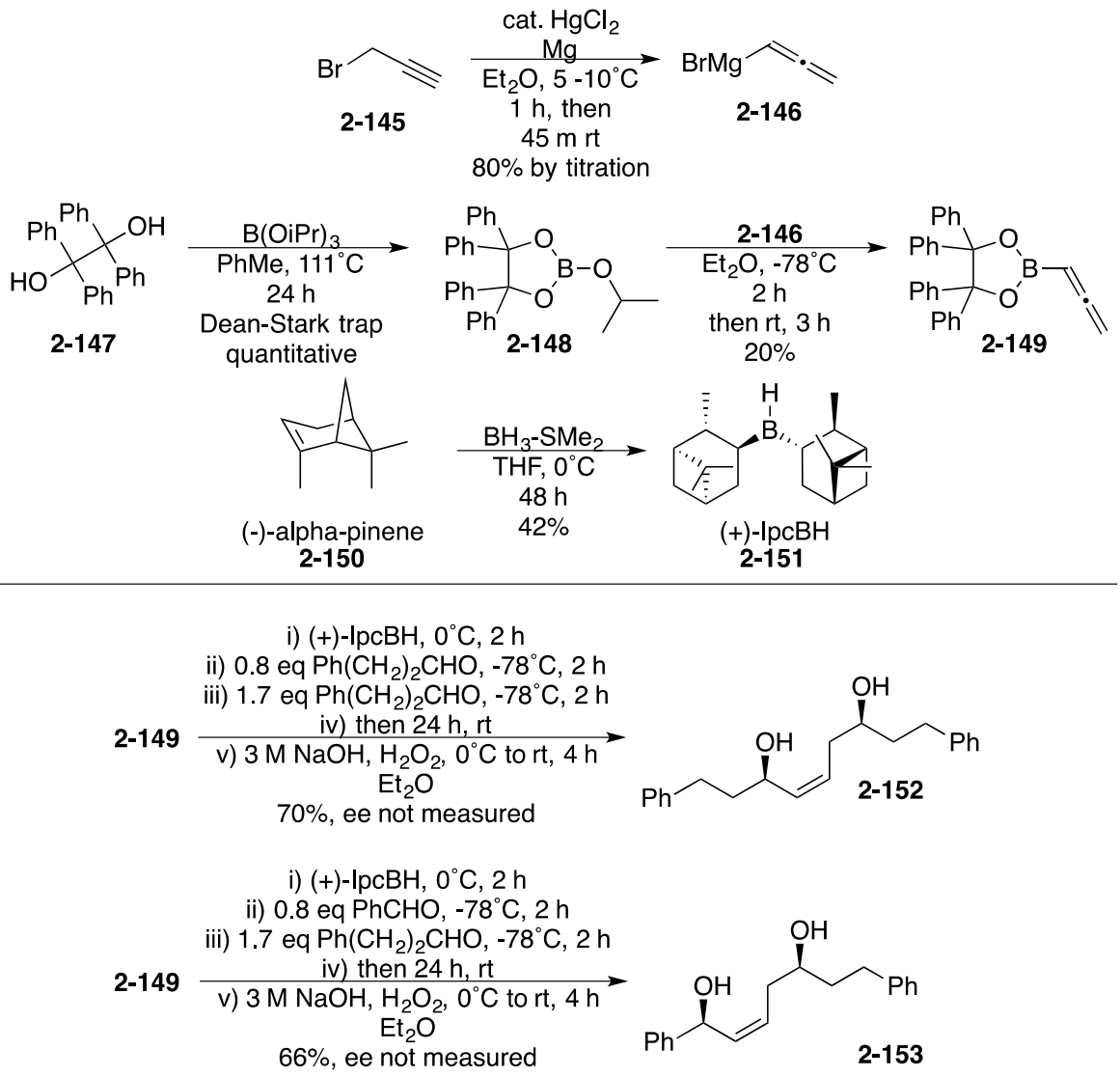

Figure 2-26. Synthesis of diols **2-152** and **2-153**.

Z-1,5-monoallylic diols **2-152** and **2-153** (Table 2-9) were screened at various solvents and temperatures. Unfortunately, no conditions were found to give moderate yields and selectivity. Entry 6 was shown not to even produce a protected 1,3-diol but a 2,3-dihydropyran instead in low yield. Entry 7 used chloral hydrate instead of

isobutyraldehyde, which was shown to give good reactivity furnishing 85% product in a 1 : 1 ratio of diastereomers. Bismuth triflate was also screened as the catalyst but did not undergo dehydrative cyclization; instead it quantitatively furnished the 8-membered acetal.

Table 2-9. Re-optimization of methodology for Roush type Z-1,5-monoallylic diols.

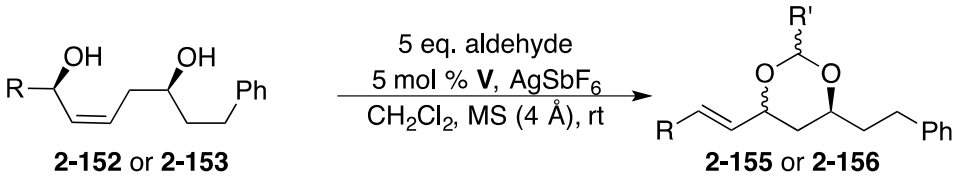

2-152 or **2-153** → **2-155** or **2-156**

entry	diol (R)		aldehyde	solvent	temp. (˚C)	time (h)	yield[a]	d.r.[b]
1	$Ph(CH_2)_2$	**2-152**	iPrCHO	DCM	r.t.	18	n.r.	-
2	$Ph(CH_2)_2$	**2-152**	iPrCHO	THF	r.t.	17	n.r.	-
3	$Ph(CH_2)_2$	**2-152**	iPrCHO	DCM	39	17	n.r.	-
4	Ph	**2-153**	iPrCHO	DCM	r.t.	24	n.r.	-
5	$Ph(CH_2)_2$	**2-152**	iPrCHO	DCE	55	20	n.r.	-
6	Ph	**2-153**	iPrCHO	DCE	55	18	DHP (30)	(1 : 1)
7	$Ph(CH_2)_2$	**2-152**	chloral	DCM	r.t.	5.5	85	1 : 1

[a]Isolated yield. [b]Determined by crude NMR.

Re-optimization was also undertaken for the Roush type E-1,5-monoallylic diols **2-158** and **2-159**. These were synthesized in analogous fashion to diols **2-152** and **2-153**, but used a different borolane **2-157** (Figure 2-27). These diols showed a marked improvement in reactivity as nearly each entry gave some amount of product (Table 2-10). Entry 6 was shown to give the highest yield in only 5 minutes. Unfortunately no diastereoselectivity was observed in entries 1-3, 5, and 7; which instead gave a complex mixture of four diastereomers. Entries 4 and 6 gave only two diastereomers, but in equal amounts.

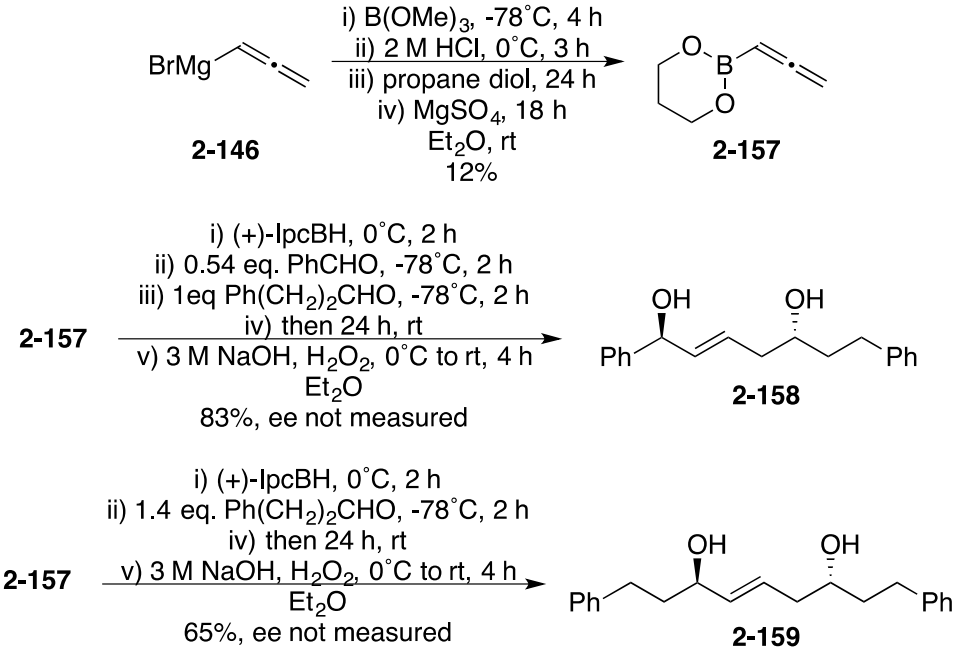

Figure 2-27. Synthesis of diols **2-158** and **2-159**.

Table 2-10. Re-optimization of methodology for Roush type E-1,5-monoallylic diols.

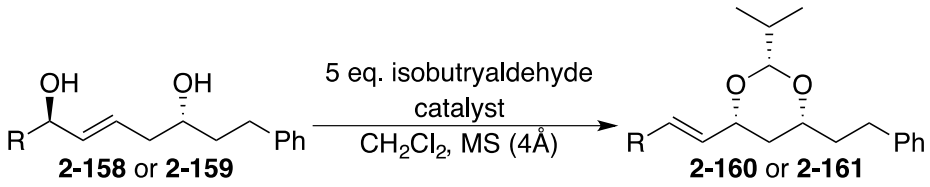

entry	diol (R)		catalyst (mol%)	temp. (˚C)	time (h)	yield (%)[a]	dr[b]
1	Ph	**2-158**	$Bi(OTf)_3$ (5)	rt	1	40	nd
2	Ph	**2-158**	$Bi(OTf)_3$ (1)	rt	18	25	nd
3	Ph	**2-158**	$Bi(OTf)_3$ (2.5)	-35	3	20	nd
4	Ph	**2-158**	**V**/$AgSbF_6$ (5)	rt	20	26	1 : 1
5	Ph	**2-158**	$Bi(OTf)_3$ (2.5)	-35	3	19	nd
6	Ph	**2-158**	$Bi(OTf)_3$ (5)	rt	0.08	84	1 : 1
7	$Ph(CH_2)_2$	**2-159**	$Bi(OTf)_3$ (5)	rt	18	70	nd

[a] Isolated yields. [b]Determined by crude NMR.

2.2.9 Investigation of Other Electrophiles

Because the previously investigated tandem hemiacetalization/dehydrative cyclization was producing decidedly complex mixtures of diastereomers, the electrophile was changed from isobutyraldehyde **2-62** to acetone. In this way, only two stereocenters would be found in the product. In addition, acetone was used as a solvent instead of a whole number equivalent in methylene chloride. By doing so, it was thought that the relative concentration of electrophile would be increased significantly and thus facilitate the formation of hemiketal. Roush type E-1,5-monoallylic diols **2-158** and **2-159** were tested (Table 2-11) since these two substrates showed modest reactivity with the isobutyraldehyde study (Table 2-10).

Table 2-11. Investigation of tandem hemiketalization/dehydrative cyclization.

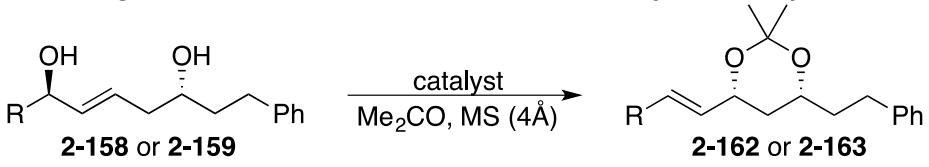

2-158 or **2-159** → **2-162** or **2-163**

entry	diol (R)		catalyst (mol%)	temp. (˚C)	time (m)	yield (%)[a]	dr[b]
1	Ph	**2-158**	$Bi(OTf)_3$ (5)	rt	45	dec	-
2	Ph	**2-158**	$Bi(OTf)_3$ (2.5)	-78	30	dec	-
3	$Ph(CH_2)_2$	**2-159**	$Bi(OTf)_3$ (5)	rt	2	76	1 : 1.6
4	$Ph(CH_2)_2$	**2-159**	$Bi(OTf)_3$ (5)	-78	300	trace	-

[a] Isolated yields. [b]Determined by crude NMR.

From these results, it was theorized that the Roush type E-1,5-monoallylic diols **2-158** and **2-159** were actually in the wrong configuration to undergo dehydrative cyclization. In other words, we needed to experiment on E-syn-1,5-monoallylic diols rather than the anti diols **2-158** and **2-159** furnished by the Roush methodology. Unfortunately, to date, there does not exist a method to synthesize these diols. Instead, we continued to optimize the acetonide variant of the tandem hemiacetalization/

dehydrative cyclization methodology (Table 2-12) using Z-1,5-monoallylic diols **2-83** and **2-106**. This would not only bypass any issues that might exist with relative stereochemistry, but also the number of products formed as there are no diastereomers formed.

Table 2-12. Investigation of tandem hemiketalization/dehydrative cyclization.

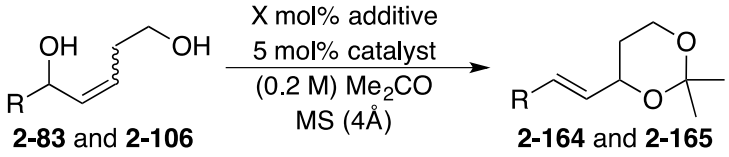

2-83 and **2-106** → **2-164** and **2-165**

entry	diol (R)		olefin	catalyst	addative (mol%)	temp. (˚C)	time (h)	yield (%)[a]
1	Ph	**2-83**	Z	**V**/$AgSbF_6$	-	rt	20	nr
2	Ph	**2-83**	Z	**V**/$AgSbF_6$	pTSA (5)	rt	21	10
3	Ph	**2-83**	Z	**V**/$AgSbF_6$	pTSA (5)	56	18	7
4	Ph	**2-83**	Z	**V**/$AgSbF_6$	PPTS (5)	rt	20	nr
5	Ph	**2-83**	Z	**V**/$AgSbF_6$	CSA (5)	rt	20	trace
6	Ph	**2-83**	Z	**V**/$AgSbF_6$	pTSA (30)	rt	21	dec
7	$Ph(CH_2)_2$	**2-106**	Z	**V**/$AgSbF_6$	pTSA (30)	rt	20	50
8	$Ph(CH_2)_2$	**2-106**	Z	**V**/$AgSbF_6$	pTSA (30)	56	18	45
9	$Ph(CH_2)_2$	**2-106**	Z	**V**/$AgSbF_6$	pTSA (30)	56	5	48
10	$Ph(CH_2)_2$	**2-106**	E	$Bi(OTf)_3$	pTSA (30)	rt	2	nr
11	$Ph(CH_2)_2$	**2-106**	E	$Bi(OTf)_3$	-	rt	0.01	85

[a] Isolated yields.

Upon the results of entry 1, Table 2-12; it was thought that an additive would be required to further facilitate formation of hemiketal. However, entry 11 gave the best reactivity and yield, thus proving that the acetonide variation of our methodology does indeed work – but only with E-1,5-monoallylic diols as catalyzed by bismuth (III) triflate. Interestingly, when Z-1,5-monoallylic diol **2-106** was treated with gold catalyst **V** and

silver co-catalyst $AgSbF_6$, the acetonide product **2-165** was not observed. Instead, a 3,6-dihydro-2H-pyran was instead observed in 66% yield and will be discussed in

Table 2-13. Investigation of vinyl ketal **2-166** formation.

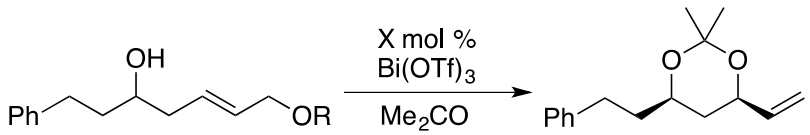

2-137 and **2-142** **2-166**

entry	diol (R)		X (mol%)	Me_2CO (M)	M.S.	temp. (˚C)	time (h)	yield (%)[a]	dr[b]
1	H	**2-137**	5	0.2	4 Å	rt	1	nr	n/a
2	H	**2-137**	5	0.2	4 Å	60	16	< 4	n/a
3	H	**2-137**	5	0.2	4 Å	115	20	34	1 : 1
4	H	**2-137**	5	0.8	4 Å	rt	20	nr	n/a
5	H	**2-137**	5	0.2	4 Å	115	22	73	1 : 3
6	H	**2-137**	5	0.8	4 Å	rt	22	nr	n/a
7	H	**2-137**	10	0.8	-	rt	20	nr	n/a
8	H	**2-137**	10	0.8	-	60	20	44	1 : >25
9	H	**2-137**	10	0.8	4 Å	60	48	nr	-
10	H	**2-137**	10	0.8	-	60	48	dec	-
11	H	**2-137**	10	0.8	-	60	14	nr	-
12	H	**2-137**	10	0.8	-	60	18	nr	-
13	H	**2-137**	10	0.8	-	60	55	dec	-
14	Me	**2-142**	5	0.2	4 Å	rt	48	nr	-
15	Me	**2-142**	5	0.2	4 Å	56	16	nr	-
16	Me	**2-142**	5	0.8	4 Å	rt	24	nr	-
17	Me	**2-142**	5	0.8	4 Å	56	20	nr	-
18	Me	**2-142**	5	0.2	-	125	0.08	dec	-
19	Me	**2-142**	5	0.2	-	84	0.04	nr	-
20	Me	**2-142**	5	0.2	-	90	0.04	dec	-

[a] Isolated yields. [b]Determined by crude NMR.

greater detail in chapter 3. Because this new variation was shown to work, we next decided to investigate the tandem hemiketalization/dehydrative cyclization of isomeric 1,5-monoallylic diols **2-137** and **2-142** to afford vinyl acetonide **2-166** (Table 2-13).

Entry 5 of table 2-13 showed the most promise, yielding product in 73% with modest diastereomeric ratio of 1 : 3. This entry was heated in a sealed tube. Thus it was thought that this high temperature and pressure was the cause for the poor selectivity. Entry 8 did in fact give better selectivity, yet the yield was only 44%. All other conditions gave no better results than these two entries.

It was then thought to switch leaving groups from OH to OMe because methyl ether derivatives have previously been shown to undergo tandem hemiacetalization/dehydrative cyclization (see Table 2-8, entry 8) in low yield but high diastereoselectivity. However no improvement was observed, even upon treatment with a variety of different microwave irradiation conditions.

Finally, other electrophiles were investigated to see if other variants of the methodology could work. Because aldehydes had been shown to undergo the transformation, it was decided to test imines and paraformaldehyde (Figure 2-28). Interestingly, paraformaldehyde did not produce the predicted 1,3-dioxolane product but instead produced divinyl-1,4-dioxane **2-173**. This 1,4-dioxane was thought to come about by a dehydrative dimerization of Z-1,4-butenediol **2-55**. However, when **2-55** is treated with no electrophile and subjected to standard conditions, no reaction is observed. The electrophile must play some role in the formation of the 1,4-dioxane **2-173**.

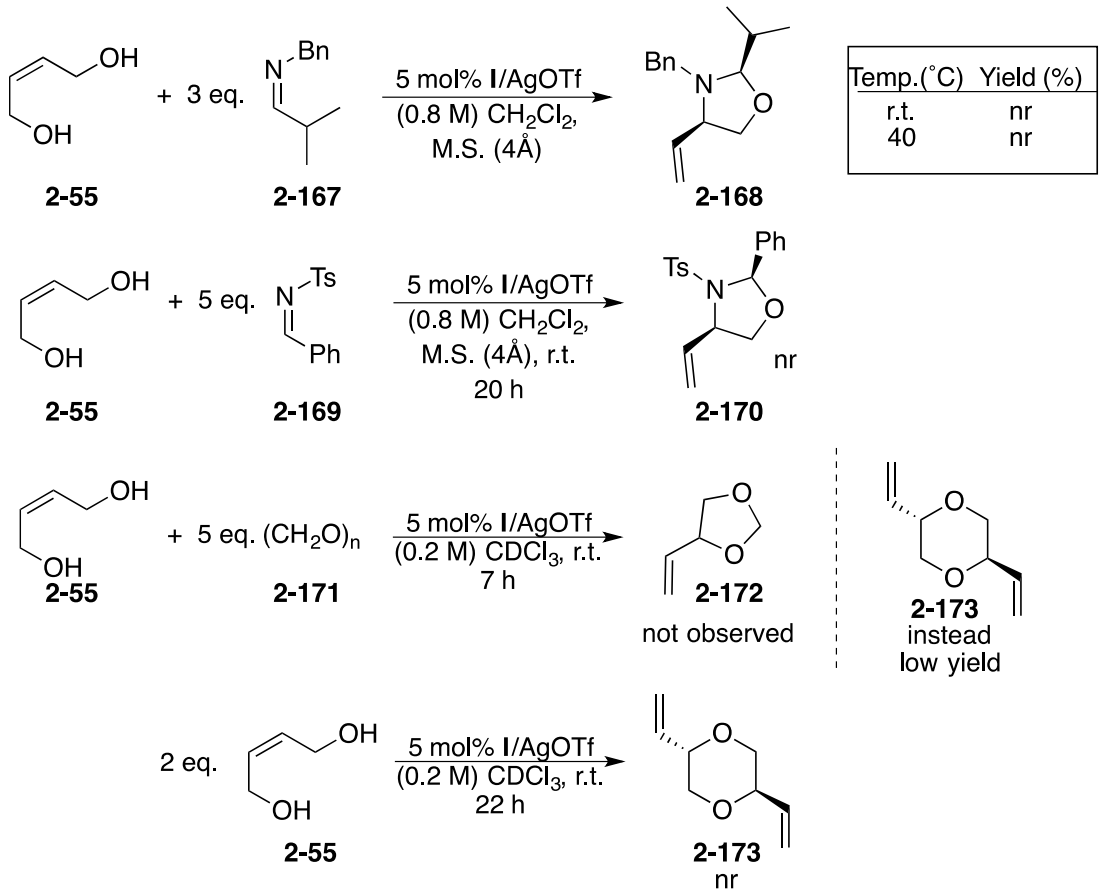

Figure 2-28. Investigation of imines and paraformaldehyde as electrophiles.

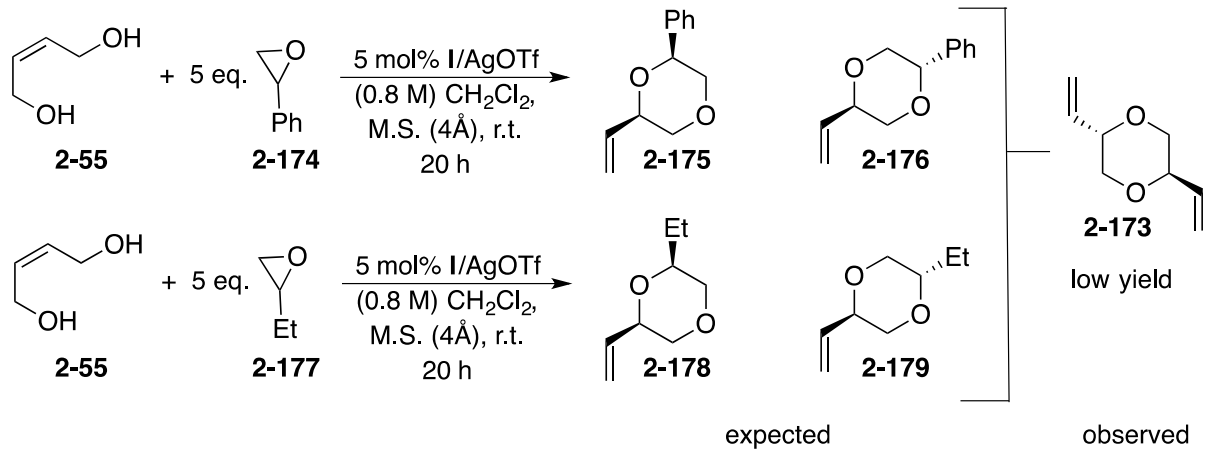

Figure 2-29. Investigation of epoxides as electrophiles.

Tandem ring opening/dehydrative cyclization of epoxides using our standard conditions to furnish substituted 1,4-dioxanes (Figure 2-29) was also considered.

Unfortunately, these failed to produced the desired compound but did interestingly furnish the same divinyl-1,4-dioxane **2-173**. This seems to suggest that the nature of the electrophile does not matter in the formation of byproduct **2-173**. The formation of this byproduct was not further studied.

2.2.10 Investigation of 1,3-Dioxane De-protection

In order to determine the diastereomeric ratio of dioxane **2-151** or **2-152**, and to demonstrate the applicability of the tandem hemiacetalization/dehydrative cyclization methodology; a method of de-protection needed to be found to yield the 1,3-diol.

Table 2-14. Investigation of 1,3-dioxane de-protection methods.

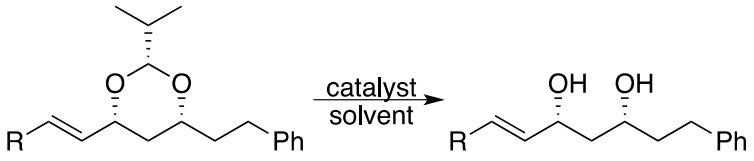

2-151 or **2-152** **2-180** or **2-181**

entry	dioxane (R)		catalyst/solvent	temp. (˚C)	time (h)	yield (%)[a]	dr[b]
1	Ph	**2-151**	cat. CSA/MeOH	rt	24	nr	-
2	Ph	**2-151**	cat. pTSA/MeOH	rt	20	nr	-
3	Ph	**2-151**	cat. pTSA/MeOH:H_2O	rt	72	nr	-
4	Ph	**2-151**	cat. pTSA/MeCN:H_2O	85	18	dec	-
5	$Ph(CH_2)_2$	**2-152**	cat. CSA/MeOH	rt	72	dec	-
6	$Ph(CH_2)_2$	**2-152**	conc. HCl/MeOH	rt	5.5	47	1 : 5
7	$Ph(CH_2)_2$	**2-152**	AcOH	rt	20	nr	-
8	$Ph(CH_2)_2$	**2-152**	conc. HCl/MeOH	rt	72	dec	-
9	$Ph(CH_2)_2$	**2-152**	conc. HCl/MeOH	rt	5.5	nr	-
10	$Ph(CH_2)_2$	**2-152**	15 eq. TFA/MeOH	rt	24	dec	-
11	$Ph(CH_2)_2$	**2-152**	conc. HCl/MeOH	rt	6	dec	-

[a] Isolated yields. [b]Determined by crude NMR.

Thus, various Brønsted acids were screened (Table 2-14). Entry 6 was found to give the best yield of 1,3-diol **2-181**. Better still, it did not destroy the starting material,

which was also found in 47%. Unfortunately, this result was not reproducible using different workup solvents to quench the excess base (see entries 8, 9, and 11 – which did not use pyridine to quench reaction). Alternatively, we should examine Lewis acids such as antimony trichloride, or even bismuth (III) triflate.

2.3 Future work

In order to complete the first phase of this project, more complexity should be added to the current diol scope. As it stands, the effect, if any, is not known for a nitrogen containing substrate on the tandem hemiacetalization/dehydrative cyclization methodology. Other heteroatoms should also be shown to be compatible with the standard conditions, which should work considering how facile the methodology is to use. Additionally, a chirality transfer study needs to be conducted to gather further evidence of the mechanism at work and further add utility to the new method.

Currently, both of the above are underway. In conjunction with a fellow graduate student, Justin Goodwin, new substrates featuring heteroatoms are under construction while the first attempt at a chirality transfer experiment has shown great promise (Figure 2-30). When a 1 : 1 mixture of diastereomers **2-182** was treated with standard conditions, only one diastereomer was shown to cyclize to give **2-183**, while the other diastereomer was left mostly unreacted. This experiment should be repeated with each of the separated diastereomers **2-182** to confirm this observation and also try to find where the missing amount of starting material is going. Lastly, we need to confirm the absolute configuration of **2-183** in order to conclusively show that a transfer of chirality has taken place. To do this, we need to de-protect the acetal moiety, and esterify with Mosher's ester. Through NMR analysis, the absolute configuration of the secondary

alcohol will be established. Further corroboration can come from HPLC analysis of both starting materials and products.

In order to implement our new strategy for natural product synthesis, we must still show that the formation of 1,3-dioxolanes containing a terminal vinyl moiety **2-99** is possible. Low yield but high diastereoselectivity was obtained in Table 2-8, entry 8 when gold (I) phosphite catalyst **V** was used in standard conditions. Perhaps if the reaction were heated, reactivity would be increased while maintaining good to moderate diastereoselectivity. If not, then a different electron deficient gold (I) catalyst should be investigated. Chapter one prominently featured phosphoramidate gold (I) catalysts that have shown great results. A new catalyst would not need to be chiral, but it would need to maintain steric bulk about the phosphorus in order to maintain high diastereoselectivity.

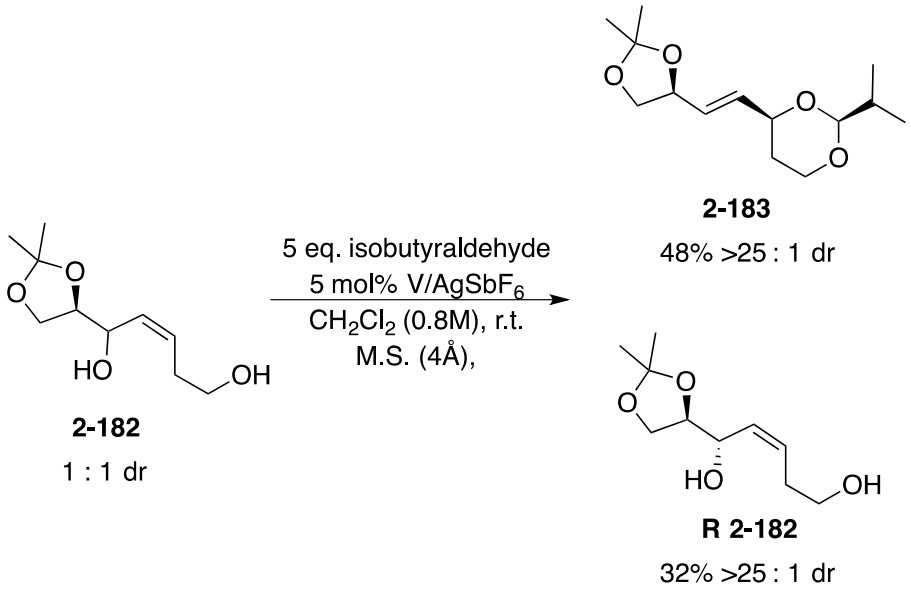

Figure 2-30. Chirality transfer investigation.

In addition to this, the potential new strategy in natural product synthesis must be realized by the clean deprotection of 1,3-dioxolanes. Currently, we have investigated

only Brønsted acids and should also consider various Lewis acids as well. A literature search has indicated that these acetals are difficult to deprotect, but if the right conditions can be found, then it would provide great utility to the synthetic community. Finally, the ultimate test for a new methodology is its application in natural product synthesis. Once all the above has been addressed, then we can then try to synthesize any of the above natural products shown in Figure 2-23.

2.4 Conclusions

A new intermolecular gold (I) catalyzed tandem hemiacetal and hemiketal/dehydrative cyclization methodology has been developed. To our knowledge, it is the first example to show a gold (I) phosphite cation capable of activating both C-C double bonds and carbonyls in the same pot. This new methodology may yet have practical applications as a new strategy in the synthesis of natural products.

CHAPTER 3
DIASTEREOSELECTIVE GOLD (I) CATALYZED SYNTHESIS OF 3,6-DIHYDRO-2H-PYRANS FROM SYN-1,5-MONOALLYLIC DIOLS

3.1 Introduction

The synthesis of 3,6-dihydro-2H-pyrans remains a challenge for the synthetic community. There are only a small handful of synthetic strategies available to the synthesis of these compounds. Traditionally, the synthetic chemist has relied on the following three strategies for the formation of these interesting moieties. These strategies are olefin metathesis, hetero-Diels-Alder, and Ferrier-type rearrangements.

These compounds are a principle component to many marine natural products. This moiety is thought to be a major contributor to the three dimensional shape of many of these compounds, and thus might also play a significant role in the biological activity demonstrated by these marine natural products. There are many examples of marine natural products containing 3,6-dihydro-2H-pyrans. A few examples include swinholides,[65] sorangicin A,[66] scytophycins,[67,68] laulimalide,[69] and isolaulimalide.[70] Three selected examples are shown below (Figure 3-1), all of which are known cytotoxins and are effective compounds that could be developed into new treatments as antifungals, antibiotics, and even anticancer drugs.

A recent report from Rayment shows a structural basis for the cytotoxicity of swinholide A.[71] This macrolide is actually one of the better-known membrane permeable compounds that is known to specifically inhibit actin filaments. As such, it is commonly used in cell biology studies, and represents a promising new class of anticancer

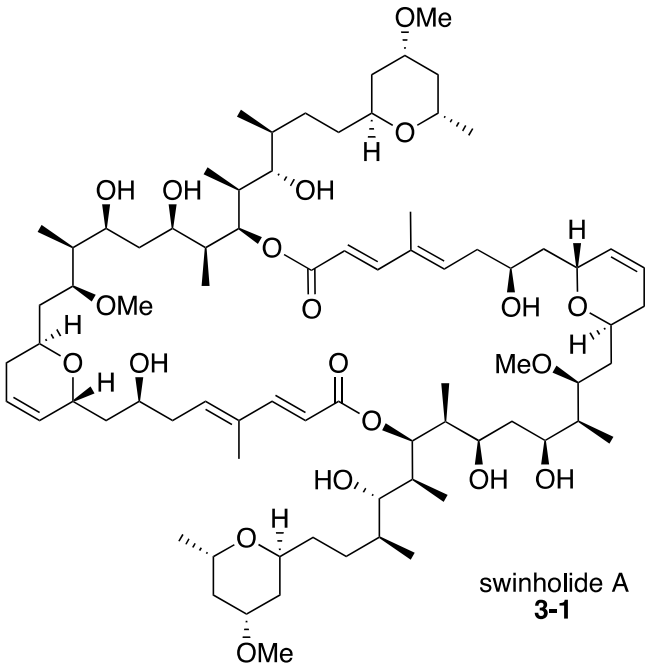

swinholide A
3-1

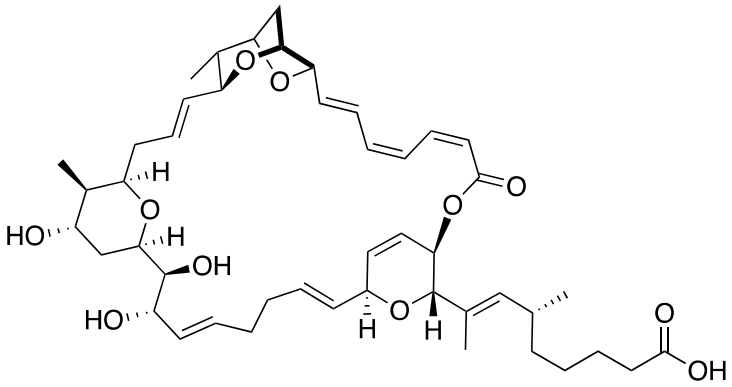

sorangicin A
3-2

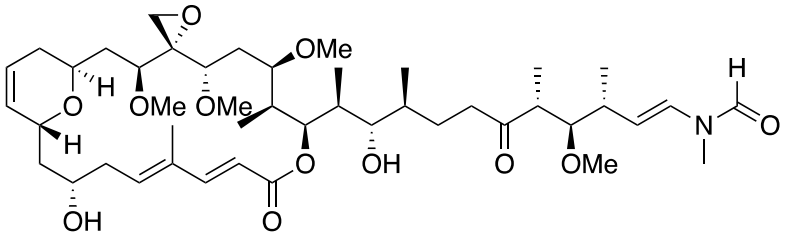

scytophycin B
3-3

Figure 3-1. Three examples of natural products containing 3,6-dihydro-2H-pyran moieties.

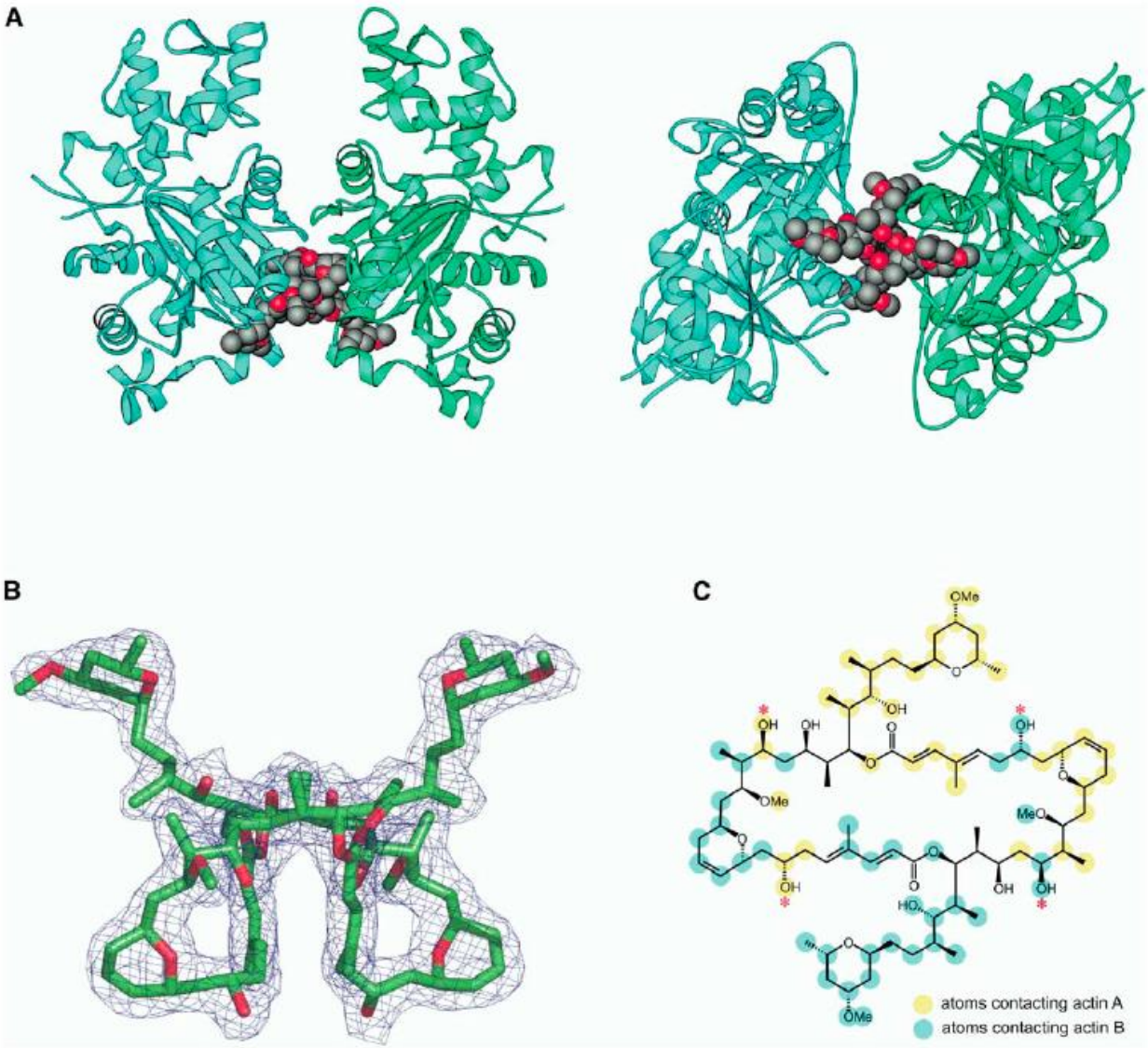

Figure 3-2. Swinholide A mode of binding two actin molecules. A: Bottom and side view of swinholide A-actin complex. B: Ornit electron density map of swinholide A. C: Map of swinholide A interactions with actin. Reprinted from Chemistry & Biology, 12, Klenchin, V. A.; King, R.; Tanaka, J; Marriott, G.; Rayment, I.,Structural Basis of Swinholide A Binding to Actin, 287-291, Copyright (2005), with permission from Elsevier.

compounds. Its cytotoxicity is believed to stem from its ability to sever and sequester actin filaments, however the exact mechanism is still not known. In the report, swinholide A is shown to be capable of binding to two actin molecules at the same binding site used by known toxins of the trisoxazole family as well as numerous actin binding proteins. Crucial to this mode of binding is the structural framework provided by

the two 3,6-dihydro-2H-pyran moieties which serve to position the binding units of swinholide A towards and within two actin molecules (Figure 3-2).

Synthesis of this important heterocycle is commonly reported using the traditional methods mentioned above. All four of these are exemplified in natural product syntheses. In a report from Mulzer,[72] the synthesis of laulimalide was accomplished via an olefin metathesis to produce both of the 3,6-dihydro-2H-pyranyl moieties. This strategy had been previously investigated by the Mulzer group, where they found that this transformation occurred smoothly with only 1-2% Grubbs first generation catalyst in either substrate **3-8** or **3-9**(Figure 3-3.).[73]

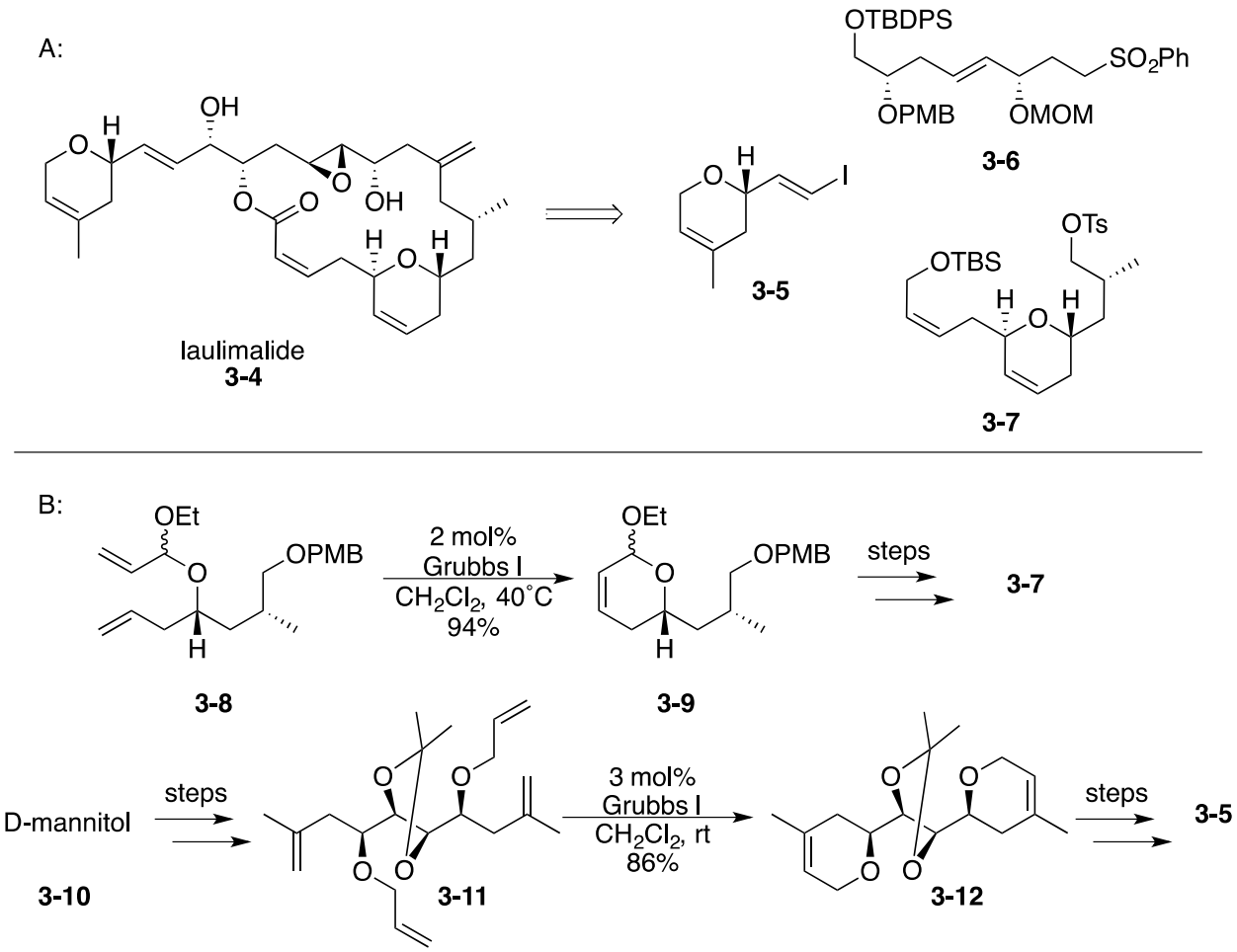

Figure 3-3. A: Mulzer's retrosynthesis of laulimalide **3-4**. B: Synthesis of **3-9** and **3-12**.

Although this strategy produces the desired dihydropyran in high yield, it requires many steps from commercially available starting materials to get to the desired substrate. As a consequence, the overall yield of the dihydropyran is quite small compared to another strategy, which might be more direct. In addition, this strategy must rely on other methods to establish the correct stereochemistry of either the substrate or the product, which only adds to the total number of steps required.

In another synthesis of laulimalide, Paterson used a hetero Diels-Alder strategy for the synthesis of the terminal 3,6-dihydro-2H-pyranyl moiety **3-13** (Figure 3-4).[74] This was accomplished using a chiral chromium complex **3-17**, which was originally developed by Jacobsen.[75] The authors were able to afford the required stereochemistry of **3-18**. Unfortunately, one of these stereocenters is obliterated in the synthesis of **3-13**.

This strategy is much more direct than the metathesis route as it can accommodate commercially available substrates. Moreover, the catalyst used in the method is the source of stereochemical information, thus it does not rely on other methods to install the correct stereochemistry upon the desired dihydropyran. However, this method does not directly produce the 3,6-dihydro-2H-pyran. Instead, this method produces an acetal that can then be reduced into the dihydropyran, which means that multiple reactions are still required to furnish the desired compound.

Ferrier rearrangements have long been known, and were first reported in 1914 by Fischer.[76] However, the synthetic utility of the method was first recognized by Ferrier in the early 1960's, and was utilized in the synthesis of glycosyl compounds.[77,78] This method is recognized as a Lewis acid catalyzed tandem elimination/alkylation to produce 3,6-dihydro-2H-pyrans or other glycosyl compounds. In the Paterson synthesis

of laulimalide, internal dihydropyran **3-14** was produced by way of a Ferrier-type I rearrangement when **3-19** was treated with titanium tetrachloride ($TiCl_4$) and trimethylallylsilane.[79,80]

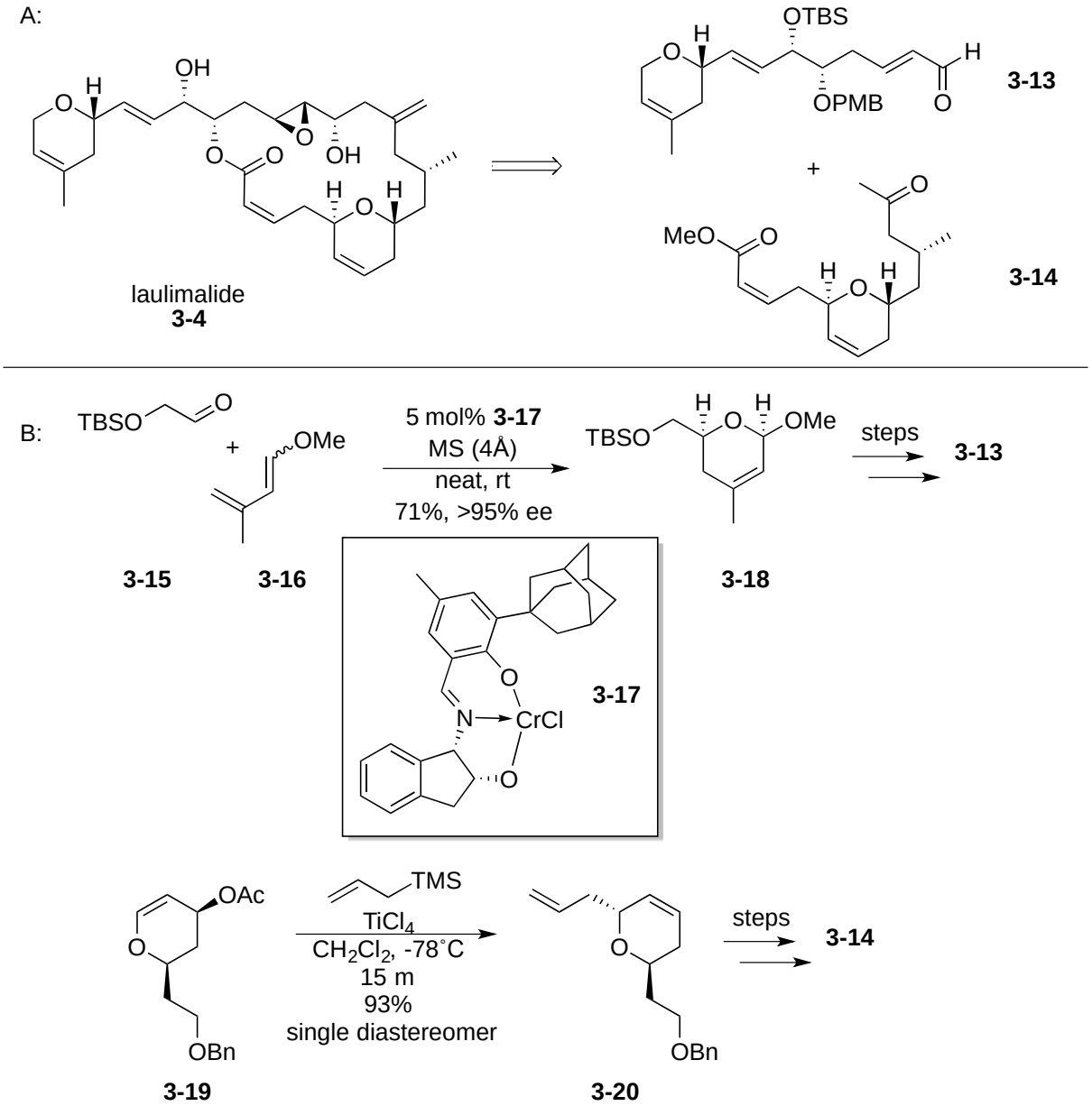

Figure 3-4. A: Paterson's retrosynthesis of laulimamide **3-4**. B: Synthesis of **3-18** and **3-20**.

Three more modern methods for producing 3,6-dihydro-2H-pyrans have recently been reported. The first of which is a [4 + 2] cycloaddition reported by Panek in the

synthesis of (-) apicularen A.[81] In this method, an aldehyde is treated with silane **3-26** and a stoichiometric amount of trimethylsilyltrifulouromethane sulfonate (TMSOTf) to produce 3,6-dihydro-2H-pyran **3-24** as a single diastereomer in good yield (Figure 3-5). This method works well to produce the desired stereochemistry, however is highly substrate dependent. In most examples shown in the report, low to moderate yields and selectivities plague this method. In addition, the synthesis of silane **3-26** requires 5 steps from commercially available materials.

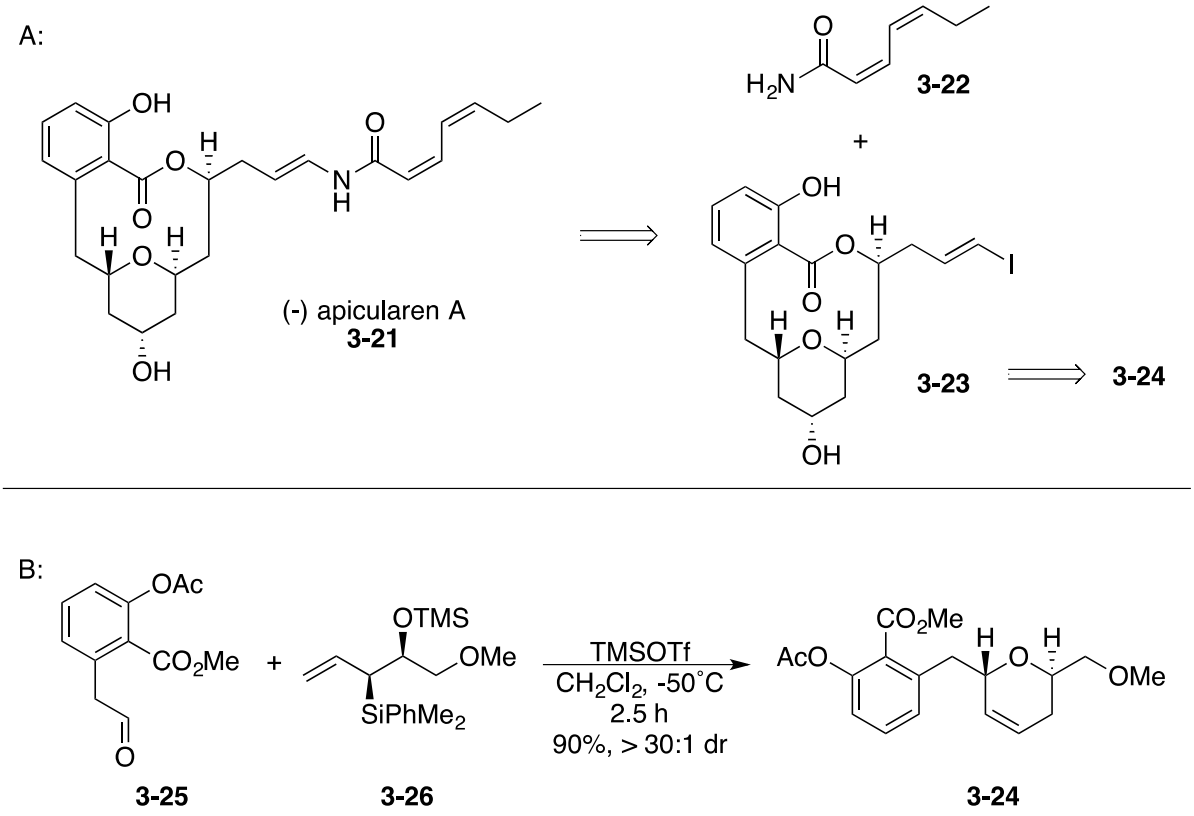

Figure 3-5. A: Panek's retrosynthesis of (-) apicularen A. B: Synthesis of **3-24**.

In a report from Uenishi, palladium (II) complexes were shown to stereospecifically cyclize 1,3-monoallylic diols into 3,6-diydro-2H-pyrans.[82] This methodology was then applied to the synthesis of laulimalide (Figure 3-6). [83,84] Diol **3-29** was first made in 21 steps before being treated with bis(acetonitrile) palladium (II) chloride to dehydratively

cyclize to **3-30** in an enantiospecific manner. Dihydropyran **3-28** was also formed through the palladium (II) catalyzed diastereoselective dehydrative cyclization of diol **3-31** to produce **3-32**. Although this methodology works quite well, and can even be used to generate the opposite epimer, high catalyst loading and sometimes very long reaction times are required.

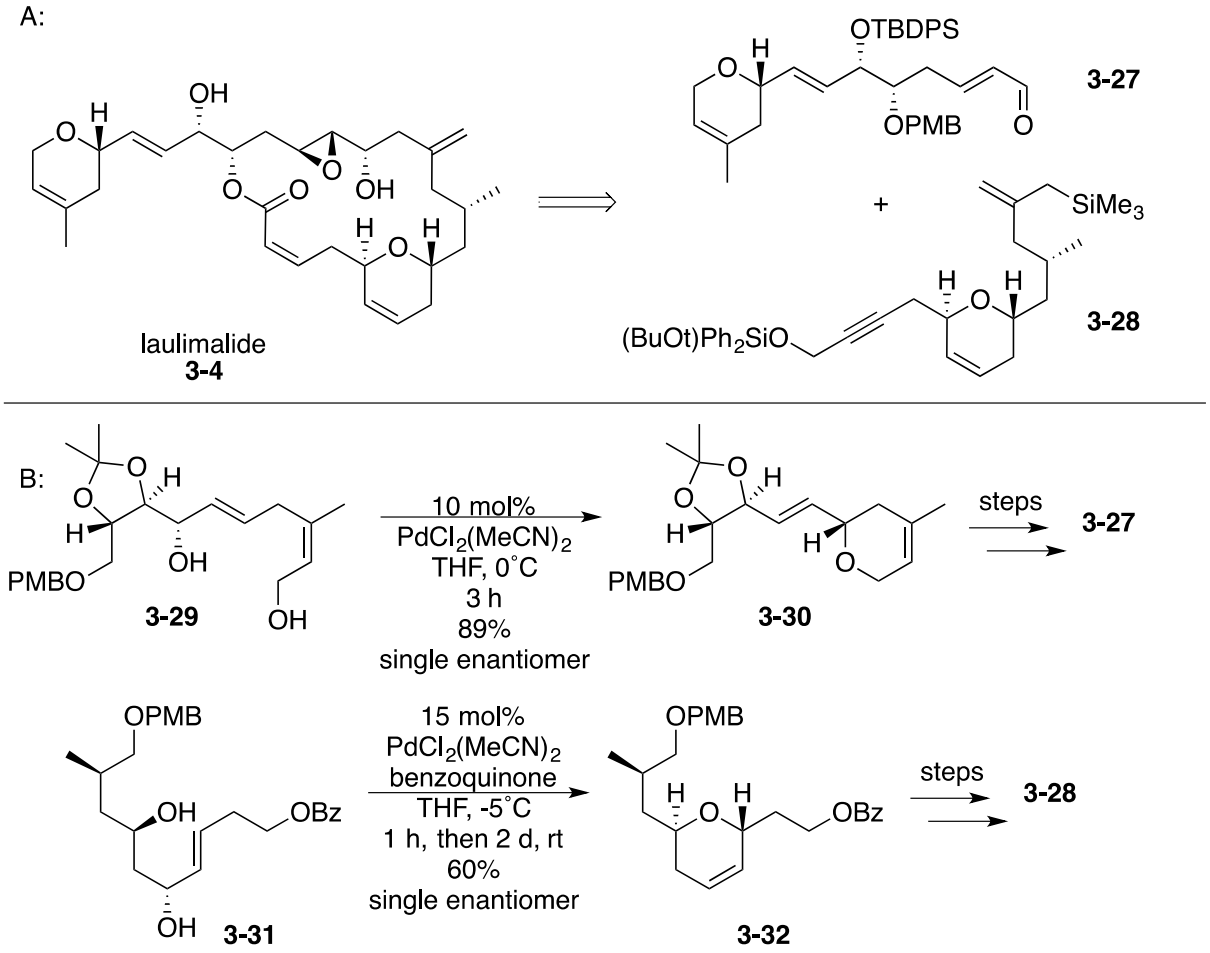

Figure 3-6. A: Uenishi's retrosynthesis of laulimalide. B: Syntheses of **3-30** and **3-32**.

In one last example of 3,6-dihydro-2H-pyran synthesis, Roush also reports a dehydrative cyclization based upon his earlier work in the synthesis of substituted 1,5-monoallylic diols discussed previously in chapter 2.[64] In their report, 1,5-monoallylic diols that were made from the Roush double allylboration methodology were treated with various catalysts and were found to give 3,6-dihydro-2H-pyrans in moderate

yields.[85] Unfortunately, the method could not furnish good diastereomeric nor enantiomeric selectivities. Therefore, other reagents and substrates were investigated. The best results came from the stannyl ether catalyzed cyclization of hydroxyl mesylate **3-33**, which occurred with a small amount of mesylate elimination to form the diene by-product **3-35** (Table 3-1).

This method has the potential to be widely used in natural product synthesis, however the formation of the hydroxymesylate is a lengthy and challenging synthesis. After the one-step synthesis 1,5-monoallylic diol, one diol must be first selectively protected. This is done by TBS protection of the allylic alcohol moiety which occurs in low selectivity and yield. This is then followed by formation of the mesylate and deprotection of the silyl ether to furnish the hydroxymesylate **3-33**. In addition, the method is substrate dependent giving only one product in entry 1, but both products in the remaining entries. Therefore the method has not been used in natural product syntheses possibly due to these problems.

Table 3-1. Roush's cyclization in the formation of 3,6-dihydro-2H-pyrans.

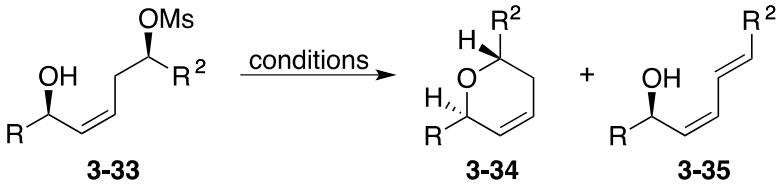

3-33 **3-34** **3-35**

entry	R	R^2	conditions	**3-34** : **3-35**	yield (%)
1	$Ph(CH_2)_2$	$Ph(CH_2)_2$	$(Bu_3Sn)_2O$, DMF, 80˚C	99 : 1	80
2	$Ph(CH_2)_2$	$(CH_3)_2CH$	$(Bu_3Sn)_2O$, DMF, 80˚C	88 : 12	76
3	$(CH_3)_2CH$	$Ph(CH_2)_2$	$(Bu_3Sn)_2O$, DMF, 75˚C	83 : 17	81
4	C_6H_{11}	C_6H_{11}	$(Bu_3Sn)_2O$, DMF, 70˚C	72 : 28	72

3.2 Results

While conducting experiments in the tandem hemiketalization/dehydrative cyclization of 1,5-monoallylic diols with acetone, the Z-1,5-monoallyic diol **3-36** was subjected to standard conditions with 30 mol% of pTSA and instead of forming the desired acetal **3-37**, 3,6-dihydro-2H-pyran **3-38** was found in a 66% yield (Figure 3-7). This was a completely unexpected outcome, and one that merited further investigation.

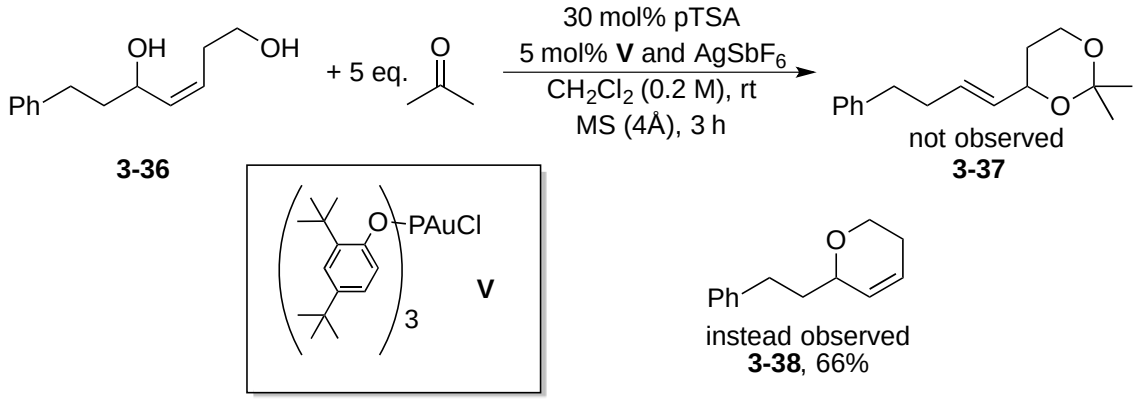

Figure 3-7. First attempt at tandem hemiketalization/dehydrative cyclization of **3-36** and acetone.

This serendipitous finding led to a screening of a variety of conditions to determine what reagents were needed to furnish this observation, and also to gain insight into how the transformation may be occurring (Table 3-2). Interestingly, it was found that the initial conditions used the gave the best results. Entry 2 suggests that pTSA was required for the transformation, in addition to the catalyst system **V**/$AgSbF_6$. Entry 6 shows that acetone was not required to produce dihydropyran, however this yields only half as much product compared to the initial conditions (entries 1 and 6).

Further investigation was conducted to determine the effect of temperature and catalyst loading on the diastereoselectivity (Table 3-3). It was theorized that by lowering temperature, or by decreasing the amount of catalyst, that the diastereomeric ratio

between the cis and trans-3,6-dihydro-2H-pyrans would increase. It was found that catalyst loading had little effect on the dr, however when the temperature was lowered

Table 3-2. Investigation of required additives and catalysts.

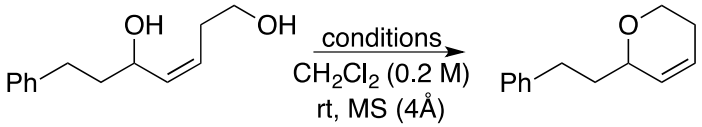

3-36 **3-38**

entry	acetone	pTSA	**V**/$AgSbF_6$	time (h)	yield (%)[a]
1	5 eq.	30 mol%	5 mol%	3	62
2	5 eq.	-	5 mol%	18	nr
3	5 eq.	30 mol%	-	20	nr
4	-	30 mol%	-	20	nr
5	-	30 mol%	5 mol%	17	nr
6	-	30 mol%	5 mol%	24	30

[a]Isolated yield.

Table 3-3. Investigation of diastereoselectivity.

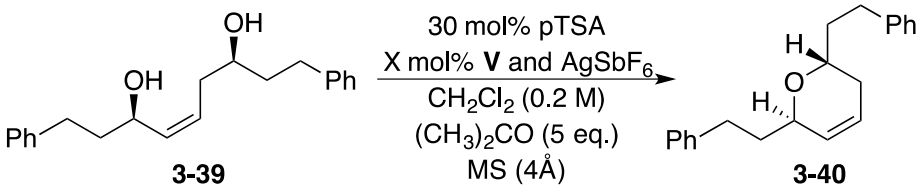

3-39 **3-40**

entry	X (mol%)	temp (˚C)	time (h)	yield (%)[a]	dr[b]
1	5	rt	1	48	5 : 1
2	3.5	rt	.16	63	6 : 1
3	5	-78	2	nr	-
4	5	0	.75	57	6 : 1
5	5	-30	24	36	>25 : 1

[a]Isolated yield. [b]Determined by crude NMR.

to -30˚C, only the cis-diastereomer **3-40** was observed (entry 5). However, this greatly decreased the reactivity giving nearly one third product and one third unreacted starting material. It is not yet known what happens to the missing third of material, though it may

be that some of the starting material decomposes and is then caught within the plug of silica used to quench the reaction.

In cooperation with fellow group member, Thomas Ghebreghiorgis, the gold/silver catalyst system was investigated to determine if **V** or $AgSbF_6$ were required for the transformation to occur (Table 3-4). Interestingly, Thomas found that under the original

Table 3-4. Investigation of gold/silver catalyst system.

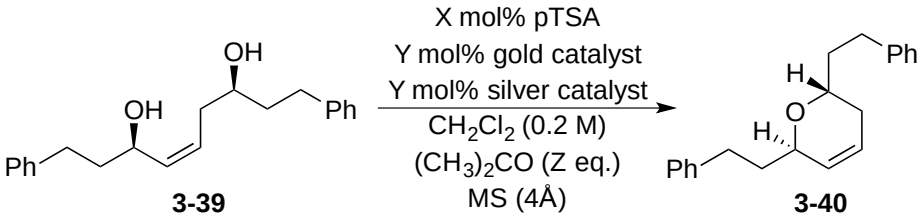

3-39 **3-40**

entry	X (mol%)	Y_{Au} (mol%)	Y_{Ag} (mol%)	Z (eq)	temp (˚C)	time (h)	yield (%)[a]	dr[b]
1	30	-	-	-	rt	18	52	4 : 1
2	30	**V** (5)	$AgSbF_6$ (5)	5	0[c]	11	68	8 : 1
3	30	**V** (5)	AgOTf (5)	5	rt	3	78	5 : 1
4	30	Ph_3PAuCl (5)	AgOTf (5)	5	rt	3.5	65	6 : 1
5	30	**V** (5)	AgOTf (5)	-	rt	4	49	3 : 1
6	30	-	AgOTf (5)	-	rt	3	53	3 : 1
7	30	-	-	5	rt	18	51	4 : 1
8	-	**V** (5)	AgOTf (5)	-	rt	20	-	-
9	-	**IV** (5)	-	-	rt	20	-	-
10	-	-	AgOTf (5)	-	rt	20	-	-
11	-	-	$AgBF_4$ (5)	-	rt	20	-	-
12	30	**V** (5)	AgOTf (5)	5	10	4	64	7 : 1
13	30	**V** (5)	AgOTf (5)	5	0	9	66	7 : 1

[a]Isolated yield. [b]Determined by crude NMR. [c]At 0˚C for 3 h, then rt for 8 h.

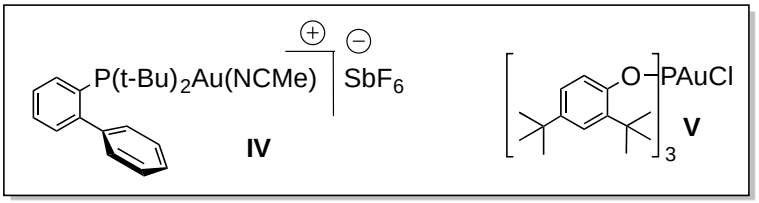

conditions with prolonged reaction times, the yield and dr were greatly improved (compare Table 3-4 entry 2 and Table 3-3 entry 1). However, when AgOTf was used instead of $AgSbF_6$, the reaction occurred more rapidly and gave the highest yield (Table 3-4 entry 3).

Thomas demonstrated that the reaction does not need each of the three catalysts pTSA, **V**, and AgOTf. The reaction was shown to proceed without gold, using only pTSA and AgOTf as catalysts (Table 3-4, entry 6), while in entry 5 neither gold nor silver were required to yield 51%. In addition, the role of pTSA is critical. In entries 8-11 no reaction is observed.

These data show that protic acidic conditions are needed to furnish the desired dihydropyran, which is expected since the overall transformation is a substitution reaction of a one hydroxyl moiety for another. Presumably, one hydroxyl group must be protonated before the other can substitute (S_N2) or that the allyl hydroxyl group leaves to form an allyl cation (S_N1). In either case, the role of pTSA is likely to protonate the leaving hydroxyl group, thus favoring its substitution. Unfortunately, the role of acetone, gold, and silver remains in question.

3.3 Future Work

Optimization of the reaction conditions appears to be complete. It is known that pTSA is the only catalyst required to make the reaction work, but that gold catalyst **V**, silver catalyst AgOTf, and 5 equivalents acetone allow the reaction to proceed more smoothly and give higher yield. The role of these auxiliary catalysts should be further investigated. In addition, the method should be tested to see if it can retain stereochemical information. Lastly, a determination of what functional groups can be tolerated must be made.

In answering these questions, the applicability of the methodology will be demonstrated as well as providing invaluable insight into a possible mechanism for the transformation. Once this level of understanding has been reached, the methodology should be applied to a natural product synthesis in order to showcase its utility.

3.4 Conclusions

To conclude, a new method for the formation of 3,6-dihydropyrans has been developed. It has the potential to be of great use in natural product synthesis. When used in conjunction with Roush's double allylboration, commercially available aldehydes can be converted into elaborate dihydro-2H-pyrans in only two steps. Hopefully, this process will be shown to conserve chirality and thus become the new standard in the state of the art in the synthesis of natural products containing 3,6-dihydro-2H-pyrans.

CHAPTER 4
EXPERIMENTAL

All reactions were carried out under an atmosphere of dry nitrogen unless otherwise specified. Anhydrous solvents were transferred via syringe to flame-dried (or oven-dried) glassware, which had been cooled under a stream of dry nitrogen. Anhydrous methylene chloride (CH_2Cl_2), tetrahydrofuran (THF), acetonitrile, ether, benzene and toluene were dried and degassed using an mBraun solvent purification system equipped with argon.

Analytical thin layer chromatography (TLC) was performed using 250 μm silica gel 60 Å, fluorescence dye pre-coated plates (Whatman Inc.). TLC analysis was primarily conducted using UV short wave light, iodine to stain, 2,4-dinitrophenylhydrazine (DNP), potassium permanganate ($KMnO_4$), and ceric ammonium molybdonate (CAM) stains. Flash column chromatography (FCC) was performed using 230-400 mesh 60 Å silica gel (Whatman Inc.). The eluents employed are reported as volume:volume percentages. Proton nuclear magnetic resonance (^{1}H NMR) spectra were recorded using Varian Unity Inova 500 MHz and Varian Mercury 300 MHz spectrometers. Chemical shift (δ) is reported in parts per million (ppm) downfield relative to tetramethylsilane (TMS, 0.0 ppm) or chloroform ($CHCl_3$ 7.26 ppm). Coupling constants (*J*) are reported in Hz. Multiplicities are reported using the following abbreviations: s, singlet; d, doublet; t, triplet; q, quartet; m, multiplet; br, broad. Carbon-13 nuclear magnetic resonance (^{13}C NMR) spectra were recorded on the same spectrometers that were used to determine proton magnetic resonance spectra. Chemical shift (δ) is reported in ppm relative to the carbon resonance of $CDCl_3$ (77.26 ppm). Infrared spectra were obtained on a PerkinElmer Spectrum RX1 FTIR spectrometer at 1.0 cm^{-1}

resolution and are reported in wave numbers. High-resolution mass spectra (HRMS) were obtained by the Mass Spectrometry Core Laboratory of the University of Florida, and are reported as m/e (relative ratio). Accurate masses are reported for the molecular ion (M+) or a suitable fragment ion. Gas chromatography (GC) traces were measured on a Hewlett-Packard 5890 Series II instrument equipped with a Restek Rtx™-5 capillary column (30m, Ø = 0.5μm), a flame ionization detector and a Hewlett-Packard 3396a integrator.

4.1 Catalyst Screening

Note: all transition metal catalysts, cocatalysts, and activated molecular sieves were weighed out in a glovebox under a dry argon atmosphere except for diacetonitrile palladium (II) chloride and tris[triphenylphosphine gold(I)]oxonium tetrafluoroborate catalysts which are considered to be air-stable.

General Procedure: Catalysts (0.01 mmol) were dissolved in solvent (1 mL) and decane (0.20 mmol, 38.0 μL) which served as an internal standard. These were stirred at room temperature for a few minutes before addition of aldehyde (0.30 mmol, 36.3 μL) by syringe. Diol (0.20 mmol, 16.4 μL) was then added right after. Progress was monitored by TLC and GC. GC measurements were made by removing a small aliquot of reaction mixture, which was then adsorbed onto silica gel (0.05 – 0.10 mL), diluted in CH_2Cl_2 (0.5 mL), and then 1-5 μL was injected into GC (4 mL/min, 60˚C for 1 minute then 5˚C/min up to 155˚C for 5 more minutes). Peak area ratios were converted into yields from the calibration plots below. Reactions were quenched by filtering crude mixture over a short plug of silica and then concentrated by rotary evaporation before purifying by FCC.

In order to determine yield as well as conversion using GC two calibration plots were made. Known quantities of cyclohexylcarboxaldehyde **2-58** (t_R = 7.2 min) to decane (t_R = 8.3 min) or acetal **2-59** (t_R = 17.5 and 17.7 min) to decane were combined

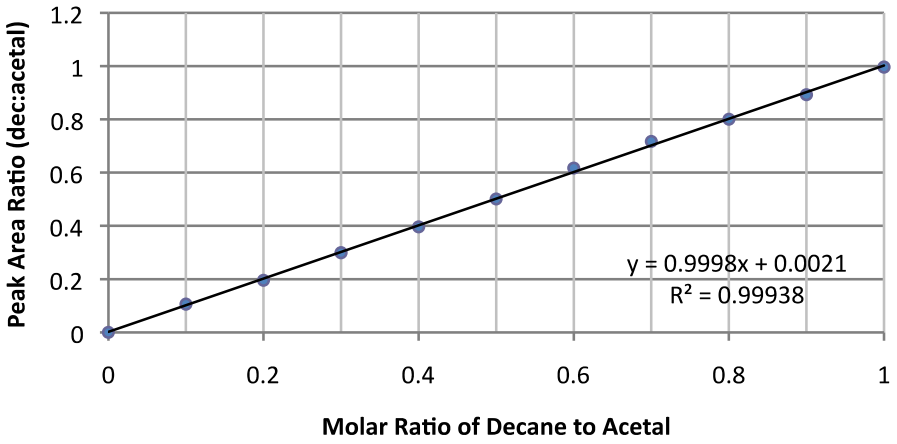

Figure 4-1. Calibration plot between molar ratio of decane to acetal versus peak area ratios.

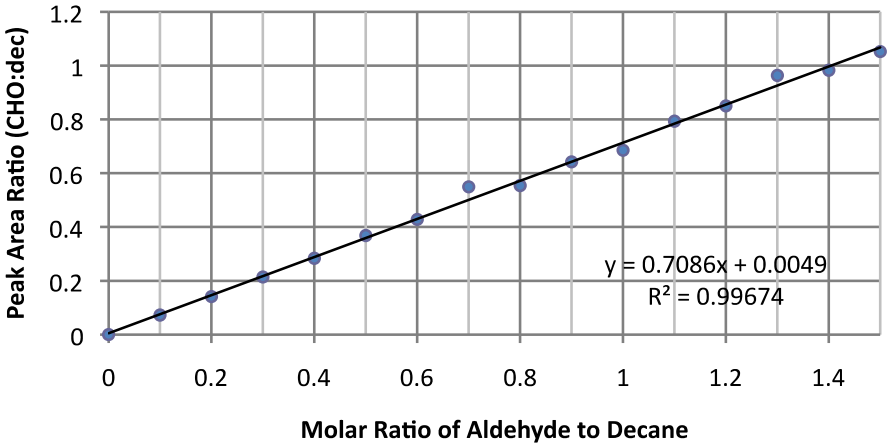

Figure 4-2. Calibration plot of molar ratio between aldehyde to decane versus peak

respectively in $CH_2Cl_2$and run on the GC (4 mL/min, 60˚C for 1 minute then 5˚C/min up to 120˚C or 155˚C) to determine peak area ratios at a given concentration. Ten or fifteen concentrations were run in order to make each calibration plot. From these plots, an equation was found to relate peak area ratio to concentration of the individual

constituents of the mixture with respect to decane. These plots and equations are given above.

4.2 Aldehyde Scope

Note: All aldehydes were freshly distilled before each reaction was run.

General Procedure: I (0.01 mmol, 5.3 mg) and AgOTf (0.01 mmol, 2.7 mg) were combined with molecular sieves (4 Å) in a test tube under argon in a glove box. The reaction vessel was wrapped in aluminum foil before being taken out of the glove box, and the mixture of solids was dissolved in CH_2Cl_2 (1 mL) at room temperature and allowed one minute to five minutes to stir in order to form the gold(I) cationic complex before the addition of aldehyde (0.30 mmol). *Z*-but-2-en-1,4-diol **2-55** (0.20 mmol, 16.4 µL) was then added. Progress was monitored by TLC for the disappearance of diol and reaction was quenched by filtering crude mixture over a plug of silica which was then concentrated by rotary evaporation and purified by flash column chromatography. If the aldehyde was not volatile, then the excess aldehyde was reduced to alcohol by $NaBH_4$ then purified by flash column chromatography.

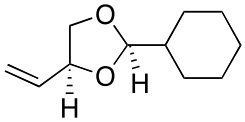

2-Cyclohexyl-4-vinyl-1,3-dioxolane (2-59): Reaction of **2-55** and cyclohexylcarboxaldehyde (**2-58**) afforded acetal as a colorless oil (93%yield, 1:8 d.r.). GC (4 mL/min, 60˚C for 1 minute then 5˚C/min up to 275˚C for an additional 5 minutes): t_R = 17.5 and 17.6 min. R_f (CH_2Cl_2/pentanes 20%): 0.23. Proton and carbon NMR spectra were found to match reported data.[86] ^{1}H NMR (300 MHz, $CDCl_3$) δ 5.82 (ddd, *J* = 17.2, 10.3, 7.0 Hz, 1H), 5.42 – 5.27 (m, 1H), 5.21 (ddd, *J* = 10.3, 1.5, 1.0 Hz, 1H), 4.77 (d, *J* = 4.9 Hz, 1H), 4.50 – 4.35 (m, 1H), 4.14 (ddd, *J* = 8.2, 6.2, 0.4 Hz, 1H), 3.51

(dd, *J* = 8.2, 7.6 Hz, 1H), 1.85 – 0.85 (m, 11H).[13]C NMR ($CDCl_3$, 75 MHz) δ 25.9, 26.6, 27.34, 27.5, 42.2, 68.4, 70.4, 108.0, 118.0, 133.2, 135.9.

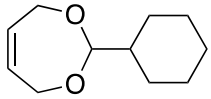

2-Cyclohexyl-4,7-dihydro1,3-dioxepine (2-60): Reaction of **2-55** and cyclohexylcarboxaldehyde (**2-58**) without molecular sieves at 0.8 M afforded acetal as a colorless oil (83%yield). R_f (CH_2Cl_2/pentanes 20%): 0.23. [1]H NMR (300 MHz, $CDCl_3$) δ 5.75 – 5.67 (m, 2H), 4.49 – 4.31 (m, 4H), 4.22 – 4.06 (m, 1H), 1.93 – 1.47 (m, 1H), 1.39 – 0.93 (m, 10H). [13]C NMR ($CDCl_3$, 75 MHz) δ 25.9, 26.6, 27.34, 27.5, 42.2, 70.4, 108.0, 118.0, 135.9.

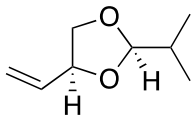

2-Isopropyl-4-vinyl-1,3-dioxolane (2-61a): Reaction of **2-55** and isobutyraldehyde (**2-62**) afforded acetal as a colorless oil (80% yield, 1:8 dr). R_f (CH_2Cl_2/hexane 40%): 0.23. Proton and carbon NMR spectra were found to match reported data.[87] [1]H NMR (500 MHz, $CDCl_3$, major diastereomer) δ 5.90 – 5.76 (m, 1H), 5.34 (dq, *J* = 17.1, 1.5 Hz, 1H), 5.22 (dq, *J* = 10.6, 1.5 Hz, 1H), 4.79 (d, *J* = 4.6 Hz, 1H), 4.53 – 4.40 (m, 3H), 4.16 (ddd, *J* = 8.8, 6.3, 2.2 Hz, 1H), 3.53 (ddd, *J* = 9.8, 7.7, 2.3 Hz, 1H), 1.94 – 1.76 (m, 3H), 1.02 – 0.87 (d, 6H).[13]C NMR (126 MHz, $CDCl_3$) δ 135.9, 118.1, 108.7, 105.0, 70.5, 32.6, 32.4, 30.7, 30.4, 17.0, 16.9.

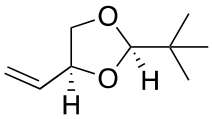

2-Tert-butyl-4-vinyl-1,3-dioxolane (2-61b): Reaction of **2-55** and pivaldehyde (**2-63**) afforded acetal as a colorless oil (70% yield, 1:18 dr). R_f (EtOAc/hexane 5%): 0.50. [1]H NMR (500 MHz, $CDCl_3$, major diastereomer) δ 5.83 (ddd, *J* = 14.4, 10.3, 7.1 Hz, 1H),

5.40 – 5.26 (m, 1H), 5.22 (ddd, *J* = 9.9, 2.2, 1.1 Hz, 1H), 4.68 (s, 1H), 4.42 (q, *J* = 6.9 Hz, 1H), 4.15 (ddd, *J* = 8.3, 5.7, 2.2 Hz, 1H), 3.53 (dd, *J* = 9.1, 6.8 Hz, 1H), 0.93 (s, 9H). ^{13}C NMR (126 MHz, $CDCl_3$) δ 135.9, 118.1, 110.7, 77.8, 77.5, 77.2, 77.0, 70.7, 34.9, 24.5, 24.4.

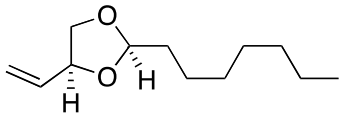

2-Heptyl-4-vinyl-1,3-dioxolane (2-61c): Reaction of **2-55** and octanal (**2-64**) afforded acetal as a colorless oil (81% yield, 1:3 dr). ^{1}H NMR (300 MHz, $CDCl_3$) δ 5.91 – 5.74 (m, 1H), 5.40 – 5.28 (m, 1H), 5.22 (dt, *J* = 10.3, 1.2 Hz, 1H), 5.02 (t, *J* = 4.8 Hz, 1H), 4.53 – 4.39 (m, 1H), 4.17 (dd, *J* = 8.3, 6.3 Hz, 1H), 3.52 (dd, *J* = 8.3, 7.5 Hz, 1H), 1.75 – 1.58 (m, 2H), 1.49 – 1.12 (m, 10H), 0.95 – 0.78 (m, 3H). ^{13}C NMR (75 MHz, $CDCl_3$) δ 14.3, 22.9, 24.2, 29.4, 29.8, 32.0, 34.4, 70.5, 100.2, 105.0, 118.0, 136.0.

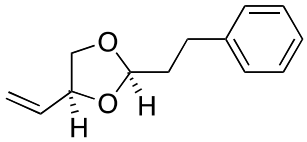

2-Phenylethyl-4-vinyl-1,3-dioxolane (2-61d): Reaction of **2-55** and hydrocinnamaldehyde (**2-65**) afforded acetal as a clear and colorless oil (68% yield, 1:5 dr). R_f (2 runs CH_2Cl_2/pentane 10%): 0.30. ^{1}H NMR (300 MHz, Chloroform-d) δ 7.36 – 7.13 (m, 5H), 5.92 – 5.75 (m, 1H), 5.36 (dq, *J* = 17.2, 1.5 Hz, 1H), 5.28 – 5.19 (m, 1H), 5.07 (t, *J* = 4.7 Hz, 1H), 4.58 – 4.42 (m, 1H), 4.21 (dd, *J* = 8.3, 6.3 Hz, 1H), 3.54 (dd, *J* = 8.3, 7.5 Hz, 1H), 2.84 – 2.67 (m, 2H), 2.12 – 1.89 (m, 2H). ^{13}C NMR (75 MHz, $CDCl_3$) δ 30.0, 30.3, 35.9, 36.0, 70.5, 100.0, 104.2, 104.6, 118.1, 126.1, 128.6, 135.8, 141.8.

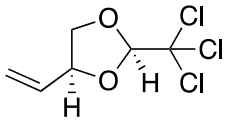

2-Trychloromethyl-4-vinyl-1,3-dioxolane (2-62e): Reaction of **2-55** and chloral hydrate (**2-61c**) afforded acetal as a clear and colorless oil (98% yield, 2:3 dr). R_f (EtOAc/hexanes 20%): 0.60. ^{1}H NMR (500 MHz, $CDCl_3$, both diastereomers) δ 5.83 (ddd, *J* = 14.4, 10.3, 7.1 Hz, 1H), 5.40 – 5.26 (m, 1H), 5.22 (ddd, *J* = 9.9, 2.2, 1.1 Hz, 1H), 5.02 (s, 1H), 4.42 (q, *J* = 6.9 Hz, 1H), 4.15 (ddd, *J* = 8.3, 5.7, 2.2 Hz, 1H), 3.53 (dd, *J* = 9.1, 6.8 Hz, 1H). ^{13}C NMR (126 MHz, $CDCl_3$) δ 135.9, 118.1, 110.7, 77.8, 76.9, 70.7.

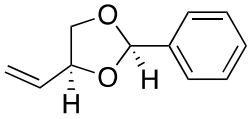

2-phenyl-4-vinyl-1,3-dioxolane (2-62f): Reaction of **2-55** and benzaldehyde (**2-67**) afforded acetal as an oil (55% yield, 1:2 dr). R_f (CH_2Cl_2:hexanes 20%): 0.40. Proton and carbon NMR spectra were found to match reported data.[88] ^{1}H NMR (500 MHz, $CDCl_3$, both diastereomers) δ 7.70 – 7.59 (m, 1H), 7.54 – 7.46 (m, 2H), 7.45 – 7.32 (m, 2H), 5.99 – 5.88 (m, 1H), 5.41 (ddt, *J* = 17.2, 2.0, 1.2 Hz, 1H), 5.27 (ddt, *J* = 11.1, 6.7, 1.2 Hz, 1H), 4.71 – 4.60 (m, 1H), 4.32 (dd, *J* = 8.3, 6.4 Hz, 1H), 3.82 – 3.75 (m, 1H), 3.72 (ddd, *J* = 8.1, 7.3, 0.6 Hz, 1H). ^{13}C NMR (126 MHz, $CDCl_3$) δ 135.9, 135.7, 128.6, 127.8, 126.3, 119.4, 109.6, 95.4, 72.9.

4.3 Substrate Syntheses

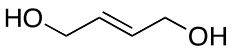

(E)-2-butene-1,4-diol (E-2-55): To a stirred solution of LAH (24 mmol, 0.9108 g) in THF (100 mL) at 0 ˚C was added 2-butyn-1,4-diol **2-76** (20 mmol, 1.7218 g) in THF (8 mL) in a dropwise fashion. Mixture was allowed to reach room temperature while reaction progress was monitored by TLC. After 4.5 h full reduction was observed, and

crude mixture was quenched via the Fieser and Fieser (n:n:3n) method whereby 1 mL/g of water/LAH is added very slowly and with great care to 0 ˚C reaction mixture and allowed at least fifteen minutes to stir before doubling the volume of the reaction with ether. Addition of 1 mL/g 10% NaOH solution is added very slowly in a dropwise manner and then allowed an additional fifteen minutes before adding 3 mL/g of water. This mixture is then allowed at least one hour to reach room temperature or until white precipitate has formed. The slurry is filtered, dried over magnesium sulfate, and concentrated by vacuum before purification by flash column chromatography to yield a clear, colorless oil (65 %). R_f (ethyl acetate 100%): 0.22. ^{1}H NMR (300 MHz, $CDCl_3$) δ = 1.30 – 1.43 (bs, 2H), 4.20 (s, 2H), 5.90 (s, 2H). ^{13}C NMR (126 MHz, $CDCl_3$) δ = 72.4, 130.9.

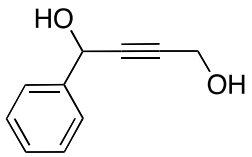

1-Phenylbut-2-yne-1,4-diol (2-95): To a stirred solution of propargylic alcohol **2-94** (20 mmol, 1.18 mL) in THF (82 mL) was added *n*-butyl lithium (17.6 mL, 2.5 M) dropwise over a period of 30 minutes at -78 ˚C. Mixture was warmed to -35 ˚C before addition of benzaldehyde **2-67** (24 mmol, 2.44 mL). Mixture was allowed to reach room temperature over 6 hours. Crude was obtained by washing the mixture with a saturated solution of ammonium chloride and brine with ethyl acetate, dried over magnesium sulfate, and concentrated in vaccuo. Product was obtained as a yellow solid by flash column chromatography (63% yield, mp 82 – 84 ˚C). R_f (ethyl acetate/hexanes 60%): 0.52. Melting point and NMR data matches previously reported data.[89] ^{1}H NMR (500

MHz, $CDCl_3$) δ = 2.20 – 2.80 (bs, 2H), 4.35 (s, 2H), 5.55 (s, 1H), 7.30 – 7.56 (m, 5H). ^{13}C NMR (126 MHz, $CDCl_3$) δ = 51.3, 64.8, 85.1, 85.7, 126.8, 128.7, 128.9, 140.5.

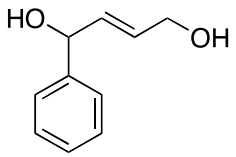

(E)-1-phenylbut-2-ene-1,4-diol (E 2-96): To a stirred solution of LAH (6 mmol, 0.2277 g) in THF (10 mL) at 0˚C was added **2-95** (3 mmol, 0.4865 g) with THF (5 mL) and allowed to stir until disappearance of starting material by TLC (22 h). Reaction was quenched via the n:n:3n method as previously described and purified via flash column chromatography to yield the yellow solid (87% yield, mp 76 – 78 ˚C). Melting point matches previously reported data.[90] R_f (ethyl acetate/hexanes 50%): 0.22. ^1H NMR (500 MHz, $CDCl_3$) δ = 2.40 – 3.10 (bs, 2H), 4.18 – 4.22 (d, 1H), 4.38 – 4.44 (d, 1H), 5.30 (s, 1H), 5.75 – 5.80 (s, 2H), 7.30 – 7.56 (m, 5H). ^{13}C NMR (126 MHz, $CDCl_3$) δ = 58.8, 70.1, 126.3, 127.9, 128.9, 130.2, 134.8, 143.2.

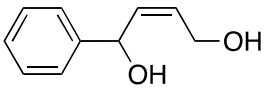

(Z)-1-phenylbut-2-ene-1,4-diol (Z 2-96): To a stirred solution of **2-95** (3 mmol, 0.4865 g) in ethyl acetate at room temperature was added quinoline (2.1 mmol, 0.25 mL) and Lindlar's catalyst (15% wt., 73 mg). This mixture was put under an atmosphere of hydrogen and allowed to stir until the disappearance of starting material could be observed by NMR (17 h). Crude was filtered over celite, concentrated in vaccuo and purified by flash column chromatography to yield a yellow solid (86% yield, mp 71 – 73 ˚C). R_f (ethyl acetate/hexane 50%): 0.24. Melting point and NMR data match previously reported data.[89] ^1H NMR (500 MHz, $CDCl_3$) δ = 2.70 – 3.30 (bs, 2H), 4.18 –

4.20 (d, 2H), 5.25 (s, 1H), 5.92 (s, 2H), 7.30 – 7.56 (m, 5H). ^{13}C NMR (126 MHz, $CDCl_3$) δ =63.1, 74.7, 126.5, 128.1, 128.8, 130.5, 133.7, 142.9.

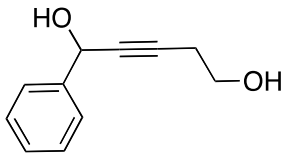

1-Phenylpent-2-yne-1,5-diol (2-78): To a stirred solution of 3-butyn-1-ol **2-77** (20 mmol, 1.52 mL) in THF (100 mL) at -78 ˚C was added *n*-butyl lithium (19.2 mL, 2.5 M) dropwise over a period of 15 minutes. Reaction mixture was warmed to -45 ˚C for the addition of benzaldehyde **2-67** (24 mmol, 2.44 mL) and allowed to reach room temperature over 20 hours. Crude mixture was washed with ammonium chloride and brine with ethyl acetate and was dried over magnesium sulfate, concentrated in vaccuo before purification by flash column chromatography to yield a colored solid (81% yield, mp 66 – 69 ˚C). R_f (ethyl acetate/hexanes 50%): 0.20. IR: 3347, 2945, 2887, 1452, 1279, and 1043 cm^{-1}. ^{1}H NMR (300 MHz, $CDCl_3$) δ 2.00 – 2.24 (bs, 1 H), 2.40 – 2.45 (m, 2 H), 2.50 – 2.65 (bs, 1 H), 3.60 – 3.65 (t, 2 H), 5.40 (s, 1 H), 7.20 – 7.50 (m, 5 H). ^{13}C NMR (75 MHz, $CDCl_3$) δ = 23.4, 64.7, 64.9, 84.3, 98.6, 114.5, 128.8.

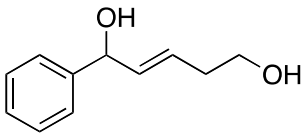

(E)-1-phenylpent-2-ene-1,5-diol (E 2-79): To a stirred solution of LAH (2.4 mmol, 0.0911 g) in THF (4 mL) at 0 ˚C was added **2-78** (1 mmol, 0.1762 g) with THF (1 mL) and allowed to stir until disappearance of starting material by TLC (22 h). Reaction was quenched via the n:n:3n method as previously described and purified via flash column chromatography to yield a clear and colorless oil (85% yield). R_f (ethyl acetate/hexanes 50%): 0.20. ^{1}H NMR (500 MHz, $CDCl_3$) δ 1.60 – 2.00 (bs, 1 H), 2.20 – 2.58 (bs, 1H),

2.32 (q, *J* = 6.18 Hz, 2 H), 3.65 - 3.70 (m, 2 H), 5.19 (d, *J* = 5.77 Hz, 1 H), 5.71 - 5.83 (m, 2 H), 7.25 - 7.39 (m, 5 H). ^{13}C NMR (126 MHz, $CDCl_3$) δ = 35.7, 61.9, 75.2, 126.4, 127.9, 128.4, 128.8, 135.6, 143.2.

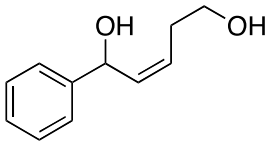

(Z)-1-phenylpent-2-ene-1,5-diol (Z 2-79): To a stirred solution of **2-78** (2 mmol, 0.3524 g) in ethyl acetate (10 mL) was added quinoline (1.4 mmol, 0.17 mL) and Lindlar's catalyst (15% wt., 5.3 mg). This mixture was put under an atmosphere of hydrogen and allowed to stir 16 hours. Reaction progress was monitored by NMR, product was afforded as a clear, red colored oil upon filtration over celite followed by flash column chromatography (91% yield). R_f (ethyl acetate/hexanes 50%): 0.39. ^{1}H NMR (300 MHz, $CDCl_3$) δ 2.35 - 2.42 (bs, 2H), d 2.50 - 2.73 (m, 2 H), 3.65 (td, *J* = 9.21, 4.62 Hz, 2 H), 3.70 - 3.85 (m, 1 H), 5.52 (d, *J* = 8.60 Hz, 1 H), 5.62 (dd, *J* = 17.11, 10.10 Hz, 1 H), 5.76 - 5.93 (m, 1 H), 7.23 - 7.53 (m, 5 H). ^{13}C NMR (75 MHz, $CDCl_3$) δ 31.1, 61.5, 69.3, 126.1, 126.2, 126.4, 127.7, 128.7, 128.8, 135.7, 143.7.

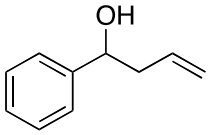

1-Phenylbut-3-ene-1-ol (2-80): To a stirred solution of benzaldehyde **2-67** (20 mmol, 2.0 mL) in THF (100 mL) at -35 ˚C was added allylmagnesium bromide (30 mL, 1.0 M) over five minutes and allowed to reach room temperature over one hour. Mixture was washed with 0.1 N HCl and brine with ethyl acetate, dried over magnesium sulfate, and concentrated in vaccuo before purification by flash column chromatography. Alcohol was afforded as a clear yellow oil (86% yield). R_f (ethyl acetate/hexanes 10%):

0.30. ^{1}H NMR (300 MHz, $CDCl_3$) δ 2.01 -2.04 (bs, 1 H), 2.42 -2.60 (m, 2 H), 4.65 – 4.78 (m, 1 H), 5.05 – 5.21 (dd, 2 H), 5.75 – 5.91 (m, 1 H), 7.21 – 7.42 (m, 5 H). ^{13}C NMR (75 MHz, $CDCl_3$) δ 11.2, 40.4, 44.1, 73.5, 93.4, 118.7, 118.7, 126.0, 127.8, 128.6, 134.7, 172.9, 181.9.

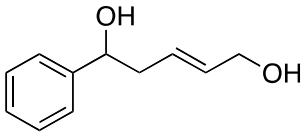

(E)-1-phenylpent-3-ene-1,5-diol (2-82): In a round bottom flask equipped with an immersion condenser, a stirred solution of Grubbs second generation catalyst (0.02 mmol, 17.0 mg) in CH_2Cl_2 (5 mL) at 45 ˚C was added a premixed solution of **2-80** (2 mmol, 0.2964 g) and crotonaldehyde (predominantly trans, 10 mmol, 0.83 mL) in CH_2Cl_2 (5 mL) and allowed to stir for 8 hours but starting material was never observed to disappear. Flash chromatography silica gel (10 mL) was added to refluxing solution and left open to air without condenser for at least 20 minutes to reach room temperature. Solvent was removed from slurry by rotary evaporation, and colored silica gel was filtered over a bed of clean silica gel with ethyl acetate to afford crude aldehyde **2-81**. About 20% conversion was observed and kept crude. R_f (ethyl acetate 20%): 0.15. ^{1}H NMR (300 MHz, $CDCl_3$) δ 2.76 – 2.83 (q, 2 H), 4.84 - 4.90 (m, 1 H), 6.12 – 6.22 (ddd, *J* = 15.7 Hz, 8.0 Hz, 1.2 Hz, 1 H), 6.80 – 6.90 (dd, *J* = 15.7 Hz, 7.2 Hz, 1 H), 7.20 – 7.40 (m, 5 H), 9.48 – 9.52 (d, *J* = 1.2 Hz, 1 H).

Crude aldehyde **2-81** was then taken into MeOH (2.8 mL) and cooled to 0 ˚C before addition of sodium borohydride (0.68 mmol, 25.7 mg); temperature was allowed to reach room temperature. After 3 hours, aldehyde was still present and so 1.2 more equivalents of sodium borohydride was added. Reaction was allowed to proceed until the disappearance of starting material via TLC, at which time mixture was reduced in

volume by 2/3 via rotary evaporation. This mixture was then dissolved in ethyl acetate, washed with brine and concentrated in vaccuo before purification by flash column chromatography to yield a colored oil (9.5% yield over two steps). R_f (ethyl acetate/hexanes 50%): 0.20. ^{1}H NMR (300 MHz, $CDCl_3$) δ 2.01 -2.04 (bs, 1 H), 2.42 - 2.60 (m, 2 H), 4.65 – 4.78 (m, 1 H), 5.05 – 5.21 (dd, 2 H), 5.75 – 5.91 (m, 1 H), 7.21 – 7.42 (m, 5 H). ^{13}C NMR (75 MHz, $CDCl_3$) 22.2, 32.6,38.9, 42.4, 62.8, 63.6, 73.8, 74.8, 126.0, 126.1, 127.8, 127.9, 128. 6, 128.7, 133.0, 144.1, 145.0.

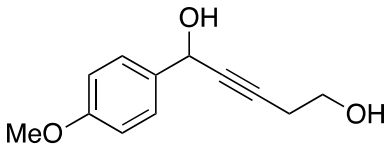

1-(4-Methoxyphenyl)pent-2-yne-1,5-diol (2-97): To a cooled solution of **2-77** (15 mmol, 1.13 mL) in THF (50mL), -50 ˚C was added n-butyllithium (36 mmol, 15 mL) and allowed 30 minutes to stir. Then anisaldehyde **2-69** (22.5 mmol, 2.74 mL) in THF (10 mL) was added, and the mixture was allowed to warm to ambient temperature over 18 hours. Ice cold ammonium chloride was added to the mixture, and extracted three times with ethyl acetate. The layers were separated, dried with magnesium sulfate, and concentrated to yield crude viscous oil. This was purified by flash column chromatography to yield an orange oil (43%). R_f (EtOAc/hexanes 50%): 0.12. ^{1}H NMR (500 MHz, $CDCl_3$) δ 7.53 – 7.37 (m, 2H), 6.99 – 6.77 (m, 2H), 5.40 (t, *J* = 2.1 Hz, 1H), 3.80 (d, *J* = 1.1 Hz, 3H), 2.58 – 2.47 (m, 2H), 1.5 (bs, 2H). ^{13}C NMR (126 MHz, $CDCl_3$) δ 159.8, 133.4, 128.2, 114.1, 84.0, 82.3, 77.4, 77.2, 76.9, 64.5, 61.1, 55.5, 23.4.

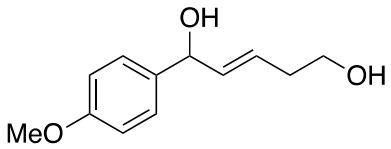

(E)-1-(4-methoxyphenyl)pent-2-ene-1,5-diol (E 2-98): To a cooled solution of **2-97** (1.21 mmol, 250 mg) in THF (6 mL) at 0 ˚C, was added LAH (2.9 mmol, 110.2 mg) portion wise over a few minutes. This mixture was allowed to stir for 18 hours and was quenched via n:n:3 method previously described above. This slurry was filtered over a bed of celite to remove all solids, and was concentrated to yield crude oil. This oil was purified by flash column chromatography to yield **E 2-98** as a clear colorless oil (94%). R_f (EtOAc/hexanes 50%): 0.12. ^{1}H NMR (500 MHz, $CDCl_3$) δ 7.34 – 7.28 (m, 2H), 6.95 – 6.85 (m, 2H), 5.86 – 5.70 (m, 2H), 5.16 (d, *J* = 6.0 Hz, 1H), 3.81 (d, *J* = 0.7 Hz, 3H), 3.70 (q, *J* = 5.9 Hz, 2H), 2.39 – 2.30 (m, 2H), 2.00 (bs, 1H), 1.59 (bs, 1H). ^{13}C NMR (126 MHz, $CDCl_3$) δ 135.7, 135.4, 127.8, 127.7, 114.1, 74.7, 62.0, 55.5, 35.7.

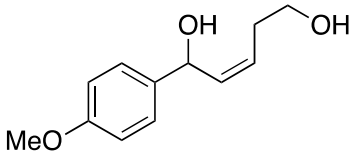

(Z)-1-(4-methoxyphenyl)pent-2-ene-1,5-diol (Z 2-98): To a solution of **2-97** (1.21 mmol, 250 mg), quinoline (0.85 mmol, 0.1 mL), Lindlar's catalyst (37.5 mg) in EtOAc (9 mL) was added hydrogen gas. This mixture was allowed to stir for 15 hours, afterwards this mixture was filtered over celite to remove catalyst. The filtrate was concentrated to yield yellow crude oil, which was purified via flash column chromatography to yield a clear orange colored oil (88%). R_f (EtOAc/hexanes 50%): 0.12. ^{1}H NMR (500 MHz, $CDCl_3$) δ 7.32 (dd, *J* = 8.9, 2.6 Hz, 2H), 6.88 (dd, *J* = 8.8, 2.7 Hz, 2H), 5.85 (ddt, *J* = 13.3, 7.9, 1.8 Hz, 1H), 5.66 – 5.54 (m, 1H), 5.48 (d, *J* = 8.6 Hz, 1H), 3.84 – 3.70 (m, 4H), 3.69 – 3.58 (m, 1H), 2.67 – 2.53 (m, 1H), 2.44 – 2.29 (m, 1H),

1.5 (bs, 2H). ^{13}C NMR (126 MHz, $CDCl_3$) δ 159.2, 135.8, 135.8, 128.2, 127.4, 127.2, 114.1, 69.0, 61.5, 55.4, 38.7, 31.0.

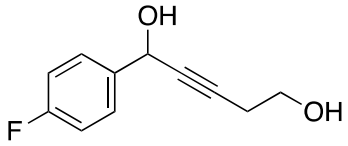

1-(4-Fluorophenyl)pent-2-yne-1,5-diol (2-99): To a cooled solution of **2-77** (10 mmol, 0.76 mL) in THF (20 mL) 0 ˚C was added ethylmagnesium bromide (22 mmol, 28 mL) slowly. The mixture was then heated to reflux for 1 hour, before cooling the solution back down to 0 ˚C for the addition of 4-fluorobenzaldehyde (10 mmol, 1.07 mL) in THF (5 mL). This mixture was allowed to stir for 16 hours. After this, the reaction was quenched with ice cold ammonium chloride, separated, and extracted with EtOAc before being dried with magnesium sulfate and concentrated to furnish crude oil. This was purified by flash column chromatography to yield a clear colorless oil (37%). R_f (EtOAc/Hexanes 50%):0.35. ^{1}H NMR (500 MHz, $CDCl_3$) δ 7.30 – 7.26 (m, 2H), 7.23 – 7.19 (m, 2H), 5.40 (t, *J* = 2.1 Hz, 1H), 3.80 (d, *J* = 1.1 Hz, 3H), 2.58 – 2.47 (m, 2H) 1.5 (bs, 2H). ^{13}C NMR (126 MHz, $CDCl_3$) δ 161.8, 133.4, 128.7, 114.1, 84.0, 82.3, 64.5, 61.1, 55.5, 23.4.

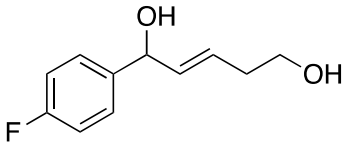

(E)-1-(4-fluorophenyl)pent-2-ene-1,5-diol (E 2-100): To a cooled solution of **2-99** (1.87 mmol, 364.1 mg) in THF (9.35 mL) at 0 ˚C, was added LAH (9.35 mmol, 354.8 mg) in small portions over a few minutes, and allowed to stir for 18 hours. After this time had elapsed, the reaction was quenched by way of the n:n:3 method previously described above. Solids were removed by filtering over a bed of celite, and

concentrating the filtrate to yield a crude oil, which was purified by flash column chromatography to yield a clear colorless oil (63%). R_f (EtOAc/Hexanes 50%): 0.24. ^{1}H NMR (300 MHz, $CDCl_3$) δ 7.44 – 7.30 (m, 2H), 7.09 – 6.96 (m, 2H), 5.85 – 5.56 (m, 2H), 5.51 (d, *J* = 8.5 Hz, 1H), 3.79 (dt, *J* = 10.4, 5.2 Hz, 1H), 3.73 – 3.59 (m, 1H), 2.87 (s, 1H), 2.74 – 2.53 (m, 1H), 2.46 – 2.27 (m, 1H). ^{13}C NMR (126 MHz, $CDCl_3$) δ 161.8, 133.4, 129. 6, 128.7, 128.0, 114.1, 64.5, 61.1, 55.5, 23.4.

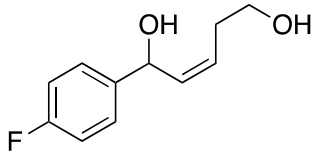

(Z)-1(4-fluorophenyl)pent-2-ene-1,5-diol (Z 2-100): To a solution of **2-99** (1.87 mmol, 364.1 mg), quinoline (1.31 mmol, 0.16 mL), Lindlar's catalyst (54.0 mg) in EtOAc (9.35 mL) was added hydrogen gas. This mixture was allowed to stir for 15 hours, afterwards this mixture was filtered over celite to remove catalyst. The filtrate was concentrated to yield yellow crude oil, which was purified via flash column chromatography to yield a clear colorless oil (77%). R_f (EtOAc/hexanes 50%): 0.24. ^{1}H NMR (300 MHz, $CDCl_3$) δ 7.44 – 7.30 (m, 2H), 7.09 – 6.96 (m, 2H), 5.82 (ddt, *J* = 11.0, 8.5, 1.3 Hz, 1H), 5.72 – 5.56 (m, 1H), 5.51 (d, *J* = 8.5 Hz, 1H), 3.79 (dt, *J* = 10.4, 5.2 Hz, 1H), 3.73 – 3.59 (m, 1H), 2.87 (s, 1H), 2.74 – 2.53 (m, 1H), 2.46 – 2.27 (m, 1H). ^{13}C NMR (126 MHz, $CDCl_3$) δ 161.8, 133.4, 129. 65 128.7, 128.0, 114.1, 64.5, 61.1, 55.5, 23.4.

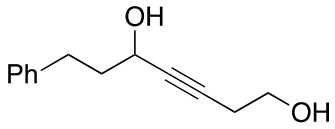

7-Phenylhept-3-yne-1,5-diol (2-101): To a cooled solution of **2-77** (10 mmol, 0.76 mL) in THF (20 mL) 0 ˚C was added ethylmagnesium bromide (22 mmol, 28 mL) slowly. The mixture was then heated to reflux for 1 hour, before cooling the solution back down to 0˚C for the addition of hydrocinnamaldehyde **2-65** (10 mmol, 1.32 mL) in THF (5 mL). This mixture was allowed to stir for 16 hours. After this, the reaction was quenched with ice cold ammonium chloride, separated, and extracted with EtOAc before being dried with magnesium sulfate and concentrated to furnish crude oil. This was purified by flash column chromatography to yield a clear colorless oil (66%). R_f (EtOAc/Hexanes 50%):0.27. Proton NMR spectrum was found to match reported data.[91] ^{1}H NMR (500 MHz, $CDCl_3$) δ 7.37 – 7.12 (m, 5H), 4.37 (s, 1H), 3.73 (q, *J* = 5.7 Hz, 2H), 2.79 (t, *J* = 7.8 Hz, 2H), 2.50 (tdd, *J* = 6.2, 2.7, 1.3 Hz, 2H), 2.11 – 1.88 (m, 2H), 1.56 (bs, 2H). ^{13}C NMR (126 MHz, $CDCl_3$) δ 136.1, 128.6, 128.5, 128.1, 126.0, 82.3, 62.0, 38.9, 35.7, 31.9.

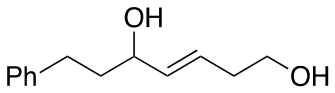

(E)-7-phenylhept-3-ene-1,5-diol (E 2-102): To a cooled solution of **2-101** (0.90 mmol, 183.8 mg) in THF (4.5 mL) at 0 ˚C, was added LAH (2.16 mmol, 82.0 mg) in small portions over a few minutes, and allowed to stir for 17 hours. After this time had elapsed, the reaction was quenched by way of the n:n:3 method previously described above. Solids were removed by filtering over a bed of celite, and concentrating the filtrate to yield a crude oil, which was purified by flash column chromatography to yield a clear colorless oil (93%). R_f (EtOAc/Hexanes 50%): 0.27. Proton NMR spectrum was

found to match reported data.[92] ^{1}H NMR (500 MHz, $CDCl_3$) δ 7.33 – 7.13 (m, 5H), 5.74 – 5.56 (m, 2H), 4.16 – 4.04 (m, 1H), 3.68 (dd, *J* = 6.7, 5.7 Hz, 2H), 2.78 – 2.61 (m, 2H), 2.36 – 2.26 (m, 2H), 1.95 – 1.77 (m, 2H), 1.75-1.50 (bs, 2H). ^{13}C NMR (126 MHz, $CDCl_3$) δ 136.1, 128.6, 128.5, 128.1, 126.0, 72.3, 62.0, 38.9, 35.7, 31.9.

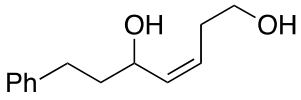

(Z)-7-phenylhept-3-ene-1,5-diol (Z 2-102): To a solution of **2-101** (0.37 mmol, 75.0 mg), quinoline (0.26 mmol, 0.03 mL), Lindlar's catalyst (11.0 mg) in EtOAc (1.85 mL) was added hydrogen gas. This mixture was allowed to stir for 17 hours, afterwards this mixture was filtered over celite to remove catalyst. The filtrate was concentrated to yield yellow crude oil, which was purified via flash column chromatography to yield a clear colorless oil (86%). R_f (EtOAc/hexanes 50%): 0.27. Proton NMR spectrum was found to match reported data.[92] ^{1}H NMR (300 MHz, $CDCl_3$) δ 7.38 – 7.08 (m, 5H), 5.77 – 5.48 (m, 2H), 4.42 (q, *J* = 7.0 Hz, 1H), 3.82 – 3.49 (m, 2H), 2.85 – 2.59 (m, 2H), 2.48 (dtt, *J* = 14.0, 9.0, 5.1 Hz, 1H), 2.26 (tq, *J* = 11.0, 5.3 Hz, 1H), 2.09 – 1.68 (m, 3H), 1.56 (bs, 1H). ^{13}C NMR (75 MHz, $CDCl_3$) δ 136.0, 129.1, 128.6, 128.5, 126.0, 66.5, 61.4, 38.8, 31.9, 31.0.

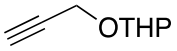

2-(Prop-2-yn-1-yloxy)tetrahydro-2H-pyran (2-126): To a solution of **2-125** (20 mmol, 1.16 mL) and 3,4-dihydropyran (24 mmol, 2.19 mL) in CH_2Cl_2 (100mL) was added pTSA (0.06 mmol, 11.0 mg). This mixture was allowed to stir for 24 hours. Reaction was quenched with $NaHCO_3$ in brine, extracted with CH_2Cl_2, dried with $MgSO_4$ and concentrated to yield crude mixture of **2-126**. Crude NMR showed only product, and as such was used without further purification. Proton NMR spectrum was found to

match reported data.[93] ^{1}H NMR (300 MHz, $CDCl_3$) δ 4.85 – 4.79 (m, 1H), 4.36 – 4.17 (m, 2H), 3.90 – 3.77 (m, 1H), 3.60 – 3.46 (m, 1H), 2.41 (t, *J* = 2.4 Hz, 1H), 1.92 – 1.45 (m, 8H).

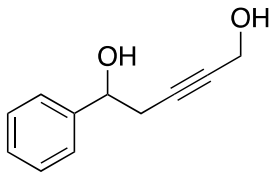

5-Phenylpent-2-yne-1,5-diol (2-127): To a cooled solution of **2-126** (20 mmol, 2.8036 g) in THF (63 mL) at -78 ˚C was added nBuLi (18.75 mmol, 7.5 mL) dropwise by way of an addition funnel. This mixture was allowed 30 minutes to stir before addition of styrene oxide (12.5 mmol, 1.5 mL) in THF (6 mL), followed immediately afterward by addition of BF_3 – etherate (18.75 mmol, 2.36 mL). This mixture was allowed to warm to ambient temperature over 28 hours and was quenched with ammonium chloride, separated, and extracted with EtOAc before being dried with magnesium sulfate, and concentrated to yield crude mixture. Crude NMR showed both diastereomers cleanly, and was kept crude for the next step.

The above crude mixture was dissolved in MeOH (63 mL) and treated with pTSA (0.04 mmol, 7.6 mg) and allowed to stir for 72 hours. The mixture was washed with sodium bicarbonate, extracted with EtOAc, dried over magnesium sulfate, and concentrated to yield crude oil. This was purified by flash column chromatography to yield a clear colorless oil (75% over three steps). R_f (EtOAc/Hexanes 50%): 0.20. Proton NMR spectrum was found to match reported data.[94] ^{1}H NMR (300 MHz, $CDCl_3$) δ 7.38 – 7.18 (m, 5H), 4.42 – 4.26 (m, 1H), 4.21 – 4.03 (m, 1H), 3.99 – 3.78 (m, 2H), 3.78 – 3.64 (m, 1H), 2.85 – 1.86 (s, 2H). ^{13}C NMR (75 MHz, $CDCl_3$) δ 140.6, 128.9, 127.6, 127.1, 87.8, 71.6, 51.1, 27.5.

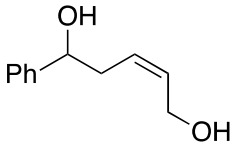

(Z)-5-phenylpent-2-ene-1,5-diol (2-128): To a solution of **2-127** (1.52 mmol, 286.1 mg), quinoline (1.06 mmol, 0.13 mL), Lindlar's catalyst (40.0 mg) in EtOAc (7.6 mL) was added hydrogen gas. This mixture was allowed to stir for 17 hours, afterwards this mixture was filtered over celite to remove catalyst. The filtrate was concentrated to yield yellow crude oil, which was purified via flash column chromatography to yield a clear colorless oil (78%). R_f (EtOAc/hexanes 50%): 0.30. Proton NMR spectrum was found to match reported data.[95] ^{1}H NMR (300 MHz, $CDCl_3$) δ 7.38 – 7.18 (m, 5H), 5.93 (dddd, *J* = 10.9, 7.2, 6.3, 0.8 Hz, 1H), 5.80 (ddt, *J* = 10.7, 9.6, 1.0 Hz, 1H), 4.42 – 4.26 (m, 1H), 4.21 – 4.03 (m, 1H), 3.99 – 3.78 (m, 2H), 3.78 – 3.64 (m, 1H), 2.85 – 1.86 (s, 2H). ^{13}C NMR (75 MHz, $CDCl_3$) δ 140.6, 129.4,128.9, 127.6, 127.1, 126.3, 51.1, 27.5.

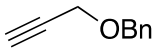

((Prop-2-yn-1-yloxy)methyl)benzene (2-129): To a suspension of NaH (22 mmol, 555.8 mg) in DMF (20 mL) at 0 ˚C, was added **2-125** (20 mmol, 1.16 mL) neat. This mixture was allowed to stir for 30 minutes before the addition of benzylbromide (22 mmol, 2.62 mL). This was then allowed to reach ambient temperature over 16 hours. The reaction was quenched with HCl (1 N, 40 mL), separated and extracted with EtOAc before being dried over magnesium sulfate, and concentrated to produce a crude oil. This was purified by flash column chromatography. R_f (EtOAc/Hexanes 10%): 0.30. Proton NMR spectrum was found to match reported data.[96] ^{1}H NMR (500 MHz, $CDCl_3$)

δ 7.45 – 7.27 (m, 5H), 4.61 (s, 2H), 4.24 (s, 1H), 4.18 (d, *J* = 2.4 Hz, 2H). ^{13}C NMR (126 MHz, $CDCl_3$) δ 128.6, 128.4, 128.2, 128.1, 127.8, 74.8, 72.3, 71.8, 71.7, 57.6.

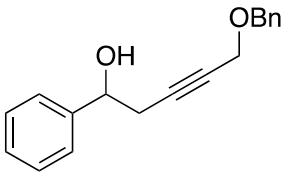

5-(Benzyloxy)-1-phenylpent-3-yn-1-ol (2-130): To a cooled solution of **2-129** (5 mmol, 715.0 mg) in THF (25 mL) at -78 ˚C was added nBuLi (7.5 mmol, 3 mL) dropwise by way of an addition funnel. This mixture was allowed 30 minutes to stir before addition of styrene oxide (5 mmol, 0.57 mL) in THF (2 mL), followed immediately afterward by addition of BF_3 – etherate (15 mmol, 1.88 mL). This mixture was allowed to warm to ambient temperature over 20 hours and was quenched with ammonium chloride, separated, and extracted with EtOAc before being dried with magnesium sulfate, and concentrated to yield crude mixture. This was purified by flash column chromatography to yield a clear colorless oil (28%). R_f (EtOAc/Hexanes 10%): 0.29. Proton NMR spectrum was found to match reported data.[97] ^{1}H NMR (500 MHz, $CDCl_3$) δ 7.48 – 7.26 (m, 10H), 4.88 (t, *J* = 6.4 Hz, 1H), 4.53 (s, 2H), 4.16 (t, *J* = 2.1 Hz, 2H), 2.77 – 2.66 (m, 2H), 2.38 (s, 1H). ^{13}C NMR (126 MHz, $CDCl_3$) δ 128.7, 128.6, 128.4, 128.2, 128.1, 128.0, 83.3, 78.9, 72.6, 71.6, 57.7, 28.9.

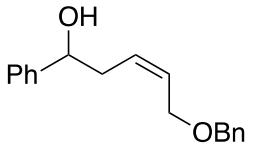

(Z)-5-(benzyloxy)-1-phenylpent-3-ene-1-ol (2-131): To a solution of **2-130** (1.77 mmol, 476.3 mg), quinoline (1.24 mmol, 0.15 mL), Lindlar's catalyst (70.5 mg) in EtOAc (9 mL) was added hydrogen gas. This mixture was allowed to stir for 16 hours,

afterwards this mixture was filtered over celite to remove catalyst. The filtrate was concentrated to yield yellow crude oil, which was purified via short path distillation to remove quinoline, thus yielding a clear colorless oil (55%). R_f (EtOAc/hexanes 20%): 0.30, but overlaps with quinoline spot. Proton NMR spectrum was found to match reported data.[98] ^{1}H NMR (500 MHz, $CDCl_3$) δ 7.44 – 7.24 (m, 10H), 5.89 – 5.76 (m, 1H), 5.76 – 5.57 (m, 1H), 4.72 (dd, *J* = 8.2, 5.2 Hz, 1H), 4.50 (s, 2H), 4.01 (dddd, *J* = 30.7, 11.9, 6.6, 1.4 Hz, 2H), 2.66 – 2.40 (m, 2H), 1.58 (s, 1H). ^{13}C NMR (126 MHz, $CDCl_3$) δ 129.8, 129.4, 128.6, 128.6, 128.5, 128.1, 128.0, 127.9, 127.6, 125.9, 77.4, 77.2, 76.9, 73.4, 72.7, 66.0, 65.6, 37.9, 37.1.

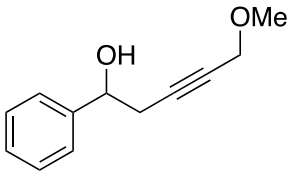

5-Methoxy-1-phenylpent-3-yn-1-ol (2-133): To a suspension of NaH (22 mmol, 555.8 mg) in dioxane (100 mL) at 0 ˚C, was added **2-125** (20 mmol, 1.16 mL) neat. This mixture was allowed to stir for 30 minutes before the addition of methyliodide (20 mmol, 1.25 mL). This was then allowed to reach ambient temperature over 16 hours. Full conversion was observed by TLC. R_f (EtOAc/Hexanes 20%): 0.27. The reaction was filtered to remove solid NaI, and kept as a 0.2 M solution of methyl ether **2-132** in dioxane due to the volatility of **2-132**.

To a cooled solution of **2-132** (10 mmol, 50 mL) at -78˚C was added nBuLi (9.38 mmol, 3.75 mL) dropwise by way of an addition funnel. This mixture was allowed 30 minutes to stir before addition of styrene oxide (6.25 mmol, 0.71 mL) in THF (2 mL), followed immediately afterward by addition of BF_3 – etherate (9.38 mmol, 1.18 mL). This mixture was allowed to warm to ambient temperature over 2 hours and was quenched

with ammonium chloride, separated, and extracted with EtOAc before being dried with magnesium sulfate, and concentrated to yield crude mixture. This was purified by flash column chromatography to yield **2-133** as a clear colorless oil (21% over two steps). R_f (EtOAc/Hexanes 30%): 0.36. ^{1}H NMR (500 MHz, $CDCl_3$) δ 7.44 – 7.27 (m, 5H), 4.94 – 4.80 (m, 1H), 4.08 (t, *J* = 2.3 Hz, 2H), 3.33 (d, *J* = 2.2 Hz, 3H), 2.75 – 2.63 (m, 2H), 2.45 – 2.32 (m, 1H). ^{13}C NMR (126 MHz, $CDCl_3$) δ 142.8, 128.7, 128.7, 128.7, 128.1, 125.9, 83.3, 78.7, 72.6, 60.2, 57.7, 30.0.

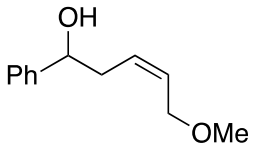

(Z)-5-methoxy-1-phenylpent-3-ene-1-ol (2-134): To a solution of **2-133** (0.5 mmol, 100 mg), quinoline (0.35 mmol, 0.04 mL), Lindlar's catalyst (15.0 mg) in EtOAc (2.5 mL) was added hydrogen gas. This mixture was allowed to stir for 18 hours, afterwards this mixture was filtered over celite to remove catalyst. The filtrate was concentrated to yield yellow crude oil, which was purified via short path distillation to remove quinoline, thus yielding a clear colorless oil (60%). R_f (EtOAc/hexanes 30%): 0.30, but overlaps with quinoline spot. ^{1}H NMR (500 MHz, $CDCl_3$) δ 7.41 – 7.21 (m, 5H), 5.83 – 5.72 (m, 1H), 5.72 – 5.61 (m, 1H), 4.74 (t, *J* = 6.4 Hz, 1H), 4.02 – 3.82 (m, 2H), 3.36 – 3.29 (m, 3H), 2.65 (s, 1H), 2.55 (dddd, *J* = 20.6, 18.8, 10.3, 6.0 Hz, 2H). ^{13}C NMR (126 MHz, $CDCl_3$) δ 144.3, 129.9, 129.3, 128.7, 128.6, 127.6, 126.9, 125.9, 73.3, 67.9, 58.2, 37.9.

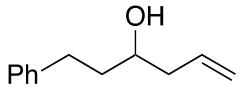

1-Phenylhex-5-en-3-ol (2-135): To a cooled solution of **2-65** (10 mmol, 1.32 mL) in THF (33 mL) at -78 ˚C, was added allylmagnesium bromide (15 mmol, 16.7 mL) dropwise by way of addition funnel. Mixture was allowed to warm to ambient temperature over 1.5 hours, and was then quenched with dilute HCl, extracted with EtOAc, dried over magnesium sulfate, and concentrated to give crude mixture which was purified by flash column chromatography to yield a clear, yellow liquid (60%). R_f (EtOAc/Hexanes 10%): 0.35. Proton NMR spectrum was found to match reported data.[99] ^{1}H NMR (500 MHz, $CDCl_3$) δ 7.34 – 7.12 (m, 5H), 5.91 – 5.74 (m, 1H), 5.21 – 5.09 (d, 2H), 3.76 – 3.60 (m, 1H), 2.81 (dt, *J* = 14.6, 7.5 Hz, 1H), 2.69 (dt, *J* = 14.3, 8.0 Hz, 1H), 2.40 – 2.27 (m, 1H), 2.25 – 2.12 (m, 1H), 1.86 – 1.73 (m, 3H), 1.58 (bs, 1H).

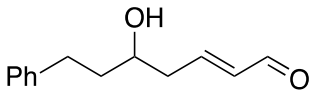

(E)-5-Hydroxy-7-phenylhept-2-enal (2-136): To an oven dried round bottom flask equipped with stir bar, was added Grubbs second generation catalyst (0.12 mmol, 101.9 mg) while warm to the touch and allowed to cool to room temperature under a stream of nitrogen. Once cooled, the catalyst was dissolved in CH_2Cl_2 (3.5 mL) then treated with a solution of premixed **2-135** (2.45 mmol, 431.8 mg) and crotonaldehyde (31.9 mmol, 2.6 mg) in CH_2Cl_2 (1.5 mL). Bubbles were observed within a few minutes of addition. Progress was monitored by TLC until the complete disappearance of **2-135** was observed after about 3 hours. The reaction was stopped by opening the reaction vessel to air and adding 5 mL of silica gel to the mixture. This was allowed 30 minutes to stir, and remaining CH_2Cl_2 was removed by rotary distillation. The resulting red powder was immediately purified via flash column chromatography to yield a clear, dark green liquid

(84%). R_f (EtOAc/Hexanes 25%): 0.25 and stains bright orange with DNP stain. Proton NMR spectrum was found to match reported data.[100] ^{1}H NMR (300 MHz, $CDCl_3$) δ 9.61 – 9.44 (m, 1H), 7.39 – 7.07 (m, 5H), 7.00 – 6.76 (m, 1H), 6.29 – 6.06 (m, 1H), 3.85 (qd, *J* = 6.7, 4.7 Hz, 1H), 2.76 (dddd, *J* = 21.8, 17.0, 14.0, 7.7 Hz, 2H), 2.63 – 2.39 (m, 2H), 1.97 – 1.72 (m, 3H), 1.57 (bs, 1H).

(E)-7-phenylhept-2-ene-1,5-diol (E 2-137): To a cooled solution of **2-136** (1.96 mmol, 400.0 mg) and $CeCl_3$ heptahydrate (4.9 mmol, 1.8256 g) in MeOH (10 mL) at 0 ˚C was added $NaBH_4$ (4.9 mmol, 185.4 mg) portionwise and was allowed to reach ambient temperature over 16 hours. An aliquot of mixture was treated with water in order to decomplex the aldehyde from cerium and thus give a clear TLC. Extra equivants of $NaBH_4$ were sometimes needed for full conversion. Once full conversion

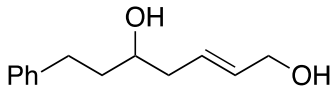

was observed, the reaction was quenched with water, and extracted three times with EtOAc, dried over magnesium sulfate, and concentrated to yield crude mixture. This was purified by flash column chromatography to yield a clear colorless oil (70%). R_f (EtOAc/Hexanes 50%): 0.18. Proton NMR spectrum was found to match reported data.[100] ^{1}H NMR (300 MHz, $CDCl_3$) δ 7.35 – 7.12 (m, 5H), 5.84 – 5.62 (m, 2H), 4.22 – 4.04 (m, 2H), 3.75 – 3.60 (m, 1H), 2.91 – 2.58 (m, 2H), 2.42 – 2.11 (m, 2H), 1.91 – 1.44 (m, 4H).

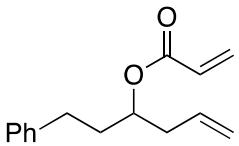

1-Phenylhex-5-en-3-yl acrylate (2-138): To a cooled solution of **2-135** (0.87 mmol, 179.1 mg) in CH_2Cl_2 at 0˚C was added acryloyl chloride (1.53 mmol, 137.8 mg)

followed by freshly distilled triethylamine (3 mmol, 0.42 mL) and was allowed to reach ambient temperature. TLC indicated full conversion after 2 hours and was then filtered over celite to remove triethylamine hydrochloride salt, then washed with water, extracted with CH_2Cl_2, dried over magnesium sulfate and concentrated to give crude mixture. This was purified by flash column chromatography to produce a clear colorless oil (96%). %). R_f (EtOAc/Hexanes 10%): 0.55. Proton NMR spectrum was found to match reported data.[101] ^{1}H NMR (300 MHz, $CDCl_3$) δ 7.39 – 7.05 (m, 5H), 6.41 (ddd, *J* = 17.3, 1.6, 0.7 Hz, 1H), 6.26 – 6.02 (m, 1H), 5.93 – 5.60 (m, 2H), 5.15 – 4.97 (m, 3H), 2.80 – 2.49 (m, 2H), 2.46 – 2.32 (m, 2H), 2.03 – 1.80 (m, 2H).

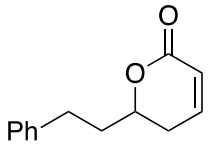

6-Phenethyl-5,6-dihydro-2H-pyran-2-one (2-139): To an oven dried round bottom 2 necked flask equipped with stir bar and condenser, was added Grubbs second generation catalyst (0.0043 mmol, 3.7 mg) while warm to the touch and allowed to cool to room temperature under a stream of nitrogen. Once cooled, the catalyst was dissolved in CH_2Cl_2 (1 mL) then heated to reflux by oil bath. This was then treated with a solution of **2-138** (0.43 mmol, 100 mg) in CH_2Cl_2 (1 mL). Bubbles were observed within a few minutes of addition. Progress was monitored by TLC until the complete disappearance of **2-138** was observed after about 3 hours. The reaction was stopped by opening the reaction vessel to air and adding 2 mL of silica gel to the mixture, then allowing the mixture to cool to ambient temperature. This was allowed 30 minutes to stir and remaining CH_2Cl_2 was removed by rotary distillation. The resulting red powder was immediately purified via flash column chromatography to yield an oil (50%). R_f

(CH_2Cl_2/Hexanes 75%): 0.29. Proton NMR spectrum was found to match reported data.[101] ^{1}H NMR (300 MHz, $CDCl_3$) δ 7.37 – 7.11 (m, 5H), 6.94 – 6.80 (m, 1H), 6.08 – 5.97 (m, 1H), 4.41 (dddd, *J* = 10.2, 8.4, 6.0, 4.3 Hz, 1H), 3.02 – 2.70 (m, 2H), 2.40 – 2.29 (m, 2H), 2.14 (dtd, *J* = 14.1, 8.7, 5.5 Hz, 1H), 1.94 (dddd, *J* = 13.9, 9.5, 7.2, 4.3 Hz, 1H).

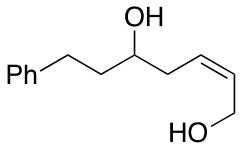

(Z)-7-phenylhept-2-ene-1,5-diol (Z 2-137): To a cooled solution of **2-139** (0.06 mmol, 12.8 mg) and $CeCl_3$ heptahydrate (0.173 mmol, 64.4 mg) in MeOH (7 mL) at 0 ˚C was added $NaBH_4$ (0.173 mmol, 6.5 mg) portionwise and was allowed to stir for 5 hours. An aliquot of mixture was treated with water in order to decomplex the aldehyde from cerium and thus give a clear TLC. Extra equivants of $NaBH_4$ were sometimes needed for full conversion. Once full conversion was observed, the reaction was quenched with water, and extracted three times with EtOAc, dried over magnesium sulfate, and concentrated to yield crude mixture. This was purified by flash column chromatography to yield a clear colorless oil (61%). R_f (CH_2Cl_2/Hexanes 75%): 0.29. Proton NMR spectrum was found to match reported data.[102] ^{1}H NMR (300 MHz, $CDCl_3$) δ 7.37 – 7.12 (m, 5H), 5.88 (dtt, *J* = 11.0, 6.9, 1.3 Hz, 1H), 5.64 (dddt, *J* = 10.9, 8.6, 7.5, 1.1 Hz, 1H), 4.26 – 4.04 (m, 2H), 2.87 – 2.62 (m, 2H), 2.40 – 2.24 (m, 2H), 1.89 – 1.73 (m, 2H), 1.25 (bs, 2H).

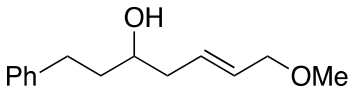

(E)-7-methoxy-1-phenylhept-5-en-3-ol (2-142): To a suspension of NaH (195 mmol, 7.78 g) in dioxane (140 mL) at 0˚C, was added **2-140** (166 mmol, 11.3 mL) neat. This mixture was allowed to stir for 30 minutes before the addition of methyliodide (139 mmol, 8.6 mL). This was then allowed to reach ambient temperature over 19 hours. Full conversion was observed by TLC. R_f (EtOAc/Hexanes 20%): 0.27. The reaction was filtered to remove solid NaI, and kept as a 1 M solution of methyl ether **2-141** in dioxane due to the volatility of **2-141**.

To an oven dried round bottom flask equipped with stir bar, was added Grubbs second generation catalyst (0.047mmol, 40 mg) while warm to the touch and allowed to cool to room temperature under a stream of nitrogen. Once cooled, the catalyst was dissolved in CH_2Cl_2 (5 mL) then treated with a solution of premixed **2-141** (47 mmol, 47 mL) and **2-135** (4.7 mmol, 819.8 mg) in CH_2Cl_2 (4.5 mL). Bubbles were observed within a few minutes of addition. Progress was monitored by TLC until the complete disappearance of **2-135** was observed after about 3 hours. The reaction was stopped by opening the reaction vessel to air and adding 9 mL of silica gel to the mixture. This was allowed 30 minutes to stir, and remaining CH_2Cl_2 was removed by rotary distillation. The resulting red powder was immediately purified via flash column chromatography to yield a clear, orange liquid (30%). R_f (EtOAc/Hexanes 10%): 0.61. Proton NMR spectrum was found to match reported data.[103] ^{1}H NMR (300 MHz, $CDCl_3$) δ 7.36 – 7.17 (m, 5H), 5.83 – 5.56 (m, 2H), 3.89 (d, *J* = 4.6 Hz, 2H), 3.67 (dq, *J* = 11.5, 5.5, 4.3 Hz, 1H), 3.32 (d, *J* = 1.1 Hz, 3H), 2.73 (ddt, *J* = 30.1, 14.6, 7.3 Hz, 2H), 2.39 – 2.08 (m, 2H), 1.87 – 1.70 (m, 2H), 1.61 (t, *J* = 6.4 Hz, 1H).

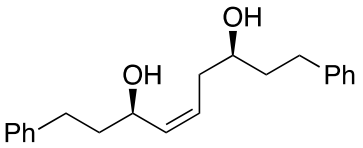

(3R, 7S, Z)-1,9-diphenylnon-4-ene-3,7-diol (Z 2-152): To a cooled solution of **2-149** (2.5 mmol, 1.0357g)[64] in CH_2Cl_2 (5 mL) at 0 ˚C was added **2-151** (2.5 mmol, 0.7158g)[104] in CH_2Cl_2 (5 mL) and was allowed to stir for 2 hours, after which the temperature was lowered to -78 ˚C. Hydrocinnamaldehyde **2-65** (6.25 mmol, 0.82 mL) was then added neat and allowed 4 hours to stir before the temperature was raised to ambient temperature over night. The reaction was then quenched 24 hours after the addition of aldehyde by the addition of 3 M NaOH (2.5 mL) and H_2O_2 (1 mL). The layers were separated, extracted with CH_2Cl_2, dried over magnesium sulfate, and concentrated to give crude mixture. This was purified via flash column chromatography to yield the diol as a clear colorless oil (70%). R_f (EtOAc/Hexanes 30%): 0.21. Proton NMR spectrum was found to match reported data. [64] ^{1}H NMR (500 MHz, $CDCl_3$) δ 7.34 – 7.12 (m, 10H), 5.72 – 5.63 (m, 1H), 5.63 – 5.54 (m, 1H), 4.41 (ddd, *J* = 8.1, 7.0, 5.7 Hz, 1H), 3.78 – 3.66 (m, 1H), 2.84 – 2.59 (m, 4H), 2.46 – 2.32 (m, 1H), 2.29 – 2.18 (m, 1H), 2.00 – 1.87 (m, 1H), 1.86 – 1.73 (m, 3H), 1.56 (bs, 2H).

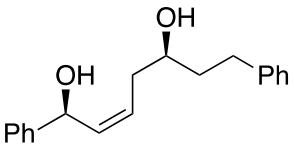

(1S, 5S, Z)-1,7-diphenylhept-2-ene-1,5-diol (2-153): To a cooled solution of **2-149** (2.5 mmol, 1.0357g)[64] in CH_2Cl_2 (5 mL) at 0 ˚C was added **2-151** (2.5 mmol, 0.7158g)[104] in CH_2Cl_2 (5 mL) and was allowed to stir for 2 hours, after which the temperature was lowered to -78 ˚C. Benzaldehyde **2-67** (2 mmol, 0.20 mL) was then added neat and allowed 2 hours to stir before the addition of hydrocinnamaldehyde **2-65**

(4.25 mmol, 0.56 mL), which was then allowed another 2 hours before the temperature was raised to ambient temperature over night. The reaction was then quenched 24 hours after the addition of benzaldehyde by the addition of 3 M NaOH (2.5 mL) and H_2O_2 (1 mL). The layers were separated, extracted with CH_2Cl_2, dried over magnesium sulfate, and concentrated to give crude mixture. This was purified via flash column chromatography to yield the diol as a clear colorless oil (66%). R_f (EtOAc/Hexanes 30%): 0.26. Proton NMR spectrum was found to match reported data. [64] ^{1}H NMR (500 MHz, $CDCl_3$) δ 7.34 – 7.12 (m, 10H), 5.72 – 5.63 (m, 1H), 5.63 – 5.54 (m, 1H), 4.41 (ddd, *J* = 8.1, 7.0, 5.7 Hz, 1H), 3.78 – 3.66 (m, 1H), 2.84 – 2.59 (m, 2H), 2.46 – 2.32 (m, 1H), 2.29 – 2.18 (m, 1H), 2.00 – 1.87 (m, 1H), 1.86 – 1.73 (m, 1H), 1.56 (bs, 2H).

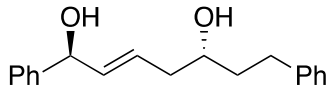

(1S, 5R, E)-1,7-diphenylhept-2-ene-1,5-diol (2-158): To a cooled solution of **2-157** (2.5 mmol, 1.0357g)[64] in CH_2Cl_2 (5 mL) at 0 ˚C was added **2-151** (2.5 mmol, 0.7158g)[104] in CH_2Cl_2 (5 mL) and was allowed to stir for 2 hours, after which the temperature was lowered to -78 ˚C. Benzaldehyde **2-67** (2 mmol, 0.20 mL) was then added neat and allowed 2 hours to stir before the addition of hydrocinnamaldehyde **2-65** (4.25 mmol, 0.56 mL), which was then allowed another 2 hours before the temperature was raised to ambient temperature over night. The reaction was then quenched 24 hours after the addition of benzaldehyde by the addition of 3 M NaOH (2.5 mL) and H_2O_2 (1 mL). The layers were separated, extracted with CH_2Cl_2, dried over magnesium sulfate, and concentrated to give crude mixture. This was purified via flash column chromatography to yield the diol as a clear colorless oil (66%). R_f (EtOAc/Hexanes 30%): 0.26. Proton NMR spectrum was found to match reported data. [64] ^{1}H NMR (500

MHz, $CDCl_3$) δ 7.34 – 7.12 (m, 10H), 5.72 – 5.63 (m, 1H), 5.63 – 5.54 (m, 1H), 4.41 (ddd, *J* = 8.1, 7.0, 5.7 Hz, 1H), 3.78 – 3.66 (m, 1H), 2.84 – 2.59 (m, 2H), 2.46 – 2.32 (m, 1H), 2.29 – 2.18 (m, 1H), 2.00 – 1.87 (m, 1H), 1.86 – 1.73 (m, 1H), 1.56 (bs, 2H).

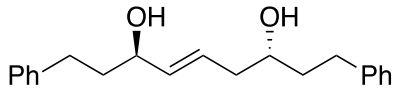

(3R, 7R, E)-1,9-diphenylnon-4-ene-3,7-diol (2-159): To a cooled solution of **2-157** (2.5 mmol, 1.0357g)[64] in CH_2Cl_2 (5 mL) at 0 ˚C was added **2-151** (2.5 mmol, 0.7158g)[104] in CH_2Cl_2 (5 mL) and was allowed to stir for 2 hours, after which the temperature was lowered to -78 ˚C. Hydrocinnamaldehyde **2-65** (6.25 mmol, 0.82 mL) was then added neat and allowed 4 hours to stir before the temperature was raised to ambient temperature over night. The reaction was then quenched 24 hours after the addition of aldehyde by the addition of 3 M NaOH (2.5 mL) and H_2O_2 (1 mL). The layers were separated, extracted with CH_2Cl_2, dried over magnesium sulfate, and concentrated to give crude mixture. This was purified via flash column chromatography to yield the diol as a clear colorless oil (70%). R_f (EtOAc/Hexanes 30%): 0.21. Proton NMR spectrum was found to match reported data. [64] ^{1}H NMR (500 MHz, $CDCl_3$) δ 7.34 – 7.12 (m, 10H), 5.72 – 5.63 (m, 1H), 5.63 – 5.54 (m, 1H), 4.41 (ddd, *J* = 8.1, 7.0, 5.7 Hz, 1H), 3.78 – 3.66 (m, 1H), 2.84 – 2.59 (m, 4H), 2.46 – 2.32 (m, 1H), 2.29 – 2.18 (m, 1H), 2.00 – 1.87 (m, 1H), 1.86 – 1.73 (m, 3H), 1.56 (bs, 2H).

4.4 Acetals from Diol Scope and Other Studies

Note: Isobutyraldehyde was freshly distilled before each reaction was run.

General Procedure A: V (0.01 mmol, 8.8 mg) and $AgSbF_6$ (0.01 mmol, 3.4 mg) were combined with molecular sieves (4 Å) in a test tube under argon in a glove box. The reaction vessel was wrapped in aluminum foil before being taken out of the glove

box, and the mixture of solids was dissolved in CH_2Cl_2 (0.25 mL) at room temperature and allowed one minute to five minutes to stir in order to form the gold (I) cationic complex before the addition of isobutyraldehyde **2-62** (1.00 mmol, 0.09 mL). Z-1,5-monoallylic diol (0.20 mmol) was then added. Progress was monitored by TLC for the disappearance of diol and reaction was quenched by filtering crude mixture over a plug of silica which was then concentrated by rotary evaporation and purified by flash column chromatography.

General Procedure B: Bismuth (III) triflate (0.01 mmol, 6.6 mg) was combined with molecular sieves (4 Å) in a test tube under argon in a glove box. The reaction vessel was taken out of the glove box, and the mixture of solids was dissolved in CH_2Cl_2 (1 mL) at room temperature before the addition of isobutyraldehyde (1.00 mmol, 0.09 mL). E-1,5-monoallylic diol (0.20 mmol) was then added. Progress was monitored by TLC for the disappearance of diol and reaction was quenched by filtering crude mixture over a plug of silica which was then concentrated by rotary evaporation and purified by flash column chromatography.

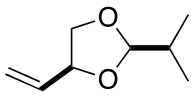

2-Isopropyl-4-vinyl-1,3-dioxolane (2-61a): Following general procedure A, the reaction of *Z*-2-butene-1,4-diol (**Z 2-55**) afforded acetal as a colorless oil (80% yield, 1:8 dr). Following general procedure B, the reaction of *E*-2-butene-1,4-diol (**E 2-55**) afforded acetal as a colorless oil (55% yield, 1:4 dr). R_f (CH_2Cl_2/hexane 40%): 0.23. Proton and carbon NMR spectra were found to match reported data.[87] ^{1}H NMR (500 MHz, $CDCl_3$, major diastereomer) δ 5.90 – 5.76 (m, 1H), 5.34 (dq, *J* = 17.1, 1.5 Hz, 1H), 5.22 (dq, *J* = 10.6, 1.5 Hz, 1H), 4.79 (d, *J* = 4.6 Hz, 1H), 4.53 – 4.40 (m, 3H), 4.16 (ddd, *J* = 8.8, 6.3,

2.2 Hz, 1H), 3.53 (ddd, *J* = 9.8, 7.7, 2.3 Hz, 1H), 1.94 – 1.76 (m, 3H), 1.02 – 0.87 (d, 6H).^{13}C NMR (126 MHz, $CDCl_3$, both diastereomers) δ 135.8, 118.0, 108.6, 104.9, 70.5, 32.6, 32.4, 30.7, 30.4, 17.0, 16.9.

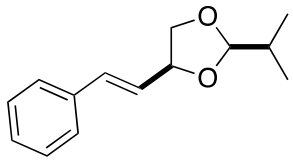

2-Isopropyl-4-((E)-styryl)-1,3-dioxolane (2-103): Following general procedure A, the reaction **Z 2-96** afforded acetal as a colorless oil (87% yield, 1:15 dr). R_f (CH_2Cl_2/hexane 40%): 0.20. ^{1}H NMR (500 MHz, $CDCl_3$) δ 7.43 – 7.20 (m, 5H), 6.70 – 6.60 (m, 1H), 6.17 (ddd, *J* = 15.8, 7.5, 0.5 Hz, 1H), 4.87 (d, *J* = 4.7 Hz, 1H), 4.67 – 4.57 (m, 1H), 4.23 (ddt, *J* = 8.3, 6.1, 0.4 Hz, 1H), 3.67 – 3.56 (m, 1H), 1.87 (dtdd, *J* = 13.7, 6.8, 4.7, 0.7 Hz, 1H), 1.02 – 0.95 (m, 6H). ^{13}C NMR (126 MHz, $CDCl_3$) δ 136.4, 133.4, 128.7, 128.1, 126.8, 126.8, 108.8, 70.8, 32.5, 16.9.

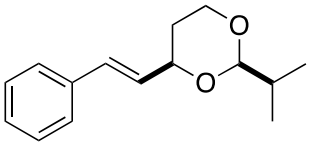

2-Isopropyl-4-((E)-styryl)-1,3-dioxane (2-92): Following general procedure A, the reaction **Z 2-79** afforded acetal as a colorless oil (91% yield, 1:22 dr). Following general procedure B, the reaction **E 2-79** afforded acetal as a clear colorless oil (98% yield, 1:22 dr). R_f (CH_2Cl_2/hexane 40%): 0.20. ^{1}H NMR (300 MHz, $CDCl_3$) δ 7.47 – 7.19 (m, 7H), 6.61 (dd, *J* = 16.4, 6.5 Hz, 1H), 6.30 – 6.16 (m, 1H), 4.50 (dd, *J* = 5.5, 1.2 Hz, 1H), 4.38 – 4.24 (m, 2H), 4.23 – 4.10 (m, 1H), 3.88 – 3.71 (m, 1H), 1.96 – 1.74 (m, 3H), 0.96 (ddd, *J* = 11.4, 6.1, 1.4 Hz, 11H). ^{13}C NMR (75 MHz, $CDCl_3$) δ 136.9, 130.4, 129.7, 128.7, 127.8, 126.7, 105.8, 77.0, 66.6, 32.6, 32.0, 16.8.

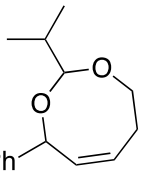

Z-2-Isopropyl-8-phenyl-5,8-dihydro-4H-1,3-dioxocine (2-93): Following general procedure B, the reaction **Z 2-79** afforded acetal as a clear colorless oil (98% yield). R_f (CH_2Cl_2/hexane 40%): 0.20. ^{1}H NMR (300 MHz, $CDCl_3$) δ 7.46 – 7.26 (m, 5H), 6.01 (dddd, *J* = 9.4, 4.8, 3.0, 2.2 Hz, 1H), 5.87 – 5.76 (m, 1H), 5.15 (dq, *J* = 5.3, 2.5 Hz, 1H), 4.50 (d, *J* = 5.4 Hz, 1H), 4.08 – 3.95 (m, 1H), 3.82 (dddd, *J* = 11.2, 8.7, 4.2, 0.7 Hz, 1H), 2.47 – 2.28 (m, 1H), 1.97 – 1.76 (m, 1H), 0.95 (dd, *J* = 6.8, 0.8 Hz, 6H). ^{13}C NMR (75 MHz, $CDCl_3$) δ 129.6, 128.6, 128.0, 127.6, 125.4, 104.9, 76.2, 63.3, 32.6, 25.3, 16.9.

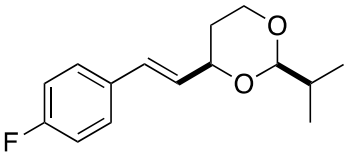

2-Isopropyl-4-((E)-4-fluorostyryl)-1,3-dioxane (2-105): Following general procedure A, the reaction **Z 2-100** afforded acetal as a colorless oil (98% yield, 1: >25 dr). Following general procedure B, the reaction **E 2-100** afforded acetal as a clear colorless oil (80% yield, 1: >25 dr). R_f (CH_2Cl_2/hexane 40%): 0.20. ^{1}H NMR (500 MHz, $CDCl_3$) δ 7.41 – 7.31 (m, 2H), 7.07 – 6.95 (m, 2H), 6.58 (dd, *J* = 16.0, 1.4 Hz, 1H), 6.14 (dd, *J* = 16.0, 5.7 Hz, 1H), 4.50 (dd, *J* = 5.5, 1.0 Hz, 1H), 4.34 (d, *J* = 5.1 Hz, 1H), 4.32 – 4.24 (m, 1H), 4.17 (ddd, *J* = 11.3, 4.9, 1.4 Hz, 1H), 3.83 – 3.73 (m, 1H), 1.93 – 1.76 (m, 1H), 1.60 – 1.49 (m, 1H), 1.02 – 0.90 (m, 6H). ^{13}C NMR (126 MHz, $CDCl_3$) δ 129.4, 129.3, 128.2, 128.1, 115.7, 115.5, 104.9, 77.5, 66.6, 33.1, 31.9, 16.9.

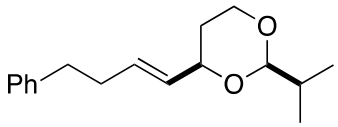

2-Isopropyl-4-((E)-phenylbut-1-en-yl)-1,3-dioxane (2-106): Following general procedure A, the reaction **Z 2-102** afforded acetal as a colorless oil (83% yield, 1: >25 dr). Following general procedure B, the reaction **E 2-102** afforded acetal as a clear colorless oil (95% yield, 1: >25 dr). R_f (CH_2Cl_2/hexane 40%): 0.20. ^{1}H NMR (300 MHz, Chloroform-d) δ 7.34 – 7.11 (m, 5H), 5.83 – 5.65 (m, 1H), 5.53 (ddt, *J* = 15.5, 6.0, 1.4 Hz, 1H), 4.28 (dd, *J* = 5.2, 1.1 Hz, 1H), 4.18 – 3.99 (m, 2H), 3.81 – 3.65 (m, 1H), 2.78 – 2.63 (m, 2H), 2.36 (dtt, *J* = 8.7, 6.5, 1.1 Hz, 2H), 1.91 – 1.69 (m, 3H), 0.98 – 0.91 (m, 6H). ^{13}C NMR (126 MHz, $CDCl_3$) δ 142.0, 131.4, 130.9, 128.6, 128.4, 126.0, 105.7, 77.1, 66.6, 35.7, 34.3, 33.0, 31.9, 17.5, 17.2.

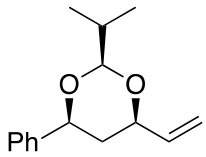

(2S, 4S, 6R)-2-Isopropyl-4-phenyl-6-vinyl-1,3-dioxane (2-143): Following general procedure A at 39˚C, the reaction of **2-131** afforded acetal as a clear colorless oil (20%). R_f (EtOAc/hexane 5%): 0.50. ^{1}H NMR (500 MHz, $CDCl_3$) δ 7.43 – 7.19 (m, 5H), 5.98 – 5.84 (m, 1H), 5.33 (dt, *J* = 17.3, 1.6 Hz, 1H), 5.16 (dt, *J* = 10.6, 1.5 Hz, 1H), 4.72 – 4.65 (m, 1H), 4.54 (d, *J* = 4.8 Hz, 1H), 4.42 – 4.36 (m, 1H), 4.32 – 4.23 (m, 1H), 2.03 – 1.89 (m, 1H), 1.85 (dt, *J* = 13.2, 2.5 Hz, 1H), 1.03 (dd, *J* = 6.9, 1.2 Hz, 6H). ^{13}C NMR (126 MHz, $CDCl_3$) δ 142.3, 138.1, 128.5, 127.7, 125.8, 125.5, 124.3, 105.3, 77.9, 76.8, 39.2, 33.1, 31.5, 17.4.

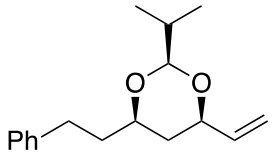

(2S, 4S, 6R)-2-Isopropyl-4-phenethyl-6-vinyl-1,3-dioxane (2-144): Following general procedure A, the reaction of **E 2-142** afforded acetal as a clear colorless oil (40%, 1 : 1 dr). R_f (CH_2Cl_2/hexane 25%): 0.30. ^{1}H NMR (500 MHz, $CDCl_3$) δ 7.43 – 7.19 (m, 5H), 5.98 – 5.84 (m, 1H), 5.33 (dt, *J* = 17.3, 1.6 Hz, 1H), 5.16 (dt, *J* = 10.6, 1.5 Hz, 1H), 4.72 – 4.65 (m, 1H), 4.54 (d, *J* = 4.8 Hz, 1H), 4.42 – 4.36 (m, 1H), 4.32 – 4.23 (m, 1H), 2.03 – 1.89 (m, 3H), 1.91 – 1.69 (m, 3H), 1.03 (dd, *J* = 6.9, 1.2 Hz, 6H). ^{13}C NMR (126 MHz, $CDCl_3$) δ 142.3, 138.1, 128.5, 127.7, 125.8, 125.5, 124.3, 105.3, 77.9, 76.8, 39.2, 33.1, 33.0, 31.9, 17.5, 17.2.

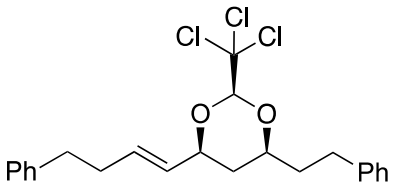

(2S, 4S, 6S) 4-Phenethyl-6-((E)-phenylbut-1-en-1-yl)-2-(trichloromethyl)-1,3-dioxane (2-156): Following general procedure A, the reaction of **E 2-142** with chloral hydrate in leiu of isobutyraldehyde afforded acetal as a clear colorless oil (40%, 1 : 1 dr). R_f (CH_2Cl_2/hexane 25%): 0.30. ^{1}H NMR (500 MHz, $CDCl_3$, as a mixture of diastereomers) δ 7.35 – 7.09 (m, 20H), 5.73 (dtt, *J* = 15.8, 6.8, 1.3 Hz, 1H), 5.63 – 5.44 (m, 2H), 4.58 – 4.53 (m, 1H), 4.34 (dd, *J* = 5.9, 1.2 Hz, 1H), 4.24 – 4.20 (m, 1H), 4.14 (dtt, *J* = 11.4, 5.0, 1.4 Hz, 1H), 4.00 (dt, *J* = 7.6, 4.9 Hz, 1H), 3.59 (tt, *J* = 8.8, 3.3 Hz, 1H), 3.52 (ddd, *J* = 11.1, 7.4, 5.0 Hz, 1H), 3.47 – 3.40 (m, 1H), 2.85 – 2.59 (m, 8H), 2.45 – 2.29 (m, 4H), 2.14 – 1.58 (m, 4H). ^{13}C NMR (126 MHz, $CDCl_3$, as a mixture of diastereomers) δ 141.5, 133.8, 131.6, 131.1, 131.1, 130.5, 130.4, 128.7, 128.7, 128.6, 128.6, 128.6, 128.6, 128.5, 128.5, 128.4, 126.3, 126.2, 126.2, 126.1, 125.5, 101.0, 99.2,

97.5, 97.1, 96.9, 95.6, 79.8, 71.9, 71.7, 71.0, 70.7, 53.6, 38.1, 37.9, 36.6, 36.6, 35.7, 35.5, 34.7, 33.0, 32.4, 32.3, 31.7, 31.5, 31.5, 31.4, 30.7.

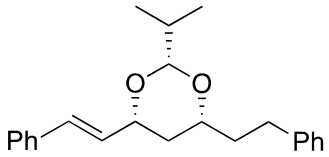

(2R, 4R, 6R)-2-Isopropyl-4-phenethyl-6-((E)-styryl)-1,3-dioxane (2-160):

Following general procedure B, the reaction of **E 2-158** afforded acetal as a clear colorless oil (84%, 1 : 1 dr). R_f (CH_2Cl_2/hexane 25%): 0.30. ^{1}H NMR (500 MHz, $CDCl_3$, both diastereomers) δ 7.43 – 7.15 (m, 28H), 6.60 (dt, *J* = 16.0, 1.6 Hz, 2H), 6.26 – 6.15 (m, 2H), 4.63 (d, *J* = 5.5 Hz, 1H), 4.58 – 4.55 (m, 0H), 4.53 – 4.43 (m, 1H), 4.30 (d, *J* = 5.6 Hz, 1H), 4.29 – 4.20 (m, 1H), 4.14 (dt, *J* = 11.2, 5.8 Hz, 1H), 3.60 (tdd, *J* = 11.1, 4.1, 2.4 Hz, 1H), 2.88 – 2.63 (m, 5H), 2.44 (ddt, *J* = 19.0, 9.8, 5.1 Hz, 1H), 2.12 – 1.69 (m, 10H), 1.07 – 0.96 (m, 16H). ^{13}C NMR (126 MHz, $CDCl_3$, both diastereomers) δ 142.0, 130.5, 130.3, 129.9, 129.7, 128.7, 128.7, 128.7, 128.6, 128.5, 127.8, 127.8, 127.2, 126.7, 126.5, 126.1, 125.9, 105.5, 104.9, 76.7, 74.9, 72.6, 71.0, 34.6, 33.2, 33.1, 32.6, 32.5, 32.1, 17.8, 17.7, 17.4, 17.3, 17.2, 17.2, 16.9.

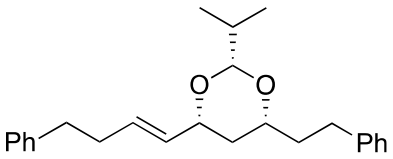

2-Isopropyl-4-phenethyl-6-((E)-4-phenylbut-1-en-1-yl)-1,3-dioxane (2-161):

Following general procedure B, the reaction of **E 2-159** afforded acetal as a clear colorless oil (70%). R_f (CH_2Cl_2/hexane 25%): 0.30. ^{1}H NMR (500 MHz, $CDCl_3$, as a mixture of diastereomers) δ 7.35 – 7.09 (m, 20H), 5.73 (dtt, *J* = 15.8, 6.8, 1.3 Hz, 1H), 5.63 – 5.44 (m, 2H), 4.58 – 4.53 (m, 1H), 4.34 (dd, *J* = 5.9, 1.2 Hz, 1H), 4.24 – 4.20 (m, 1H), 4.14 (dtt, *J* = 11.4, 5.0, 1.4 Hz, 1H), 4.00 (dt, *J* = 7.6, 4.9 Hz, 1H), 3.59 (tt, *J* = 8.8,

3.3 Hz, 1H), 3.52 (ddd, *J* = 11.1, 7.4, 5.0 Hz, 1H), 3.47 – 3.40 (m, 1H), 2.85 – 2.59 (m, 8H), 2.45 – 2.29 (m, 4H), 2.14 – 1.58 (m, 6H), 1.01 – 0.94 (m, 12H). ^{13}C NMR (126 MHz, $CDCl_3$, as a mixture of diastereomers) δ 141.5, 133.8, 131.6, 131.1, 131.1, 130.5, 130.4, 128.7, 128.7, 128.6, 128.6, 128.6, 128.6, 128.5, 128.5, 128.4, 126.3, 126.2, 126.2, 126.1, 125.5, 101.0, 99.2, 97.5, 97.1, 96.9, 95.6, 79.8, 71.9, 71.7, 71.0, 70.7, 53.6, 38.1, 37.9, 36.6, 36.6, 35.7, 35.5, 34.7, 33.0, 32.4, 32.3, 31.7, 31.5, 31.5, 31.4, 30.7.

4.5 Ketals

General Procedure : Bismuth (III) triflate (0.02 mmol, 13.2 mg) was combined with molecular sieves (4 Å) in a test tube under argon in a glove box. The reaction vessel was taken out of the glove box, and the mixture of solids was dissolved in $(CH_3)_2CO$ (1 mL) at room temperature before the addition of E-1,5-monoallylic diol (0.20 mmol). Progress was monitored by TLC for the disappearance of diol and reaction was quenched by filtering crude mixture over a plug of silica which was then concentrated by rotary evaporation and purified by flash column chromatography.

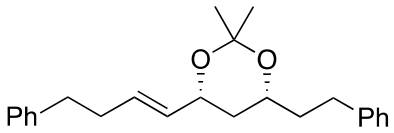

(4R, 6R)-2,2-Dimethyl-4-phenethyl-6-((E)-4-phenylbut-1-en-1-yl)-1,3-dioxane (2-163): Following general procedure, the reaction of **E 2-159** afforded acetal as a clear colorless oil (76%, 1 : 2 dr). R_f (CH_2Cl_2/hexane 50%): 0.22. Proton and carbon NMR spectra were found to match reported data. ^{1}H NMR (300 MHz, $CDCl_3$) δ 7.28 – 7.02 (m, 5H), 5.65 (dt, *J* = 15.5, 6.7 Hz, 1H), 5.50 – 5.33 (m, 1H), 4.20 (ddd, *J* = 14.7, 6.2, 2.9 Hz, 1H), 3.89 – 3.65 (m, 2H), 2.74 – 2.49 (m, 4H), 2.27 (q, *J* = 7.0 Hz, 1H), 1.84 –

1.51 (m, 4H), 1.40 – 1.28 (m, 6H). ^{13}C NMR (75 MHz, $CDCl_3$) δ 142.2, 142.0, 131.8, 131.7, 131.4, 131.1, 128.7, 128.6, 125.9, 98.8, 70.4, 68.0, 67.7, 65.8, 38.3, 38.1, 37.7, 37.4, 35.6, 34.3, 34.3, 31.8, 31.2, 30.5, 30.1, 20.1.

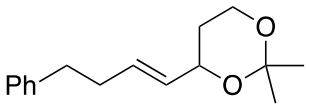

(E)-2,2-Dimethyl-4-(4-phenylbut-1-en-1-yl)-1,3-dioxane (2-165): Following general procedure, the reaction of **E 2-102** afforded acetal as a clear colorless oil (85%). R_f (EtOAc/hexane 10%): 0.21. ^{1}H NMR (300 MHz, $CDCl_3$) δ 7.36 – 7.09 (m, 5H), 5.72 (dt, *J* = 13.1, 6.4 Hz, 1H), 5.56 (m, 1H), 4.34 (m, 1H), 3.91 – 3.56 (m, 3H), 2.79 – 2.55 (m, 2H), 2.37 (h, *J* = 8.6, 6.7 Hz, 2H), 1.32 – 1.21 (s, 6H). ^{13}C NMR (75 MHz, $CDCl_3$) δ 128.6, 128.5, 126.1, 123.2, 118.6, 75.8, 73.9, 54.0, 36.6, 34.0, 32.2, 29.4.

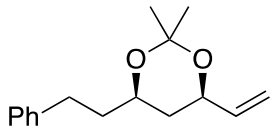

2,2-Dimethyl-4-phenethyl-6-vinyl-1,3-dioxane (2-166): Following general procedure, the reaction of **E 2-137** afforded acetal as a clear colorless oil (85%). R_f (EtOAc/hexane 10%): 0.21. Proton NMR spectrum was found to match reported data.[105] ^{1}H NMR (500 MHz, $CDCl_3$) δ 7.33 – 7.13 (m, 5H), 5.88 – 5.76 (m, 1H), 5.28 – 5.18 (m, 1H), 5.12 (dd, *J* = 10.6, 1.6 Hz, 1H), 4.38 – 4.25 (m, 1H), 3.82 (ttd, *J* = 10.0, 7.8, 6.2, 3.7 Hz, 1H), 2.90 – 2.55 (m, 3H), 1.91 – 1.62 (m, 3H), 1.43 (s, 6H). ^{13}C NMR (75 MHz, $CDCl_3$) δ 142.1, 139.0, 128.7, 128.5, 125.9, 115.5, 115.2, 98.8, 70.4, 67.6, 38.0, 37.0, 31.2, 30.4, 20.0

.

4.6 De-protection of Acetal 2-152

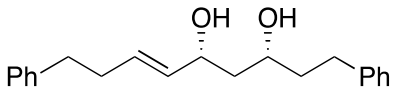

(3R, 5R, E)-1,9-diphenylnon-6-ene-3,5-diol (2-181): To a stirred solution of concentrated HCl (3 mmol, 0.092 mL) in MeOH (5 mL) was added **2-152** (0.05 mmol, 17.5 mg) and was allowed to stir 5.5 hours before quenching with pyridine (3 mmol, 0.24 mL).The mixture was filtered over celite to remove pyridine hydrochloride salt, and concentrated to yield crude oil which was purified by flash column chromatography to yield a clear colorless oil (47%, and 47% leftover starting material). R_f (EtOAc/hexane 50%): 0.50. ^{1}H NMR (299 MHz, $CDCl_3$) δ 7.35 – 7.11 (m, 10H), 5.77 – 5.63 (m, 1H), 5.53 (ddt, *J* = 15.4, 6.4, 1.3 Hz, 1H), 4.47 – 4.34 (m, 1H), 3.88 (dt, *J* = 7.7, 3.7 Hz, 1H), 2.87 – 2.55 (m, 4H), 2.50 – 2.05 (m, 4H), 1.96 – 1.51 (m, 2H). ^{13}C NMR (75 MHz, $CDCl_3$) δ 142.2, 131.8, 131.7, 131.4, 131.1, 128.7, 128.6, 125.9, 70.4, 67.7, 38.3, 35.6, 34.3, 31.2, 30.1.

4.7 3,6-Dihydro-2H-pyran Syntheses

General Procedure: V (0.005 mmol, 4.4 mg), $AgSbF_6$ (0.005 mmol, 1.7 mg), and pTSA (0.03 mmol, 5.7 mg) were combined with molecular sieves (4 Å) in a test tube under argon in a glove box. The reaction vessel was wrapped in aluminum foil before being taken out of the glove box, and the mixture of solids was dissolved in CH_2Cl_2 (0.5 mL) at room temperature and allowed one minute to five minutes to stir in order to form the gold (I) cationic complex before the addition of $(CH_3)_2CO$ (0.5 mmol, 0.036 mL). Z-1,5-monoallylic diol (0.10 mmol) was then added. Progress was monitored by TLC for the disappearance of diol and reaction was quenched by filtering crude mixture over a

plug of silica which was then concentrated by rotary evaporation and purified by flash column chromatography.

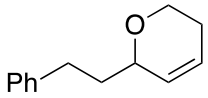

6-Phenylethyl-3,6-dihydro-2H-pyran (3-38): Following the general procedure, the reaction of **3-36** afforded dihydropyran as a clear colorless oil (62%). R_f (EtOAc/hexane 5%): 0.23. Proton and carbon NMR spectra were found to match reported data.[106] ^{1}H NMR (300 MHz, $CDCl_3$) δ 7.38 – 7.08 (m, 5H), 5.93 – 5.81 (m, 1H), 5.64 (ddt, *J* = 10.3, 2.4, 1.6 Hz, 1H), 4.11 (tdq, *J* = 6.9, 3.3, 1.8, 1.2 Hz, 1H), 4.01 (dddd, *J* = 11.2, 5.7, 2.6, 0.9 Hz, 1H), 3.74 – 3.61 (m, 1H), 2.75 (qdd, *J* = 13.8, 9.0, 6.7 Hz, 2H), 2.41 – 2.22 (m, 2H), 1.88 – 1.77 (m, 2H). ^{13}C NMR (75 MHz, $CDCl_3$) δ 142.4, 130.5, 128.7, 128.5, 125.9, 125.1, 73.3, 63.6, 37.2, 31.7, 25.6.

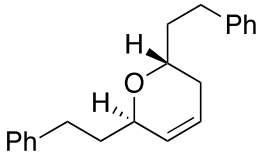

(2R, 6R)-2,6-Diphenylethyl-3,6-dihydro-2H-pyran (3-40): Following the general procedure, the reaction of **3-39** afforded dihydropyran as a clear colorless oil (63%, 6 : 1 dr). R_f (EtOAc/hexane 5%): 0.23. Proton NMR spectrum was found to match reported data.[107] ^{1}H NMR (500 MHz, $CDCl_3$) δ 7.35 – 7.13 (m, 10H), 5.85 – 5.76 (m, 1H), 5.69 (dddd, *J* = 10.3, 2.9, 2.4, 1.5 Hz, 1H), 4.25 – 4.16 (m, 1H), 3.73 (tt, *J* = 8.5, 4.0 Hz, 1H), 2.97 – 2.81 (m, 3H), 2.81 – 2.60 (m, 3H), 2.04 – 1.88 (m, 2H), 1.84 – 1.67 (m, 3H).

LIST OF REFERENCES

(1) Web of Knowledge [v.5.8] - Web of Science http://apps.webofknowledge.com/RAMore.do?product=WOS&search_mode=GeneralSearch&SID=2DK1CbcLi4JfgAbKe71&qid=3&ra_mode=more&ra_name=PublicationYear&colName=WOS&viewType=raMore&more_sort_order=alpha (accessed Dec 12, 2012).

(2) Huang, H.; Zhou, Y.; Liu, H. *Beilstein Journal of Organic Chemistry* **2011**, *7*, 897–936.

(3) Hashmi, A. S. K.; Rudolph, M. *Chem Soc Rev* **2008**, *37*, 1766–1775.

(4) Widenhoefer, R. A.; Han, X. *Eur J Org Chem* **2006**, *2006*, 4555–4563.

(5) Hashmi, A. *Chem. Rev* **2007**, *107*, 3180–3211.

(6) Corma, A.; Leyva-Pérez, A.; Sabater, M. J. *Chem. Rev* **2011**, *111*, 1657–1712.

(7) Li, Z.; Brouwer, C.; He, C. *Chem. Rev* **2008**, *108*, 3239–3265.

(8) Fürstner, A.; Davies, P. W. *Angew Chem Int Edit* **2007**, *46*, 3410–3449.

(9) Hashmi, A. S. K. *Angew Chem Int Ed Engl* **2010**, *49*, 5232–5241.

(10) Nolan, S. P. *Accounts Chem Res* **2011**, *44*, 91–100.

(11) Gorin, D. J.; Sherry, B. D.; Toste, F. D. *Chem. Rev* **2008**, *108*, 3351–3378.

(12) Raubenheimer, H. G.; Schmidbaur, H. *South African Journal of Science* **2011**, *107*, 01–13.

(13) Desclaux, J. P.; Pyykkö, P. *Chemical Physics Letters* **1976**, *39*, 300–303.

(14) Gorin, D.; Toste, F. *Nature* **2007**, *446*, 395.

(15) Pitzer, K. S. *Accounts Chem Res* **1979**, *12*, 271–276.

(16) Chatt, J.; Duncanson, L. A. *Chem. Commun.* **1953**, 2939.

(17) Hertwig, R. H.; Koch, W.; Schröder, D.; Schwarz, H.; Hrušák, J.; Schwerdtfeger, P. *J. Phys. Chem.* **1996**, *100*, 12253–12260.

(18) Salvi, N.; Belpassi, L.; Tarantelli, F. *Chem-Eur J* **2010**, *16*, 7231–7240.

(19) Benitez, D.; Shapiro, N. D.; Tkatchouk, E.; Wang, Y.; Goddard, W. A.; Toste, F. D. *Nature Chem* **2009**, *1*, 482–486.

(20) Zank, J.; Schier, A.; Schmidbaur, H. *Chem. Commun.* **1999**, 415–420.

(21) Carvajal, M. A.; Novoa, J. J.; Alvarez, S. *J. Am. Chem. Soc* **2004**, *126*, 1465–1477.

(22) Wang, W.; Hammond, G. B.; Xu, B. *J. Am. Chem. Soc* **2012**, *134*, 5697–5705.

(23) Benitez, D.; Tkatchouk, E.; González, A. Z.; Goddard, W. A., III; Toste, F. D. *Org. Lett* **2009**, *11*, 4798–4801.

(24) Burdett, J. K.; Albright, T. A. *J. Am. Chem. Soc* **1979**, *18*, 2112–2120.

(25) Thiel, W. R.; Eppinger, J. *Chem-Eur J* **1997**, *3*, 696–705.

(26) Yamamoto, Y. *J. Org. Chem.* **2007**, *72*, 7817–7831.

(27) Wang, D.; Cai, R.; Sharma, S.; Jirak, J.; Thummanapelli, S. K.; Akhmedov, N. G.; Zhang, H.; Liu, X.; Petersen, J. L.; Shi, X. *J. Am. Chem. Soc* **2012**, *134*, 9012–9019.

(28) Tolman, C. *Chem. Rev* **1977**, *77*, 313–348.

(29) Hirai, T.; Hamasaki, A.; Nakamura, A.; Tokunaga, M. *Org. Lett* **2009**, *11*, 5510–5513.

(30) Giner, X.; Nájera, C. *Org. Lett* **2008**, *10*, 2919–2922.

(31) Liu, X.-Y.; Li, C.-H.; Che, C.-M. *Org. Lett* **2006**, *8*, 2707–2710.

(32) Bandini, M.; Eichholzer, A.; Gualandi, A.; Quinto, T.; Savoia, D. *ChemCatChem* **2010**, *2*, 661–665.

(33) Biannic, B.; Ghebreghiorgis, T.; Aponick, A. *Beilstein Journal of Organic Chemistry* **2011**, *7*, 802–807.

(34) Ghebreghiorgis, T.; Biannic, B.; Kirk, B. H.; Ess, D. H.; Aponick, A. *J. Am. Chem. Soc* **2012**, *134*, 16307–16318.

(35) Amijs, C. H. M.; Ferrer, C.; Echavarren, A. M. *Chem. Commun.* **2007**, 698.

(36) Dubé, P.; Toste, F. D. *J. Am. Chem. Soc* **2006**, *128*, 12062–12063.

(37) Tarselli, M. A.; Gagné, M. R. *J. Org. Chem.* **2008**, *73*, 2439–2441.

(38) Tarselli, M. A.; Liu, A.; Gagné, M. R. *Tetrahedron* **2009**, *65*, 1785–1789.

(39) Suarez Pantiga, S.; Hernández Díaz, C.; Piedrafita, M.; Rubio, E.; Gonzalez, J. M. *Adv Synth Catal* **2012**, *354*, 1651–1657.

(40) Tarselli, M.; Zuccarello, J.; Lee, S.; Gagne, M. *Org. Lett* **2009**, *11*, 3490–3492.

(41) Mauleón, P.; Zeldin, R. M.; González, A. Z.; Toste, F. D. *J. Am. Chem. Soc* **2009**, *131*, 6348–6349.

(42) González, A. Z.; Toste, F. D. *Org. Lett* **2010**, *12*, 200–203.

(43) Aponick, A.; Li, C.-Y.; Biannic, B. *Org. Lett* **2008**, *10*, 669–671.

(44) Aponick, A.; Biannic, B. *Org. Lett* **2011**, *13*, 1330–1333.

(45) Biannic, B.; Aponick, A. *Eur J Org Chem* **2011**, *2011*, 6605–6617.

(46) Aponick, A.; Li, C.-Y.; Palmes, J. A. *Org. Lett* **2009**, *11*, 121–124.

(47) Aponick, A.; Li, C.-Y.; Malinge, J.; Marques, E. F. *Org. Lett* **2009**, *11*, 4624–4627.

(48) Aponick, A.; Biannic, B.; Jong, M. R. *Chem. Commun.* **2010**, *46*, 6849–6851.

(49) Ketcham, J. M.; Biannic, B.; Aponick, A. *Chem. Commun.* **2013**.

(50) Gómez-Bombarelli, R.; González-Pérez, M.; Pérez-Prior, M. T.; Calle, E.; Casado, J. *J. Phys. Chem. A* **2009**, *113*, 11423–11428.

(51) Bartlett, P. A.; Jernstedt, K. K. *J. Am. Chem. Soc* **1977**, *99*, 4829–4830.

(52) Bartlett, P.; Meadows, J.; Brown, E.; Morimoto, A.; Jernstedt, K. *The Journal of Organic Chemistry* **1982**, *47*, 4013–4018.

(53) Evans, D. A.; Gauchet-Prunet, J. A. *The Journal of Organic Chemistry* **1993**, *58*, 2446–2453.

(54) Evans, D. A.; Connell, B. T. *J. Am. Chem. Soc* **2003**, *125*, 10899–10905.

(55) Fettes, A.; Carreira, E. M. *J. Org. Chem.* **2003**, *68*, 9274–9283.

(56) Dineen, T. A.; Roush, W. R. *Org. Lett* **2004**, *6*, 2043–2046.

(57) Palimkar, S. S.; Uenishi, J. *Org. Lett* **2010**, *12*, 4160–4163.

(58) Lu, D.; Li, Y.; Gong, Y. *J. Org. Chem.* **2010**, *75*, 6900–6907.

(59) Oriez, R.; Prunet, J. *Tetrahedron Lett* **2010**, *51*, 256–258.

(60) Evans, P. A.; Grisin, A.; Lawler, M. J. *J. Am. Chem. Soc* **2012**, *134*, 2856–2859.

(61) Li, D. R.; Murugan, A.; Falck, J. R. *J. Am. Chem. Soc* **2008**, *130*, 46–48.

(62) Herrmann, A. T.; Saito, T.; Stivala, C. E.; Tom, J.; Zakarian, A. *J. Am. Chem. Soc* **2010**, *132*, 5962–5963.

(63) Qin, H.; Yamagiwa, N.; Matsunaga, S.; Shibasaki, M. *Angew Chem Int Edit* **2007**, *46*, 409–413.

(64) Flamme, E. M.; Roush, W. R. *J. Am. Chem. Soc* **2002**, *124*, 13644–13645.

(65) Carmely, S.; Kashman, Y. *Tetrahedron Lett* **1985**, *26*, 511–514.

(66) Jansen, R.; Wray, V.; Irschik, H.; Reichenbach, H.; Höfle, G. *Tetrahedron Lett* **1985**, *26*, 6031–6034.

(67) Moore, R. E.; Patterson, G. M. L.; Mynderse, J. S.; Barchi, J., Jr.; Norton, T. R.; Furusawa, E.; Furusawa, S. *Pure Appl. Chem.* **1986**, *58*, 263–271.

(68) Ishibashi, M.; Moore, R. E.; Patterson, G. M. L.; Xu, C.; Clardy, J. *J. Org. Chem.* **1986**, *51*, 5300–5306.

(69) Jefford, C. W.; Bernardinelli, G.; Tanaka, J.-I.; Higa, T. *Tetrahedron Lett* **1996**, *37*, 159–162.

(70) Mooberry, S. L.; Tien, G.; Hernandez, A. H.; Plubrukarn, A.; Davidson, B. S. *Cancer Research* **1999**, *59*, 653–660.

(71) Klenchin, V. A.; King, R.; Tanaka, J.; Marriott, G.; Rayment, I. *Chemistry & Biology* **2005**, *12*, 287–291.

(72) Mulzer, J.; Oehler, E. *Angew Chem Int Ed Engl* **2001**, *40*, 3842–3846.

(73) Mulzer, J.; Hanbauer, M. *Tetrahedron Lett* **2000**, *41*, 33–36.

(74) Paterson, I.; De Savi, C.; Tudge, M. *Org. Lett* **2001**, *3*, 3149–3152.

(75) Dossetter, A. G.; Jamison, T. F.; Jacobsen, E. N. *catalyst* **1999**, *1*, 2.

(76) Fischer, E. *Chem. Ber.* **1914**, *47*, 196–210.

(77) Ferrier, R. J.; Overend, W. G.; Ryan, A. E. *Chem. Commun.* **1962**, 3667.

(78) Ferrier, R. J. *Chem. Commun.* **1964**, 5443–5449.

(79) Paterson, I.; Smith, J. D.; Ward, R. A. *Tetrahedron* **1995**, *51*, 9413–9436.

(80) Paterson, I.; Cumming, J. G.; Ward, R. A.; Lamboley, S. *Tetrahedron* **1995**, *51*, 9393–9412.

(81) Su, Q.; Panek, J. S. *J. Am. Chem. Soc* **2004**, *126*, 2425–2430.

(82) Uenishi, J.; Ohmi, M.; Ueda, A. *Tetrahedron: Asymmetry* **2005**, *16*, 1299–1303.

(83) Uenishi, J.; Ohmi, M. *Angew Chem Int Ed Engl* **2005**, *44*, 2756–2760.

(84) Uenishi, J.; Ohmi, M.; Matsui, K.; Iwano, M. *Tetrahedron* **2005**, *61*, 1971–1979.

(85) Flamme, E. M.; Roush, W. R. *Beilstein Journal of Organic Chemistry* **2005**, *1*, 7.

(86) Kimura, M.; Mukai, R.; Tamaki, T.; Horino, Y.; Tamaru, Y. *J. Am. Chem. Soc* **2007**, *129*, 4122–4123.

(87) Singer, E.; Hölscher, B. *US Patent 20,120,308,486* **2012**.

(88) Marguet, F.; Cavalier, J. F.; Verger, R. *Eur J Org Chem* **1999**, 1671–1678.

(89) Boeckman, R. K.; Thomas, E. W. *J. Am. Chem. Soc* **1979**, *101*, 987–994.

(90) Bates, R. W.; Díez-Martín, D.; Kerr, W. J.; Knight, J. G.; Ley, S. V.; Sakellaridis, A. *Tetrahedron* **1990**, *46*, 4063–4082.

(91) Allegretti, P. A.; Ferreira, E. M. *Org. Lett* **2011**, *13*, 5924–5927.

(92) Fernández, E.; Pietruszka, J.; Frey, W. *J. Org. Chem.* **2010**, *75*, 5580–5589.

(93) Córdova, A.; Lin, S.; Tseggai, A. *Adv Synth Catal* **2012**, *354*, 1363–1372.

(94) Sidduri, A.; Rozema, M. J.; Knochel, P. *J. Org. Chem.* **1993**, *58*, 2694–2713.

(95) Oliveira, J. M.; R Freitas, J. C.; Comasseto, J. V.; Menezes, P. H. *Tetrahedron* **2011**, *67*, 3003–3009.

(96) Li, H.-J.; Guillot, R.; Gandon, V. *J. Org. Chem.* **2010**, *75*, 8435–8449.

(97) Fischer, M.; Schmölzer, C.; Nowikow, C.; Schmid, W. *Eur J Org Chem* **2011**,

2011, 1645–1651.

(98) Naruta, Y.; Maruyama, K. *J. Chem. Soc., Chem. Commun.* **1983**, 1264–1265.

(99) Ghadigaonkar, S.; Koli, M. R.; Gamre, S. S.; Choudhary, M. K.; Chattopadhyay, S.; Sharma, A. *Tetrahedron: Asymmetry* **2012**, *23*, 1093–1099.

(100) Shafi, S. M.; Chou, J.; Kataoka, K.; Nokami, J. *Org. Lett* **2005**, *7*, 2957–2960.

(101) de Fátima, Â.; Kohn, L. K.; de Carvalho, J. E.; Pilli, R. A. *Bioorganic & Medicinal Chemistry* **2006**, *14*, 622–631.

(102) Binder, J. T.; Kirsch, S. F. *Chem. Commun.* **2007**, 4164–4166.

(103) Fujihara, T.; Tomike, Y.; Ohtake, T.; Terao, J.; Tsuji, Y. *Chem. Commun.* **2011**, *47*, 9699–9701.

(104) Brown, H. C.; Singaram, B. *The Journal of Organic Chemistry* **1984**, *49*, 945–947.

(105) Iio, H.; Mizobuchi, T.; Tokoroyama, T. *Tetrahedron Lett* **1987**, *28*, 2379–2382.

(106) Markó, I. E.; Bayston, D. J. *Tetrahedron* **1994**, *50*, 7141–7156.

(107) Fraboulet, G.; Fargeas, V.; Paris, M.; Quintard, J.-P.; Zammattio, F. *Tetrahedron* **2009**, *65*, 3953–3960.

BIOGRAPHICAL SKETCH

Carl Ballesteros was born in Columbus Air Force Base to the proud parents of Tomas J. and Ileana Ballesteros. As the middle child of three and son to an Air Force Lieutenant Colonel, Carl grew up all over the world having lived as near as Panama City, Florida and as far away as Madrid, Spain. Tomas finally retired from the Air Force in 1995, and settled down in Clermont, Florida. Carl attended South Lake High School, and graduated the spring of 2001. Thereafter, he attended the University of Florida where he conducted undergraduate research in physical chemistry under the direction of Martin Vala, Ph.D., professor emeritus and studied interstellar radiation sources. He also taught general chemistry under Dr. Vala's direction. In addition, Carl conducted undergraduate research in organic synthetic chemistry under the direction of Merle A. Battiste, Ph. D., professor emeritus. Carl graduated with a Bachelor of Sciences degree in the spring of 2005 having majored in chemistry. He went on to attend the graduate program at the University of Florida, department of chemistry in 2007 and received his Doctor of Philosophy degree in the spring of 2013.